

THE MEDIAL PREFRONTAL CORTEX CONTRIBUTES TO BINGE EATING PRONENESS
IN FEMALE RATS

By

Elaine Sinclair

A DISSERTATION

Submitted to
Michigan State University
in partial fulfillment of the requirements
for the degree of

Neuroscience—Doctor of Philosophy

2017

ABSTRACT

THE MEDIAL PREFRONTAL CORTEX CONTRIBUTES TO BINGE EATING PRONENESS IN FEMALE RATS

By

Elaine Sinclair

Eating disorders (EDs) are some of the most severe psychiatric conditions that primarily affect the female sex. Women are significantly more likely than men to suffer from EDs and the female: male bias in ED risk is one of the largest in all of psychiatry. The prevalence rates for EDs in women are on par with several other major psychiatric disorders, but the severity of medical complications and psychiatric co-morbidities inherent to EDs are far worse than most other psychiatric conditions. For this reason, uncovering the specific biological and neural mechanisms that contribute to ED risk, development, and exacerbation is crucial. To that end, functional MRI (fMRI) in women with EDs has become a common modality for investigating the neurobiological variables inherent to EDs, as fMRI techniques anatomically localize critical “hot spots” of apparently abnormal neural activity that may be associated with eating pathology. Indeed, several lines of working using fMRI in women with EDs have demonstrated aberrant activity within prefrontal cortex (PFC) circuitry specifically during tasks that engage behavioral control mechanisms, particularly in women with EDs associated with the core, maladaptive symptom of *binge eating*. These data provide compelling evidence that dysfunctional PFC-mediated regulation over food intake may underlie eating pathology, namely binge eating. To study the role of the PFC in the context of eating pathology, animal models are valuable tools as the rodent medial PFC (mPFC) has several executive functions that are analogous to the human PFC. In addition, the rodent mPFC exerts behavioral control over palatable food (PF) intake, at least in male rodents: the mPFC acts as a behavioral “brake” or limit over excessive PF intake.

Thus, pathological eating behaviors, specifically binge eating, may be due in large part to deficient, mPFC-mediated behavioral control over PF intake. However, complete understanding of the underlying neural mechanisms by which the mPFC may contribute to binge eating is still lacking. Specifically, few studies, to date, have investigated whether the mPFC is implicated in binge eating using 1) a clinically-relevant rodent model of binge eating, or 2) female rodents. To that end, the goal of this dissertation was to identify the functional significance of the mPFC to PF intake and to binge eating using a well-validated animal model of binge eating proneness in female rodents. The experiments within this dissertation test the hypothesis that ***mPFC-mediated control over PF intake is weaker in female rats that are prone to binge eating.*** The first aim revealed different patterns of activation in the mPFC of binge eating prone (BEP) vs. binge eating resistant (BER) female rats, following exposure to PF. The second aim used double-label immunohistochemistry to identify that a vast majority of PF-activated neurons within the mPFC are excitatory, glutamatergic projection neurons, and that fewer excitatory neurons are engaged by PF in BEPs as compared to BERs. Using reversible, pharmacological inactivation of the mPFC, the third aim demonstrated that the mPFC of female rats indeed serves as a behavioral limit over excessive PF intake, but that the strength of the mPFC-mediated “brake” on PF intake is weaker in BEP rats as compared to BER rats. Thus, the experiments within this dissertation identify not only the cellular players within the mPFC that contribute to PF intake but also the functional significance of the mPFC to binge eating in the female sex.

Dedicated to Alex, Leo, and Louie

ACKNOWLEDGEMENTS

I am immeasurably grateful to each and every member of the Sisk lab that I have had the absolute pleasure of working with and learning from during my graduate career, and I am so honored to have been in the company of such wonderful scientists and people. Margaret Bell and Kayla DeLorme served as exemplary role models early on, and they taught me the critical lab skills that I needed for almost every experiment within this dissertation. Maggie Mohr taught me everything that I needed to know about single and double label immunohistochemistry, and she has and always will be a wonderful friend. The friendships of Britny Hildebrandt and Kristen Culbert made the countless weeks of feeding tests and innumerable rounds of perfusions all the more tolerable. Kristen Culbert also contributed *significantly* to the statistical analyses in the first Chapter of this dissertation. Janelle LeMon helped with several of the feeding tests and surgeries within this dissertation, and I am so excited for her future in the lab. Jane Venier is irreplaceable. She has been the best source of emotional support and valuable advice since the beginning. Last but not least, Jenny Kim not only assisted with every round of stereotaxic surgery in Chapter 3 of this dissertation, but she will be the best friend and lab mate that I could have ever asked for during these critical last years in the lab.

I would also like to thank my committee members for their support and guidance along the way, especially for knowing what was and was not best for me throughout this experience. I especially want to thank my co-advisor Kelly Klump for always challenging me to consider the clinical applications of my work and for always being so enthusiastic about everything we do with our binge eating model; it has been a constant source of motivation for me since day one.

Finally, I extend immense gratitude and appreciation to my advisor, Cheryl Sisk. I feel so lucky to have had the absolute pleasure to work with such an incredible role model and scientist. I have learned professionalism, critical thinking skills, invaluable writing skills, and scientific rigor from one of the best in the field, which will inevitably advance my career as a physician scientist. I am so grateful to have been given the opportunity to be a member of her lab.

TABLE OF CONTENTS

LIST OF TABLES.....	x
LIST OF FIGURES	xii
KEY TO ABBREVIATIONS.....	xiii
Introduction.....	1
Eating Disorders in Women.....	1
Neural Circuit Dysfunction in Eating Disorders in Humans	5
Abnormal reward processing as a cause for EDs.....	6
Deficient, prefrontal cortex-mediated behavioral regulation as a cause for EDs	7
The rodent medial prefrontal cortex (mPFC): A good model for studying cortical regulation of eating behavior.....	10
Homology between the rodent mPFC and the human PFC	11
Connectivity of the rodent mPFC	11
Excitatory, glutamatergic projection neurons of the mPFC.....	12
Inhibitory, GABAergic interneurons of the rodent mPFC.....	13
<i>Parvalbumin (PV) neurons</i>	14
<i>Somatostatin (SOM) interneurons</i>	14
<i>Vasoactive Intestinal Peptide (VIP) interneurons</i>	15
Functions of the rodent mPFC	15
Executive functions.....	15
How does the mPFC regulate <i>food intake and eating behavior</i> ?.....	19
Animal models for the study of eating pathology.....	23
Studying <i>binge eating</i> as a proxy for EDs	24
Binge eating prone (BEP)/binge eating resistant (BER) animal model.....	25
Concluding Remarks	27
Summary of dissertation experiments.....	28
Chapter 1	30
Differential Mesocorticolimbic Responses to Palatable Food in Binge Eating Prone and Binge Eating Resistant Female Rats	30
Introduction.....	30
Methods	32
Animals	32
Feeding Tests and BEP/BER Classification	33
<i>Acclimation</i>	33
<i>Feeding Tests</i>	33
<i>BEP/BER Classification</i>	34
Induction of c-Fos and Quantification of Fos-Immunoreactivity (Fos-ir).....	35
<i>Induction of c-Fos Expression</i>	35
<i>Immunohistochemistry for Fos-ir</i>	36
<i>Quantification of Fos-ir in the Mesocorticolimbic Circuit</i>	37

Statistical Analyses	39
<i>Preliminary Analyses of Feeding Test Data</i>	39
<i>Fos-ir in the NA and mPFC</i>	39
Results.....	41
Preliminary Analyses of Feeding Test Data.....	41
Fos Expression in the NA and mPFC	41
Discussion.....	44
Potential mechanisms explaining higher mesocorticolimbic responsiveness to PF in BEPs vs. BERs	49
Greater mesocorticolimbic responsiveness to food and food-related stimuli in human eating disorders	50
Limitations to the current study	50
Conclusions.....	52
 Chapter 2.....	 54
Activation of excitatory and inhibitory neurons in the mPFC following palatable food exposure in binge eating prone and binge eating resistant female rats	54
Introduction.....	54
Methods	57
Animals and Housing.....	57
Feeding Test Paradigm.....	57
Identifying BEP and BER Female Rats	58
Induction of Fos expression by PF exposure	59
Single and Double Label Fos Immunohistochemistry (IHC)	60
<i>Single label Fos IHC</i>	60
<i>Double Label Fos-Satb2 Immunofluorescence</i>	61
<i>Double Label Fos-PV, Fos-SOM, Fos-VIP IHC</i>	62
Quantification of Fos-expressing excitatory and inhibitory neurons in the mPFC.....	63
<i>Stereological estimates of single label Fos-immunoreactive (Fos-ir) Cell Number</i>	63
<i>Quantification of Fos-Satb2 Immunofluorescence</i>	63
<i>Quantification of Double-Label Fos-PV, Fos-SOM, Fos-VIP IHC</i>	64
Statistical Analyses	65
<i>Behavioral differences between BEPs and BERs</i>	65
<i>Single label Fos IHC</i>	65
<i>Double label Fos IHC</i>	66
Results.....	66
Behavioral differences between BEPs and BERs across the feeding test period	66
Neural Responsiveness to PF in the mPFC.....	68
Excitatory neuron responsiveness to PF in the mPFC of BEPs and BERs	68
Inhibitory neuron responsiveness to PF in the mPFC of BEPs and BERs	71
Discussion.....	72
PF elicits neural activation in the mPFC, but overall mPFC responsiveness to PF does not differ between BEPs and BERs	76
Reduced excitatory neuron responsiveness to PF may be associated with binge eating proneness.....	78
Inhibitory neuron responsiveness to PF does not differ as a function of binge phenotype	81

Individual sub-types of inhibitory neurons differ in the magnitude of their responsiveness to PF	84
Conclusion	85
Chapter 3	87
Enhanced palatable food consumption following GABA-mediated inhibition of the medial prefrontal cortex in binge eating prone and binge eating resistant female rats	87
Introduction	87
Methods	90
Animals and Housing	90
Feeding Tests for Identifying BEP and BER Rats	90
Classifying rats as BEP or BER	91
Stereotaxic Surgical Procedures	92
Intra-mPFC Infusions of Muscimol	93
Analysis of Feeding, Locomotor, and Grooming Behavior	94
Verification of cannula placement and muscimol infusions within the mPFC	96
Statistical Analyses	97
<i>Behavioral differences between BEPs and BERs</i>	97
<i>PF and chow intake following GABA-mediated inhibition of the mPFC</i>	97
<i>Feeding, locomotor, and grooming behavior following GABA-mediated inhibition of the mPFC</i>	98
Results	99
BEPs consume significantly more PF than BERs during feeding tests	99
GABA-mediated inhibition of the mPFC increases PF, but not chow, intake in BEP and BER rats	99
GABA-mediated inhibition of the mPFC alters the structure of feeding on PF in BEPs and BERs	106
GABA-mediated inhibition of the mPFC reduces locomotor and grooming behavior	106
Cannula targets and muscimol-induced Fos expression in the mPFC	108
Discussion	111
The mPFC serves as a behavioral limit over PF intake in female rats	111
The magnitude of mPFC-mediated control over PF intake is slightly weaker in BEPs vs. BERs	113
Behavioral mechanisms underlying muscimol-induced increase in PF intake and differences in PF intake between BEPs and BERs	114
Conclusions	116
Conclusions	118
The mPFC in the context of sex differences in binge eating proneness and the onset of binge eating proneness during puberty	121
Implications for EDs in women	123
REFERENCES	126

LIST OF TABLES

Table 1.1)	Diagnostic criteria for the major sub-types of EDs	2
Table 1.2)	Medical complications associated with AN, BN, BED	4
Table 1.3)	Differences in PF intake, chow intake, and body weights between BEPs and BERs, <u>CH 1</u>	42
Table 1.4)	Fos expression in the mPFC and NA of BEP rats exposed to PF and No PF control rats, <u>CH 1</u>	46
Table 1.5)	Fos expression in the mPFC and NA of BEP and BER rats exposed to PF, <u>CH 1</u>	48
Table 2.1)	Proportions of BEP and BER rats identified in cohorts 1 and 2, <u>CH 2</u>	58
Table 2.2)	PF and chow intake and body weights in BEPs and BERs, <u>CH 2</u>	67
Table 2.3)	Single Fos expression in No PF control rats and BEP and BER rats exposed to PF	70
Table 2.4)	Proportions of Fos+ neurons co-localized with excitatory and inhibitory markers in the mPFC of BEP and BER rats	73
Table 2.5)	Total number of Fos+ neurons co-localized with excitatory neuron marker Satb2 in the mPFC of BEP and BER rats	75
Table 2.6)	Total number of Fos+ neurons co-localized with inhibitory neuron markers PV, SOM, or VIP in the mPFC of BEP and BER rats.....	82
Table 2.7)	Proportions of PV, SOM, and VIP+ neurons expressing Fos in response to PF intake in the mPFC of BEP and BER rats	83
Table 3.1)	Proportions of BEPs and BERs identified in cohorts 1, 2, and 3 <u>CH 3</u>	91
Table 3.2)	PF and chow intake and body weights in BEPs and BERs, <u>CH 3</u>	100
Table 3.3a)	Increase in 1 and 4hr PF intake following GABA-mediated inhibition of the mPFC	103
Table 3.3b)	Percent change in 1 and 4hr PF intake following GABA-mediated inhibition of the mPFC	104

Table 3.3c)	No change in 1, 4, or 24hr chow intake following GABA-mediated inhibition of the mPFC	105
--------------------	---	-----

LIST OF FIGURES

Figure 1.1)	The mPFC-mediated behavioral “brake” over excessive food intake in rodents	22
Figure 1.2)	Regions of interest and representative Fos images from the mPFC and NA, <u>CH 1</u>	38
Figure 1.3)	PF intake, chow intake, and body weights across the feeding test paradigm in BEPs and BERs, <u>CH 1</u>	43
Figure 1.4)	Fos expression within the mPFC and NA of No PF control rats, BEPs exposed to PF, and BERs exposed to PF, <u>CH 1</u>	47
Figure 2.1)	Single Fos expression in the CG, PL, and IL cortex of No PF control rats, BEPs, and BERs, <u>CH 2</u>	69
Figure 2.2)	Proportions of Fos-expressing excitatory and inhibitory neurons within the mPFC of BEP and BER rats	74
Figure 2.3)	Number of activated excitatory neurons in the mPFC of BEP and BER rats.....	77
Figure 2.4)	Proportions and total numbers of activated inhibitory neurons in the mPFC of BEP and BER rats	80
Figure 3.1)	Initial pilot studies confirm that GABA-mediated inhibition of the mPFC leads to a significant increase in PF intake	95
Figure 3.2)	PF and chow intake in BEPs and BERs following GABA-mediated inhibition of the mPFC	102
Figure 3.3)	GABA-mediated inhibition of the mPFC alters the structure of PF consumption in BEP and BER rats	107
Figure 3.4)	GABA-mediated inhibition of the mPFC alters rearing and grooming behavior in BEP and BER rats.....	109
Figure 3.5)	Cannula hit sites in the mPFC and Fos expression following pre-sacrifice infusion of muscimol within the mPFC of BEPs and BERs	110

KEY TO ABBREVIATIONS

Eating Disorder	ED
Palatable food	PF
Anorexia nervosa	AN
Bulimia nervosa	BN
Binge eating disorder	BED
Functional magnetic resonance imaging	fMRI
Prefrontal cortex	PFC
Medial prefrontal cortex	mPFC
Cingulate sub-region of the mPFC	CG
Prelimbic sub-region of the mPFC	PL
Infralimbic sub-region of the mPFC	IL
Special AT-rich sequence binding protein 2	Satb2
Parvalbumin	PV
Somatostatin	SOM
Vasoactive intestinal peptide	VIP
Binge eating resistant (rat)	BER
Binge eating prone (rat)	BEP
Analysis of variance	ANOVA
Analysis of covariance	ANCOVA
Standard error of the mean	S.E.M
Nucleus accumbens core	NAC
Nucleus accumbens shell	NAS

Introduction

Eating Disorders in Women

Eating disorders, including anorexia nervosa (AN), bulimia nervosa (BN), and binge eating disorder (BED, see **Table 1.1** for diagnostic criteria) represent a major public health concern, affecting up to 30 million individuals each year [1]. Up to 2/3rd of the affected individuals are women, and the female: male ratio is reported to be as high as 10:1, making the sex difference in eating disorder (ED) risk *the largest* in all of psychiatry [2, 3]. Prevalence rates for EDs are on par with several other major psychiatric disorders [4], but the severity of medical and psychiatric co-morbidities inherent to EDs is far worse than most other conditions in psychiatry. The rate of suicide among sufferers of EDs, owing to psychiatric co-morbidities such as depression and substance use, is one of the highest in all of psychiatry, and the mortality rate, owing to the degree of medical complications inherent to EDs (See **Table 1.2** for summary), is *the highest* in all of psychiatry [5-12].

Despite the severity of the medical and psychiatric complications associated with having an ED, research in the field of EDs still lacks a clear understanding of the specific *biological underpinnings* inherent to ED psychopathology, particularly in women. To date, current research in the field has focused on psychosocial variables, such as personality traits (i.e., obsessiveness, harm avoidance), and eating/weight-related concerns (i.e., history of dieting, drive for thinness), that underlie ED risk and eating pathology [13, 14]. Yet emerging evidence suggests that biological variables (i.e., estradiol and progesterone, HPG axis activation at puberty, genetic variables [15-17]) and disruptions within central serotonergic and dopaminergic signaling pathways [18] may be of equal importance to the development, maintenance, and

Table 1.1) Diagnostic criteria for the major sub-types of EDs

DSM-5 criteria for full and sub-threshold eating disorders ¹			
ED sub-type	Diagnostic Criteria	Behavior frequency & Illness duration	Measure of Severity
Anorexia nervosa (AN) <i>Restricting type</i>	Significantly low body weight given age, sex, developmental stage		
	Intense fear of weight gain, despite low body weight		
	Disturbance in experience of one's weight or shape	3 months	BMI
	Weight loss achieved by <u>dieting</u> , <u>fasting</u> , <u>excessive exercise</u>		
Anorexia nervosa <i>Binge-purge type</i>	Same criteria as restricting type except weight loss achieved by <u>recurrent bingeing and purging</u>	3 months in duration	BMI
Bulimia nervosa (BN)	Recurrent episodes of binge eating		
	Recurrent compensatory behaviors to prevent weight gain (vomiting, laxatives, fasting, excessive exercise)	≥1 binge-purge/week	# of episodes of compensatory behaviors per week
		3 months in duration	
	Perception of self influenced by weight and shape		

Table 1.1 (cont'd)

Binge eating disorder (BED)	Recurrent episodes of binge eating with marked distress during binge eating	≥ 1 binge/week	# of binge episodes per week
	Lack of compensatory behaviors following a binge	3 months in duration	
Atypical AN	AN behavior but body weight is within the normal range	---	---
BN of low frequency or duration	BN criteria but binge-purge	---	---
	cycles occur less than once per week or for less than 3 months		
BED of low frequency or duration	BED criteria but binge eating disorder but binge episodes occur less than once per week or for less than 3 months	---	---

[†] Table adapted from the Diagnostic and Statistical Manual of Mental Disorders, Fifth Edition

Table 1.2) Medical complications associated with AN, BN, BED

Common medical complications associated with AN, BN, and BED ¹			
<i>Organ System</i>	<i>Anorexia</i>	<i>Bulimia</i>	<i>Binge Eating Disorder</i>
Dermatologic & Orofacial	Parotid enlargement Cheilosis of oral mucosa Dry skin Hair loss	Parotid enlargement Dental caries Enamel erosion	
Cardiovascular	Bradycardia Long QT interval on EKG Hypotension Cardiomyopathy Atrial and ventricular arrhythmias Decreased left ventricular mass	Cardiomyopathy (ipecac poisoning)	
Gastrointestinal	Constipation Rectal prolapse Delayed gastric emptying	Esophagitis Hematemesis Esophageal tears Constipation Rectal prolapse Delayed gastric emptying	
Endocrine & Metabolic	Amenorrhea Infertility Osteoporosis Delayed growth Low testosterone (males) Hyponatremia Hypokalemia Hypomagnesemia Hypoglycemia Hypercortisolism	Irregular menstruation Hypokalemia Hypomagnesemia	Obesity Metabolic syndrome

Table 1.2 (cont'd)

Neurologic	Peripheral neuropathy Cortical atrophy Ventricular enlargement
Hematologic	Leukopenia Anemia Neutropenia Thrombocytopenia

¹ Table adapted from Becker, A.E. et. al., NEJM, 1999 & Herzog, D.B. and P.M. Copeland, NEJM, 1985

exacerbation of EDs. To that end, several recent lines of work have successfully utilized neuroimaging techniques (i.e., functional MRI techniques) to specifically identify and localize neural circuit dysfunction in women with EDs.

Neural Circuit Dysfunction in Eating Disorders in Humans

Initial studies investigating the neurobiological variables inherent to EDs came from decades of work by Walter Kaye and colleagues, which demonstrated a significant link between abnormalities in select neurotransmitter systems, most notably serotonin and dopamine, and ED psychopathology [19, 20]. This pioneering work was among the first to identify that core neurobiological deficits, rather than purely psychosocial variables, were critical to the psychopathology of EDs [18, 21]. More recently, the field of ED research in humans has largely expanded upon this work by using functional MRI (fMRI) imaging techniques in an attempt to identify dysfunctional neural activity within neural circuits that are critical to food intake, food reward, and behavioral control mechanisms in individuals with EDs. The use of fMRI in individuals with EDs has revealed promising avenues for future exploration, as they have

consistently demonstrated aberrant patterns of neural activation in women with EDs during reward processing tasks, in response to food or food-related stimuli, or during cognitive tasks that engage behavioral control mechanisms. As such, neuroimaging studies in women with EDs have identified critical “hot spots” of apparently dysfunctional neural activity, suggesting that the spectrum of pathological eating behaviors inherent to EDs likely stems from altered function within cortical and limbic circuitry.

Abnormal reward processing as a cause for EDs

Abnormal reward processing, as a pre-existing trait characteristic in women that develop EDs, makes intuitive sense, as the ability to regulate when and how much to eat is partially driven by the anticipated and experienced reward associated with eating. In general, women with all sub-types of EDs display some degree of altered reward sensitivity; findings have been mixed for AN (some display high reward sensitivity while others show the opposite [22]), but most women with BN, for example, appear to have greater sensitivity to reward as compared to healthy controls [23]. Altered reward sensitivity in women with EDs may stem from underlying deficits in the basic ability to process reward, specifically within cortical and/or limbic circuitry. In support of this hypothesis, women with or remitted from AN, BN, or BED tend to show aberrant cortical and limbic neural responsiveness to both basic rewards (i.e., monetary gains) and food rewards. For example, women remitted from AN and BN appear to be deficient in differentiating high vs. low reward states, using *monetary rewards*, within the ventral striatum: on a monetary reward task, healthy women display higher ventral striatal activity during monetary “wins” vs. “losses”, but women remitted from AN or BN fail to do so [24, 25]. Food rewards, on the other hand, tend to elicit a range of neural activation patterns in limbic and cortical circuitry, depending on the specific sub-type of ED. Repeated tastes of sucrose elicit

significantly lower insular activation in women remitted from AN but *significantly higher* insular activation in women remitted from BN as compared to healthy controls [26, 27]. In addition, binge eating scores in individuals with high BMI (i.e., BMI > 25) positively correlate with the magnitude of neural activation in the medial frontal gyrus and anterior cingulate cortex in response to palatable taste cues (i.e., chocolate milk, cream soda) [28], while images of highly palatable foods elicit stronger orbitofrontal cortex and anterior cingulate cortex activity in women with AN, BN, and BED as compared to healthy controls [29, 30].

Deficient, prefrontal cortex-mediated behavioral regulation as a cause for EDs

Neuroimaging studies investigating reward processing in EDs provide a compelling argument for reward circuit dysfunction as an underlying risk factor for ED development, but they do not fully explain eating pathology. For example, **hypo**-responsiveness to reward could prevent women with AN from being motivated to eat [24], but how can they continue to persistently avoid food despite being in a chronic state of starvation [31]. In addition, though **hyper**-responsiveness to reward may make women with BN, BED, or generalized binge eating more motivated to seek and eat food [32], what allows them to continue eating beyond the point of being uncomfortably full.

While reward dysfunction may contribute to ED psychopathology, an alternative explanation for the spectrum of eating pathology in EDs is that underlying deficits in *basic behavioral regulation* contribute more strongly to ED psychopathology. That is, neural circuits that subserve executive functions, such as behavioral inhibition, planning, and action selection, may be relatively deficient in controlling when to eat, what to eat, and when to stop eating in women with EDs. In a sense, the basic premise that disturbances in behavioral regulation contribute to ED risk strongly aligns with several of the core trait characteristics that exist in

women with EDs, even across the full spectrum of ED sub-types. While women with AN exhibit obsessive-compulsive personality traits [18], perfectionism [14], harm avoidance [14], and impaired behavioral flexibility [18, 33], women with BN, BED or who binge eat have enhanced impulsivity [34], deficient executive control [35], greater risk for co-morbid substance abuse and borderline personality disorder [36, 37], and high negative urgency (i.e., acting impulsively in response to distress) [38]. Basic behavioral regulation is a critical function of the prefrontal cortex (PFC), so aberrant PFC activity during tasks that engage behavioral control mechanisms would support the hypothesis that dysfunctional activity within circuitry that mediates behavioral regulation may contribute to the clear abnormalities *in the regulation of food intake* inherent to EDs.

Indeed, dysfunctional activation within PFC-circuitry has been consistently found in women with EDs, most often during neurocognitive tasks that engage behavioral control mechanisms, including self-regulation (Simon Spatial incompatibility task), response inhibition (Go-NoGo, Stroop-word color interference), or behavioral flexibility. Assessing PFC function during neurocognitive tasks does not directly relate to food intake and eating pathology *per se*, but food consumption certainly requires that one regulates their eating behavior, so the neural constructs that are engaged in response to neurocognitive demands are also likely to be activated during food consumption. As such, PFC dysfunction during neurocognitive tasks of behavioral regulation would be expected to occur during food intake as well.

Reports in women with BN, BED, or generalized binge eating, in particular, provide compelling support for the notion that disturbances in behavioral regulation are strongly associated with EDs on the binge-eating “side” of the ED spectrum. Specifically, women with EDs associated with binge eating consistently demonstrate *diminished PFC activation* during

tasks where behavioral regulation and inhibition are required [39]. During correct responding on the Simon Spatial Incompatibility Task (assessing self-regulatory control) both inferolateral and anterior cingulate cortex activity is lower in women and adolescent girls with BN as compared to healthy controls [40, 41]. The severity of bulimic pathology also negatively correlates with the magnitude of inferior frontal gyrus engagement during task performance, indicating that the lower the engagement of PFC circuitry, specifically in situations where behavioral regulation is required (i.e., food exposure), the worse the bulimic pathology [40]. During the Stroop color-word interference task, ventromedial prefrontal cortex activation is also lower in women with BED than in lean controls or obese women without BED [42]. Scores of restraint eating (a maladaptive dieting behavior that contributes to binge eating) also negatively correlate with the magnitude of activation of inferior frontal and ventromedial PFC sub-regions during Stroop task performance, suggesting that weaker PFC-mediated behavioral inhibition may underlie poor regulation over food intake in women with BED [42]. Finally, individuals with BED demonstrate poor performance on a flexible, decision-making task, as they exhibit less directed, less strategic decision-making as compared to their non-BED counterparts [43]. In the same study, ventrolateral prefrontal cortex activity was also diminished in individuals with BED during exploratory choice behavior on the task, suggesting sub-optimal functioning of PFC circuitry during goal-directed action [43]. Combined, these data strongly suggest that the inability for women with binge eating-related EDs to control the initiation and cessation of cycles of binge eating and/or purging may stem from deficiencies in basic, PFC-mediated behavioral regulation.

In summary, neuroimaging studies in women with EDs have significantly advanced the field of ED research by localizing the neural circuits that appear to be abnormally responsive to

stimuli or behavioral tasks that are relevant to eating pathology. Aberrant activity within PFC circuitry, during tasks that require behavioral regulation, has been a consistent finding and has presented a clear avenue for future exploration. Moreover, the presence of deficient PFC engagement during cognitive tasks aligns quite well with the core personality traits that are so common to women with AN and to women with BN, BED, or generalized binge eating. Yet one question that remains is whether or not the PFC even regulates normative eating behavior. PFC circuitry is certainly “online” during basic cognitive tasks of self-regulation or response inhibition, but does this extend to the regulation of food intake as well? Ultimately, developing an understanding of how the PFC inherently regulates food intake is essential for identifying whether the abnormal patterns of PFC activity in women with EDs is indeed a core neural mechanism inherent to eating pathology.

The rodent medial prefrontal cortex (mPFC): A good model for studying cortical regulation of eating behavior

Neuroimaging studies are probably the closest we can get to identifying where true neural circuit dysfunction lies in women with EDs. Yet, one caveat to neuroimaging studies in humans is that they are largely correlational, so they lack mechanistic insight and can be subject to a high degree of subjective reasoning and interpretation. To overcome these inconsistencies and shortcomings, assessing cortical function in the context of food intake and eating pathology in *animal models* is of great value. Studying the rodent PFC also affords the unique opportunity to identify the specific cellular and hormonal players, the neural circuits, and the neurotransmitter systems that drive or inhibit food intake. In addition, the rodent PFC is functionally similar to the human PFC, so studying the rodent PFC has high translational potential. That is, what we

glean from the rodent PFC in the context of food intake and eating pathology likely holds true for eating behaviors in humans as well.

Homology between the rodent mPFC and the human PFC

The rodent mPFC is a laminated structure composed of six distinct cell layers and three sub-regions, the cingulate cortex (CG), the prelimbic cortex (PL), and the infralimbic cortex (IL). Anatomical homology exists between the rodent mPFC and both the dorsal anterior cingulate cortex (dACC) and ventromedial prefrontal cortex (vmPFC) of the human PFC: the dorsal half of the rodent mPFC (i.e., the CG and the dorsal PL) is analogous to the human dACC (Brodmann area 32) while the ventral half of the rodent mPFC (i.e., the ventral PL and IL) is analogous to the pregenual (Brodmann area 33) and subgenual (Brodmann area 25) sub-divisions of the human vmPFC [44]. Anatomical homology between the dACC and the vmPFC with the rodent CG, PL, and IL is primarily based on the *functional homology* between the PFC sub-regions in the specific context of fear learning [44]. In rodents, the PL cortex of the dorsal mPFC, in particular, activates fear expression during fear conditioning paradigms while the IL cortex of the ventral mPFC supports fear suppression [44]. Similarly, data from human neuroimaging studies strongly suggest that the dACC supports fear expression while the vmPFC facilitates fear suppression during fear learning [44]. Specifically, neural activity within the dACC increases during shock delivery in healthy individuals [45], while activation within the vmPFC significantly correlates with extinction learning [46], and the vmPFC exerts inhibitory control over amygdala-mediated fear expression [47].

Connectivity of the rodent mPFC

The dorsal CG sub-region and the ventral PL and IL sub-regions of the rodent mPFC, though part of the same global structure of the mPFC, are functionally distinct, in the context of

basic behavioral regulation: CG cortex is more strongly associated with motor, sensory, and attentional functions, while PL and IL cortices sub-serve visceral, autonomic, and limbic processing and the integration of physiological states and environmental cues for the guidance of behavior [48] (see **“Functions of the rodent mPFC: Executive functions”** for details). The distinct connectivity of CG, PL, and IL with various cortical and sub-cortical targets helps to explain the functional diversity of the dorsal vs. ventral mPFC. Glutamatergic input to the CG is primarily limited to contralateral mPFC (e.g. CG and PL) and thalamus, but PL and IL receive dense glutamatergic input not only from contralateral mPFC (e.g., CG, PL and IL) and thalamus, but also limbic cortical regions, including medial and lateral orbitofrontal cortex and dorsal and ventral hippocampus, and both the basolateral and basomedial amygdala [48]. In addition, glutamatergic projections from CG cortex primarily target the contralateral mPFC, thalamus, dorsal striatum, and lateral hypothalamus, while projection targets of PL and IL cortex include the contralateral mPFC, medial orbitofrontal cortex, thalamus, dorsal striatum ventral striatum, lateral hypothalamus, and basolateral amygdala [49, 50]. Combined, CG, PL, and IL also receive dense dopaminergic input from the ventral tegmental area, which controls select executive functions [51], reward learning [52, 53], goal-directed behavior [54, 55], and food reward [56], as well as serotonergic input from dorsal raphe, which regulates not only mood and anxiety, but also attention and impulsivity [57-59].

Excitatory, glutamatergic projection neurons of the mPFC

Excitatory projection neurons, or pyramidal cells, are glutamatergic projection neurons that comprise up to 80-90% of the total neuronal pool within the mPFC, and function as the major cellular drivers of the behaviors sub-served by the mPFC [44]. Pyramidal cells are comprised of a pyramid-shaped cell body, one apical dendrite, several basal dendritic trees, and a

single, long-projecting axon that extends to the cortical and sub-cortical targets described above [60]. Pyramidal cells are housed in layers II-VI of the laminated mPFC: pyramidal cells within layers II-III are enriched in cortico-cortical projections, while layers V and VI primarily house pyramidal cells that project to sub-cortical targets [44]. Pyramidal cell dendrites house NMDA, AMPA and metabotropic glutamate receptors for glutamatergic input, D1-like and D2-like dopamine receptors for dopaminergic input, primarily 5-HT_{1A} and 5-HT_{2A} receptors for serotonergic input, alpha and beta adrenergic receptors for norepinephrine input from the locus coeruleus, and muscarinic cholinergic receptors for cholinergic input from the basal forebrain [57]. In addition, at least three different types of inhibitory, GABAergic interneurons within the mPFC (described in more detail below) provide the essential inhibitory control over intrinsic excitability within the mPFC. GABA_A (ionotropic) receptors are located on the pyramidal cell soma, axon initial segment, and proximal and distal dendrites while GABA_B (metabotropic) receptors located at pre-synaptic terminals serve as autoreceptors for the regulation of GABA uptake and release [61].

Inhibitory, GABAergic interneurons of the rodent mPFC

The inhibitory, GABAergic interneurons of the rodent mPFC regulate pyramidal neuron excitability, the magnitude of both afferent and efferent neural activity within the mPFC, and the critical balance between excitation and inhibition within the mPFC [62]. Inhibitory neurons comprise 10-20% of the total neuronal pool in the mPFC, but they are, nonetheless, crucial for optimal functioning of the mPFC [62, 63]. Inhibitory neurons are distinguished from one another based on their morphology, electrophysiological properties, cytoplasmic protein and/or neuropeptide expression, and their site of synaptic contact with the pyramidal cell [64, 65]. The three major, non-overlapping populations of inhibitory neurons in the mPFC include

parvalbumin- (PV), somatostatin- (SOM), and vasoactive intestinal peptide (VIP)-expressing neurons, and combined PV, SOM, and VIP interneurons comprise up to 90% of the total inhibitory neuron pool within the mPFC [64, 65].

Parvalbumin (PV) neurons

PV neurons are fast-spiking interneurons that synapse onto both the cell soma and the axon initial segment of pyramidal cells [65, 66]. PV neurons primarily serve to regulate the precise synchronization of pyramidal cell firing and gamma oscillations that mediate the basic attentional processing sub-served by the mPFC [66, 67]. Because they exert fast and continuous regulation of pyramidal cell activity and excitatory output, deficits in PV neuron activity induce significant disturbances in mPFC-mediated behaviors. Chemogenetic inhibition of PV neurons in the PL and IL cortex, for example, promotes the expression of helplessness behavior in mice, a depression-like behavioral phenotype [68], and functional silencing of PV neurons (i.e., by blocking GABA release from PV neurons), in the PL and IL cortex impairs performance on tasks of both working memory and behavioral flexibility [69].

Somatostatin (SOM) interneurons

SOM neurons are regular-spiking interneurons with long, ascending axons that extend into layer I of the mPFC, where they arborize extensively onto apical dendrites of pyramidal cells to modulate incoming excitatory input [61, 62, 70]. Because SOM neurons synapse onto both dendritic heads and spines of pyramidal cells, they have a purported role in regulating cortical plasticity during, for example, reward-related behavioral tasks [61]; SOM neuron firing rate has been shown to be up or down-regulated during reward-related tasks that require the expression of learned behavior. For example, SOM neuron firing rate in the CG cortex of mice is significantly suppressed when entering the reward-receipt zone of a reward foraging task [71],

while SOM neurons of the dorsal mPFC fire rapidly in response to the onset of reward licking in a Go/No-Go task in male mice [72].

Vasoactive Intestinal Peptide (VIP) interneurons

VIP neurons are distinct from both PV and SOM neurons in that they are mostly enriched in layers II and III of the mPFC and primarily target other interneurons, specifically SOM interneurons [62]. In this regard, VIP neurons specialize in **disinhibitory** control mechanisms by targeting and inhibiting SOM neurons in the cortex and, consequently, releasing inhibition from pyramidal cells [73, 74]. A noteworthy, distinguishing feature of VIP neurons is that they are virtually the only cell type in the mPFC to express the mu opioid receptor [75], which is particularly relevant to eating behaviors: infusion of a mu opioid receptor agonist into the mPFC enhances food intake and food reward in male rats [76-78].

Functions of the rodent mPFC

Executive functions

Similar to the human frontal cortex, the rodent mPFC subserves several core executive functions, including working memory, attention, decision making and action selection [79]. Several behavioral tasks in rodents have been designed to probe select executive functions, and combining such tasks in tandem with lesion or pharmacological inactivation studies of the mPFC has revealed the mechanisms by which each sub-region of the mPFC contributes to rodent executive function.

In general, the CG cortex (i.e., the dorsal mPFC) appears to be primarily involved in attention and cognitive flexibility as well as “ambition” driven behavioral performance. The attention-mediated functions of the CG cortex are quite in line with the distinct connectivity (*see*

pg.8) of the CG cortex described earlier. The contribution of the CG cortex to a rodent's attentional capacity has been demonstrated through the use of both the 5-choice task and set-shifting tasks in rodent models [79], while the role of the CG cortex in ambition-like behavior has been demonstrated in derivations of impulsive choice tasks [80, 81]. In the 5-choice task, animals must tend to five different apertures in order to wait for a cue stimulus that signals reward delivery in one of the five apertures [79]. Lesioning the CG cortex exclusively reduces performance accuracy on the 5-choice task, reflecting an impaired ability for the animal to optimally attend to stimulus presentation during task performance [82, 83]. In set-shifting tasks, on the other hand, animals must first learn that one of two different types of stimuli (i.e., odor of a food bowl vs. digging media of a food bowl) indicates food reward receipt (achieved via digging in one of the two food bowls), and then must learn when a stimulus that initially indicated reward no longer does so [84, 85]. As such, set-shifting tasks engage both attention and cognitive flexibility in rodents. Lesioning the CG cortex exclusively impairs intradimensional set shifting, that is, switching from digging for a food reward in a vanilla-scented bowl, for example, to digging in a cinnamon scented bowl [85]. In this regard, the CG cortex also facilitates cognitive flexibility in rodents, allowing them to increase their attention to relevant stimuli, while simultaneously decreasing their attention to irrelevant stimuli, for the purpose of optimizing positive outcomes. Finally, in a modified version of an impulsive choice task, rodents must choose between a T-maze arm that delivers a small, but “easy to get”, food reward and an arm that provides a larger food reward but at a cost: rodents must climb over a physical wall to obtain the reward [86]. At baseline, rodents consistently choose the larger but more effortful reward (i.e., ~8/10 high-reward arm choices), but lesioning the CG cortex causes a significant shift in preference: CG-lesioned rats consistently choose the smaller but less difficult

reward option (i.e., ~2/10 high-reward arm choices) [86]. As such, the CG cortex appears to guide effort-based decision-making (e.g., ambition) in a decision-making task that is predictive of high reward states.

Executive functions of the *ventral* mPFC (i.e. PL and IL), on the other hand, appear to be more selective for behavioral inhibition, and action selection, consistent with its more robust connectivity with limbic cortical and sub-cortical brain regions (*see pg. 8*). For example, while the 5-choice task mostly measures attention, it is also quite sensitive to two other aspects of behavioral inhibition: impulsivity and compulsivity [79]. Premature responding, or responding in an aperture before stimulus presentation, reflects impulsivity, while perseverative responding, or continued responding after reward receipt, reflects compulsivity [87]. Indeed, excitotoxic lesions of the PL or IL [82, 83, 88], or pharmacological inactivation of the PL or IL [87, 89, 90], lead to an increase in both impulsive and compulsive responding during 5-choice task performance, while sparing the attentional capacity of the rodent.

The PL and IL also regulate the expression of goal-directed vs. habitual responding (i.e., action selection), which is commonly tested through the combined use of instrumental response paradigms with reward devaluation protocols [54]. Specifically, after devaluing a reinforcer (i.e., by inducing food-specific satiety or by pairing the reinforcer with lithium chloride), instrumental performance for that particular reinforcer declines, suggesting that instrumental performance is driven by the *value* of the reinforcer: animals are driven to respond for a particular outcome only when it maintains its value [54]. The PL cortex, specifically, drives the expression of goal-directed behaviors: lesioning the PL cortex renders animals insensitive to reinforcer devaluation [91, 92], so activity within the PL cortex is needed to associate inherent value with a particular reinforcer. On the other hand, the IL cortex drives the expression of

habitual behaviors, which is displayed on reward devaluation tasks after extensive over-training; animals adopt stimulus-response behavior following over-training and, consequently, become insensitive to reward devaluation [54]. Following pharmacological inactivation of the IL cortex, however, over-trained rats become sensitive to devaluation, and revert back to the expression of goal-directed responding rather than the expected habitual response mechanism [93, 94]. Ultimately, these data, combined, suggest that the PL and IL cortex modulate action selection (i.e., food seeking and intake) based on the value of a goal state (i.e., when hungry vs. when full), and, thus, guide behavioral performance to maximize positive and minimize negative outcomes [79].

Neurocognitive tasks and instrumental responding paradigms in rodents seem far-removed from ED psychopathology, so how are these behavioral constructs relevant to EDs? Essentially, studying the cognitive functions of the mPFC in animal models proves that the rodent mPFC regulates several core neural constructs that are disrupted in women with EDs. The rodent mPFC facilitates behavioral flexibility while also suppressing impulsive and compulsive behavior, and women with EDs display behavioral rigidity [33], high compulsivity [33, 95], and high impulsivity [96]. Specifically, women with all sub-types of EDs have impaired set-shifting capabilities, generally reflecting both poor cognitive flexibility and high compulsivity [33]. Similarly, high impulsivity exists in women with virtually all sub-types of EDs, but most significantly in women on the binge-eating side of the ED spectrum [97]. Furthermore, goal-directed vs. habitual behavioral responding essentially defines the maladaptive eating behaviors displayed by women with EDs, particularly AN and BN [11, 31]. In the early stages of AN or BN, dieting, bingeing, and purging are mostly goal-directed [11], in that they yield rewarding outcomes, such as weight loss or relief from anxiety [18, 22, 98]. In

the later stages of the disease, dieting, bingeing, and purging become habitual in nature, in that they are no longer goal-directed or reinforcing, and, consequently, are quite difficult to modify [11]. Thus, data in support of the cognitive functions of the rodent mPFC suggest that the rodent mPFC subserves several core executive functions that are disrupted in women with EDs, highlighting the translational potential of rodent models for studying the mPFC in the context of eating pathology.

How does the mPFC regulate *food intake and eating behavior*?

Extensive literature suggests that the mPFC supports behavioral inhibition, controls compulsivity and impulsivity, and guides decision-making and action selection. However, the function of the mPFC in the context of food intake and food reward has remained rather understudied, despite the fact that altered mPFC-mediated regulation of behavior is one of the more consistent themes in the field of ED neuroimaging in humans. Specifically, disturbances in the core behavioral constructs of self-regulation and response inhibition likely extend to the regulation of food intake as well. The lab of Pietro Cottone, for example, has shown that high trait impulsivity and compulsivity correlate with the magnitude of binge-like consumption of PFs in rodent models, which directly addresses the point above: disruptions in core executive functions of the mPFC can also manifest as eating pathology [99, 100]. Specifically, Velazquez-Sanchez and colleagues revealed that rats with high trait impulsivity (i.e., based on differential reinforcement of low rates of responding task performance) displayed more compulsive-like intake of PF and escalated their intake of intermittently presented PF more significantly than their low trait impulsivity counterparts [99]. The inherent ability for the mPFC to exert “executive” control over food intake is also reflected in its anatomical connectivity: two of the major downstream projection targets of the mPFC, the nucleus accumbens and the lateral

hypothalamus, provide some of the strongest “go” signals in favor of food intake [101, 102]. Thus, a deficit in the ability for the mPFC to exert top-down control over the motivation for food, signaled by sub-cortical circuitry, would be expected to manifest as dysregulated (i.e., overly-restricted or uninhibited), pathological eating behaviors.

The mPFC responds to, processes, and has the capacity to direct food-seeking behavior. Subsets of neurons within the mPFC fire in response to different taste cues or reward ingestion, suggesting that the mPFC can encode consummatory reward [103, 104]. In addition, pharmacological inactivation of the PL cortex reduces responding on an active lever during a discrimination-stimulus task for sucrose delivery [105], and PL inactivation reduces food pellet seeking after presentation of a food-predictive cue [106]. Moreover, direct inactivation of the specific neuronal ensembles within the ventral mPFC that respond to the delivery of food rewards reduces lever responding for food reward self-administration [107]. Similarly, chemogenetic activation of pyramidal cells within the ventral mPFC enhances breakpoint ratios for food pellet reward delivery on a progressive ratio, operant responding task, suggesting that direct stimulation of the ventral mPFC is sufficient to enhance the expression of behaviors that are driven towards acquiring food rewards [108]. Such studies ultimately suggest that the mPFC maintains online, working representations of cues or stimuli associated with food rewards and can ultimately guide an animal to engage in seeking and consuming food rewards. Thus, the processing of food rewards certainly occurs at the level of the mPFC, but does the mPFC regulate the *consumption* of food?

Relatively few studies, to date, have directly examined how or whether the mPFC regulates food intake and feeding behavior. The microstructure of feeding behavior does appear to be regulated by the mPFC, as pharmacological inactivation of the PL cortex reduces the

number and duration of sucrose licking bouts [109], and inactivation of the ventral mPFC yields fewer but longer bouts of highly-palatable liquid ingestion [76, 110]. The effects of the mPFC on food intake are less clear, but, nevertheless, several lines of work suggest that the mPFC serves as a behavioral limit or “brake” over excessive food intake, especially palatable food intake. For example, pharmacological inactivation of the ventral mPFC leads to an increase in chow intake, highly-palatable liquid intake [76, 110], and high fat intake [111]. This apparent limit or behavioral “brake” over food intake subserved by the mPFC appears to be at least partially driven by its dense glutamatergic projections to the nucleus accumbens (**see Figure 1.1**). Specifically, infusion of an AMPA-type glutamate receptor antagonist into the nucleus accumbens shell induces a robust increase in chow intake, in non-food deprived rats [112, 113], while AMPA receptor activation within the nucleus accumbens shell significantly reduces chow intake, in food-deprived rats, as well as the consumption of a highly-palatable liquid solution [114]. Moreover, enhancing excitatory output from the IL cortex, via intra-IL infusions of a GABA-A receptor antagonist, *attenuates* the increase in chow intake that is elicited by AMPA-type glutamate receptor blockade within the accumbens shell [115]. Thus, the mPFC appears to exert tonic, top-down executive control over food intake by way of glutamatergic projections into limbic circuitry [112, 116].

Combined, these data suggest that the role of the mPFC, in the specific context of food intake, is generally *inhibitory* in nature, in that glutamatergic output from the mPFC likely serves as a behavioral limit over the consumption of food rewards. There are two notable limitations to the studies outlined above, however, that deserve comment and that are directly addressed within this dissertation. First, all studies, to date, assessing the role of the mPFC in the context of eating behavior have been performed in *male rats*. Studying the neural mechanisms

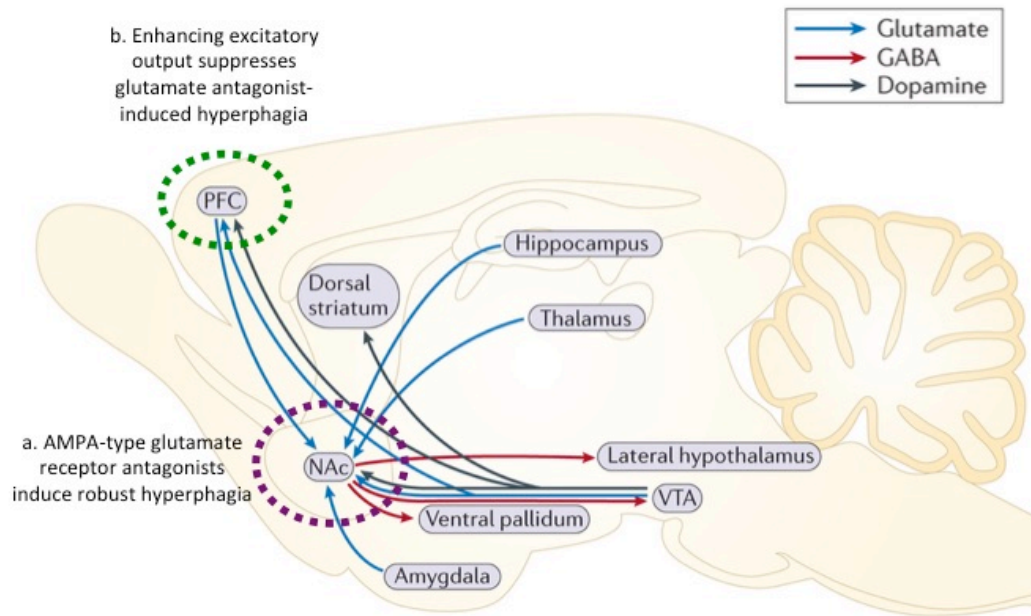


Figure 1.1) The mPFC-mediated behavioral “brake” over excessive food intake in rodents

The mPFC (green circle) sends dense glutamatergic projections (blue lines) to the NA core and shell (purple circle), where dopamine (black lines) and opioid transmission within NA core and shell drive the “wanting” and “liking” of food rewards, respectively. Infusion of an AMPA-type, glutamate receptor antagonist into the NA shell (a) elicits robust hyperphagia on both chow and sucrose solutions, but this hyperphagia is significantly attenuated if glutamatergic output from the mPFC is enhanced by co-infusing a GABA-A receptor antagonist into the mPFC (b). Thus, the mPFC can exert tonic, inhibitory control over excessive food intake through dense connectivity with accumbens circuitry. Figure adapted from Kourrich, S et. al., *Nat Reviews Neuroscience*, 2015.

that contribute to food intake have direct implications for pathological eating behavior inherent to EDs, so studying such mechanisms in the female sex is necessary, given that *women are significantly more likely than men to have an ED* [2, 117, 118]. Moreover, ovarian hormones have a very significant impact not only on food consumption in general [119], but also on the expression of pathological eating behaviors during adolescence [120] and adulthood [121], so studying the mechanisms by which the mPFC regulates eating behaviors *only in the male sex* seems counterintuitive. As such, investigating the role of the mPFC to food intake and eating pathology against the genetic, hormonal, and behavioral background of a female rodent is necessary.

Second, few of the studies assessing the mPFC in the context of food intake have used a clinically relevant animal model of disordered eating. As such, they identify the role of the mPFC to food intake, in general, but they do not identify whether a disturbance in or variations in the ability for the mPFC to regulate food intake is associated with the expression of specific pathological eating behaviors. Therefore, studying the role of the mPFC to food intake, specifically to *palatable* food intake, in female rats and in an animal model of disordered eating is warranted.

Animal models for the study of eating pathology

Because EDs are complex psychiatric disorders associated with a combination of genetic, biological, environmental, and psychosocial risk factors, it is difficult, if not impossible, to completely model every feature of an ED in animals. Nonetheless, core behavioral features and symptoms of EDs can be modeled, induced, or observed in animals. In addition, psychosocial risk factors, which are certainly important to ED psychopathology in humans, are absent in

animals, so animal models of disordered eating provide the key benefit of identifying the *isolated neurobiological* factors that contribute to EDs and that could be targeted therapeutically [122]. Similarly, experts in human ED research have suggested that studying the neurobiological basis of eating behaviors, at a more basic level, is crucial to our understanding of how normal eating turns into the abnormal, excessive, and persistent patterns of eating observed in individuals with EDs [123].

Studying *binge eating* as a proxy for EDs

Investigating the neurobiological mechanisms that contribute to *binge eating* has implications for virtually every sub-type of ED. Binge eating is defined as the consumption of an unusually large amount of food (often palatable food, high-fat/high-sugar) in a discrete period of time (i.e., < 2 hours) with a feeling of a lack of control over the binge episode [9, 124]. Binge eating, as a clinically-defined, maladaptive eating behavior cuts across all sub-types of EDs: it is a core diagnostic feature of the binge-purge subtype of AN, of BN, of BED, and of most sub-threshold types of EDs (see **Table 1**) [124]. Binge eating can also be readily observed or induced in animals by providing intermittent and limited exposure to highly-palatable foods (PFs), as the restricted schedule of access causes animals to escalate their consumption over time, yielding a binge-like phenotype [111, 125].

Several animal models of binge eating have been developed for the study of eating pathology. The lab of Bartley Hoebel designed a model of “sugar addiction” that uses 12hrs of food-deprivation followed by 12hrs of re-feeding with sucrose and chow [125, 126]. Similarly, a model developed by Mary Boggiano and colleagues exposes rats to a history of dieting and stress prior to PF exposure, to elicit higher levels of binge eating as compared to non-dieting/non-stressed rats [126, 127]. Finally, Rebecca Corwin and colleagues utilize a model of limited

access to PF, without associated food deprivation, where rats with intermittent PF access (i.e., a binge group) are compared to rats with daily access to PF (i.e., a non-binge, control group) [126, 128]. Each model of binge eating has clear strengths and translational potential for the human condition. The sugar addiction model highlights the similarities between food addiction and drug addiction: sugar bingeing rats display physical signs of withdrawal akin to drug dependence, and cross-sensitization to other drugs of abuse [129, 130]. Inducing a history of dieting and stress prior to a binge episode models key environmental variables that are known to precede a binge in women [14, 126]. Finally, the limited access model has identified changes to neurotransmitter systems within cortical and striatal brain regions of bingeing rats that are not present in non-bingeing rats [111, 128].

Binge eating prone (BEP)/binge eating resistant (BER) animal model

Despite the strengths and advantages inherent to the aforementioned models of binge eating, research within this dissertation utilizes an individual differences model of binge eating, namely the binge eating prone (BEP)/binge eating resistant (BER) rat model. One of the major strengths of the BEP/BER model rat model is that it takes advantage of natural, within-group variability in PF consumption: all rats are exposed to the same experimental condition (i.e., limited and intermittent PF exposure) but only a small percentage display the more extreme patterns of eating behavior that are classified as “prone” or “resistant” to binge eating. In this regard, the model closely mirrors the development of EDs in humans, in that PFs are relatively ubiquitous, but only some, presumably at-risk individuals develop an ED. All rats exposed to the feeding test paradigm also receive a “score” of binge eating that places them into either one of the two extremes of binge eating (BEP or BER) or somewhere along the continuum between these two extremes. As a consequence, the BEP/BER model reflects *the spectrum* of eating

pathology that exists within the human population [22, 131], which most closely describes eating pathology, in general, in women [22]. Another major advantage to the BEP/BER model is that animals are given limited, intermittent exposure to PF without any period of food deprivation throughout a feeding test paradigm. The use of food deprivation for the study of eating pathology can be advantageous, in that it models the cycles of bingeing and restricting that are assumed by women with the binge-purge type of AN and BN [124]. Yet, a major drawback to the inclusion of food deprivation in a model of binge eating is that it does not generalize to all EDs where binge eating is a core feature. Women with BED do not use compensatory measures to avoid weight gain after a binge and not all women with sub-threshold EDs engage in periods of fasting or restriction following a binge [124].

The BEP/BER model has strong face validity for the human condition, in that BEP and BER rats mirror key differences between binge eaters and non-binge eaters in humans. First, PF is presented intermittently throughout the week (3d/week) and for a limited period of time (4h/day), which models the typical time course and frequency of binge episodes in humans [124, 126]. Thereafter, BEPs and BERs are identified based on their individual patterns of PF consumption: consistently high PF intake identifies a BEP rat, while consistently low intake identifies a BER rat [132-134]. Across the feeding test period, BEPs do not consume more chow than do BERs, nor do they gain significantly more weight than BERs, suggesting that BEPs are prone to *binge eating*, rather than to generalized over-eating, and do not necessarily model obesity [135]. In addition, BEPs endure increasing levels of foot shock stress to obtain PFs, but BERs do not, suggesting that BEPs may also possess the core “loss of control” behavioral phenotype that clinically defines binge eating in humans [124, 136].

Finally, our lab has demonstrated that the influence of gonadal hormones on binge eating proneness in the BEP/BER model strongly reflects the clear role for gonadal hormones in eating pathology in the human condition. The striking sex difference in EDs is recapitulated in the BEP/BER model: female rats are significantly more likely to be identified as BEP than are male rats [134]. In addition, the core behavioral differences between BEP and BER rats emerges during mid-to-late puberty [16], similar to the dramatic onset of ED psychopathology during adolescence in girls [36]. Recent data from our lab has also demonstrated that peri-natal testosterone exposure in female rats protects against the development of binge eating proneness during puberty (Culbert, K.M., et. al., *in press*), which models the protective effects of peri-natal testosterone exposure in girls on the development of eating pathology during adolescence [137, 138]. Thus, as a whole, the key features of the BEP/BER model suggest that it is a well-validated model of binge eating with high translational potential that can extend to virtually every sub-type of ED. To that end, the BEP/BER model is ideal for specifically studying the role of the mPFC to the expression of eating pathology within the female sex.

Concluding Remarks

In conclusion, EDs are very severe psychiatric conditions that predominantly affect the female population, but the field of ED research still lacks a strong understanding of the specific neurobiological variables that contribute to the pathological eating behaviors inherent to EDs. Neuroimaging studies, however, have shed light on the neural substrates that likely underscore eating pathology in EDs. One of the more consistent findings from fMRI data in women with EDs is aberrant activity within PFC circuitry during tasks that engage behavioral control mechanisms, suggesting that disturbances in mPFC-mediated behavioral regulation, in the context of food intake, may be one mechanism that contributes to the expression of the

maladaptive, persistent, and excessive eating behaviors in women with EDs. To study whether the mPFC is at all related to eating pathology, rodent models are highly valuable tools, as the rodent mPFC subserves behavioral regulation much like the human PFC, and emerging evidence suggests that the rodent mPFC appears to regulate food and PF intake as well. However, no studies, to date, have investigated a specific role for the mPFC in the context of food intake in *female rats*, or in an *animal model of disordered eating*. To that end, the objective of this dissertation is to use a well-validated animal model of binge eating, to determine the functional role of the mPFC to binge eating proneness in the female sex.

Summary of dissertation experiments

Chapter 1: I first identified that neural responsiveness to PF differs between BEP and BER female rats, by quantifying PF-induced expression of the neural activation marker Fos in the mPFC. After identifying BEPs and BERs through a series of feeding tests, I exposed them to PF for one hour prior to sacrifice to induce Fos expression within the mPFC, and then I quantified the total number of Fos-immunoreactive cells in the CG, PL, and IL cortex of the mPFC in BEPs and BERs.

Chapter 2: In Chapter 2, I will identify the neuronal phenotypes of mPFC neurons that are responsive to PF (i.e., express Fos) in BEP and in BER female rats. Determining the proportions of all PF-activated neurons that are of the excitatory or inhibitory neuron phenotype will identify not only the major cell type that drives the mPFC response to PF, but also whether differences in the magnitude of excitatory and/or inhibitory neuron responsiveness to PF within the mPFC correlate with binge eating proneness. After identifying BEP and BER rats, I will induce Fos expression in the mPFC of BEP and BER rats as outlined in Chapter 1. Thereafter, I will use double-label immunohistochemistry to identify the proportions of Fos-expressing neurons that

co-localize with 1) the excitatory neuron marker, special AT-rich sequence binding protein 2 (Satb2), and 2) three markers of inhibitory neurons in the mPFC: PV, SOM, and VIP.

Chapter 3: In Chapter 3 I will determine the behavioral consequence of inhibiting neural output from the mPFC on PF intake and on scores of feeding behavior in BEP and in BER female rats. After identifying BEPs and BERs, I will use the GABA-A agonist muscimol to pharmacologically inactivate neural activity within the mPFC of BEPs and BERs just prior to PF exposure. I will determine the effects of mPFC inactivation on the total consumption of PF and chow in BEPs and BERs, and I will score feeding behavior in BEPs and BERs following each drug infusion. Scoring feeding behavior following inactivation of the mPFC will identify the behavioral mechanism(s) by which inactivation of the mPFC alters the consumption of PF in general, and whether, qualitatively, the mPFC exerts differential control over PF consumption in rats prone to vs. resistant to binge eating.

Chapter 1

Differential Mesocorticolimbic Responses to Palatable Food in Binge Eating Prone and Binge Eating Resistant Female Rats

Introduction

Binge eating involves the consumption of a large amount of food in a short period of time and a loss of control during the binge episode [124]. Binge eating is the core, maladaptive symptom that cuts across every major subtype of eating disorder within the DSM-5 (e.g., bulimia nervosa, binge eating disorder, anorexia-nervosa binge/purge type) [124]. Individuals who binge eat suffer from significant psychological distress, including elevated depression scores, reduced quality of life, and a general decline in psychological function [139]. Scientific inquiry into the etiology of binge eating has traditionally focused on psychosocial variables, although a growing body of evidence points to significant biological underpinnings [122, 130, 140]. Nonetheless, the neurobiology underlying binge eating remains poorly understood. The present study aimed to address this gap by using a well-validated animal model of binge eating to investigate the involvement of the mesocorticolimbic reward circuit, which encodes and mediates food reward, in binge eating risk [101]. Specifically, we asked whether enhanced mesocorticolimbic neural responsiveness to palatable food (PF) is associated with a higher propensity to binge eat.

Several components of the mesocorticolimbic reward circuit, including the nucleus accumbens (NA) and the medial prefrontal cortex (mPFC), are activated in conjunction with PF intake [101]. In animal studies, neural activation is commonly assessed by examining expression of Fos, the protein product of the immediate early gene *c-fos*, in brain regions of interest. Neural expression of the Fos protein peaks 60-90 min following a strongly depolarizing stimulus, so

microscopic quantification of Fos immunoreactivity is often used as a proxy for neural activation after stimulus exposure [141]. Specifically, Fos expression within the mesocorticolimbic reward circuit is increased after intake of PF, and the Fos response to PF is greater than that elicited by standard lab chow [78, 142]. However, no studies to date have examined PF-induced activation of the mesocorticolimbic circuit in an animal model of binge eating proneness, e.g., in high versus low binge eaters. This is an important consideration for the human condition, because access to PF is virtually ubiquitous, yet only a small proportion of humans binge eat, indicating wide-ranging individual differences in binge eating proneness [16, 131, 135]. Here we test the hypothesis that mesocorticolimbic responsiveness to PF positively correlates with the propensity to binge eat, using an individual differences rat model of binge eating, the binge eating prone (BEP)/binge eating resistant (BER) model, which identifies naturally occurring, within-group differences in binge eating.

The BEP/BER rat model has high face and construct validity for studying the biological underpinnings associated with binge eating, largely due to its ability to model a continuum of binge eating behaviors, to identify extreme binge eating phenotypes (i.e., BEP and BER rats), and to identify natural, individual variation in binge eating of PF [131]. PF exposure in this model is intermittent (3d/week) and brief (4hr/day), similar to the intermittent and discrete (i.e., a few hours) binge episodes in the human condition [16, 124, 131, 135]. BEP rats binge only on PF and not on standard rat chow in this model, suggesting that they are not general over-eaters, and BEP rats do not gain excessive weight throughout the testing period as compared to their BER counterparts [16, 131, 133-135]. Finally, similar to humans [36], sex differences are apparent in the BEP/BER paradigm, such that female rats are more likely to display binge eating proneness as compared to male rats [134].

Given the robust behavioral differences between BEP and BER rats in their propensity to binge on PF, we hypothesized that PF is a more salient reward to BEP rats than to BER rats. To test this hypothesis, we compared the neural responsiveness (i.e., Fos expression) to PF in the NA and mPFC in three different groups: 1) BEP rats exposed to PF, 2) BER rats exposed to PF, and 3) a group of control rats not exposed to PF. Our hypothesis predicted that neural responsiveness to PF (i.e., Fos expression) within the NA and mPFC would be higher in BEP rats as compared to both control (no PF) rats and BER rats exposed to PF. Our study results support these predictions, and provide preliminary evidence consistent with the hypothesis that binge eating proneness is associated with enhanced responsiveness to PF, particularly in brain regions involved in higher order, executive processing of PF reward.

Methods

Animals

Forty adult (postnatal day 60; P60) female Sprague-Dawley rats were obtained from Harlan Laboratories (Madison, Wisconsin) and individually housed upon arrival in clear Plexiglas cages (45 x 23 x 21 cm) with *ad libitum* access to chow (Harlan Teklad Global Diets: 8640, Madison, Wisconsin) and water. Rats were maintained on a 12:12 hour light: dark cycle (lights on at 0200h and off at 1400h) at $72 \pm 4^{\circ}\text{F}$ and were treated in accordance with the NIH Guide for the Care and Use of Laboratory Animals. All protocols were approved by the Michigan State University Institutional Animal Care and Use Committee.

Feeding Tests and BEP/BER Classification

Acclimation

One week prior to the start of feeding tests, all rats were acclimated to daily handling and body weight measurements. Specifically, rats were pulled from their home cages and held by the experimenter for ~2 minutes (i.e., the approximate amount of time required for cage bedding searches on feeding test days, see below) and were weighed in a covered container using a standard electronic balance.

Feeding Tests

The BEP/BER paradigm used in this study began on P67 and was adapted from the protocol outlined in [135] that has been used previously in our lab [16, 131, 133, 134]. The BEP/BER paradigm consists of feeding test days, during which PF is provided in addition to standard chow, and non-feeding test days during which only chow is provided. In the present study, the BEP/BER paradigm was conducted over a period of three weeks. On feeding test days, occurring three days per week (MWF), body weights and 24-hour chow intake were recorded in the mornings before lights out. Approximately 10 minutes prior to lights out, rats were given pre-measured PF (~15-17g high fat diet pellets, 45% kcal from fat, 35% kcal from carbohydrate, 20% kcal from protein; #D12451, Research Diets Inc., New Brunswick, NJ) placed in ceramic dishes on the floor of home cages. Of note, ceramic dishes stayed in rat home cages throughout the entire testing period, including days when rats were not exposed to PF. Rats were also allowed unlimited access to standard chow during the period of PF access on feeding test days. After 4 hours of access to PF, all remaining PF and chow were measured using standard electronic balances and PF was removed from all home cages. Cage bedding was searched to ensure that all chow and PF pellets were included in each measurement. The 4-hour

PF intake values were later used to identify BEP and BER rats, as this short, discrete amount of time models binge eating in humans (usually 1-2 hours) and has been used previously to elicit binge eating in rats [16, 131, 133-135]. On non-feeding test days (i.e., all other days of the week), body weights and total 24-hour chow intake were recorded in the mornings before lights out.

BEP/BER Classification

Using methods outlined in [16, 131, 133, 134], we identified BEP and BER rats using a tertile approach based on the 4-hour PF intake data across eight of the nine feeding tests (3 feeding tests per week; 3 weeks total of testing). Data from the first feeding test were omitted from the final analysis due to inadvertent inaccurate measurement of PF intake in a subset of rats. Prior to BEP/BER classification, all 4-hour PF intake values on each testing day were standardized by body weights $\{\text{intake (g)}/\text{body weight (g)}^{2/3}\}$ [134, 143]. Standardization removes any confound of normal body weight variation on PF intake values that could unduly influence tertile calculations and BEP/BER classifications. Mean standardized PF intake values from each feeding test day were then divided into top, middle, and bottom tertiles, such that each rat scored within one of the three tertiles on each feeding test day. Rats were categorized as BEP if they scored within the highest tertile on at least 4 of the 8 feeding tests (i.e., 50% of feeding test days) and never within the lowest tertile. Rats were categorized as BER if they scored within the lowest tertile on at least 4 of the 8 feeding tests (i.e., 50% of feeding test days) and never within the highest tertile. Past studies in our lab using the BEP/BER model have analyzed a wide range of tertile criteria for identifying BEP and BER rats (i.e., requiring 50% to 83% of feeding test days to be high/low for BER/BEP groups) [16, 131, 133, 134]. We chose to use criteria at the lower end of the range in order to maximize our sample size while still identifying

rats that were consistently eating the highest (BEP) and the lowest (BER) amounts of PF across testing [134]. Overall, this method of classifying rats as BEP or BER takes into account both the frequency and the consistency of either high or low levels of PF intake across the testing period. This approach closely follows the methods used for identifying binge eaters and non-binge eaters in the human condition: individuals who binge eat at least once per week are considered binge eaters, while those who seldom binge eat are considered non-binge eaters [124].

Induction of c-Fos and Quantification of Fos-Immunoreactivity (Fos-ir)

Induction of c-Fos Expression

The rats identified as BEP (8/40, 20% of the sample) and BER (11/40, 28% of the sample) from the feeding test protocol were used to compare mesocorticolimbic responsiveness to PF in the two extreme binge eating phenotypes. After the last feeding test on P87, rats were handled daily for one week without any further exposure to PF. During this period of time, ceramic food dishes remained in each rat's home cage, and all rats were carted daily to the room where pre-sacrifice PF exposure would occur for Fos induction. On the day of Fos induction (P94), rats were randomly assigned to receive either PF (15-17g in ceramic dishes) in their home cages (n=5 BEP; n=7 BER, referred to as "BEP w/PF" or "BER w/PF") or no PF in their home cages (n=3 BEP; n=4 BER, combined into one group and referred to as "No PF")¹ for a total of 1hr beginning just after lights out. During this exposure period, chow remained in the cages of all PF-exposed and No PF animals, and ceramic food dishes remained in the cages of all PF-exposed and No PF animals. PF and ceramic dishes were removed from all cages after the 1hr exposure period, and 30min later (i.e., 90 minutes after the introduction of PF or the empty dish),

¹The number of Fos-ir cells did not differ significantly between BEP and BER "No PF" rats within any of the analyzed brain regions (p values 0.29-0.91). Therefore, data from these rats were combined into a single "No PF" group for all statistical analyses to maximize sample size and minimize the number of statistical comparisons.

rats were given a lethal dose of Fatal Plus[®] i.p. (sodium pentobarbital diluted to 50mg/mL in sterile saline; 150mg/kg). This 90min period between initial stimulus introduction and the induction of euthanasia has been shown to be an optimal period of time for peak Fos expression to occur in response to food rewards [78, 144]. Thereafter, rats were intracardially perfused with 300mL of 0.1M buffered saline rinse followed by 300mL of 4% paraformaldehyde. Brains were removed and placed in 4% paraformaldehyde overnight and then stored in 20% sucrose in 0.1M buffered saline. Brains were cryostat-sectioned at 40µm into four series through the mPFC and the NA, and sections were stored in cryoprotectant at -20°C until further processing.

Immunohistochemistry for Fos-ir

One set of tissue sections from the 1 in 4 series from each rat was processed for Fos immunohistochemistry. Sections were rinsed in Tris Buffered Saline (TBS, 3X5 min) and then were immersed in 0.1% sodium borohydride in 0.5M TBS for 15 min, followed by 10 min in 1% hydrogen peroxide in TBS. Sections were rinsed in TBS (3X5min) and then incubated for 30 min in a blocking solution of 20% normal goat serum, (NGS; Pel Freez Biologicals) in 0.3% Triton X-100 in TBS. Blocking was followed by a 48-hr incubation at 4°C in a 1:10,000 dilution of rabbit anti-Fos primary antisera (sc-52, Santa Cruz Biotech; Santa Cruz, CA) in TBS with 2% NGS and 0.3% Triton X-100. Sections were rinsed in TBS (3X5min) and then incubated for 60 min in a 1:500 dilution of goat anti-rabbit biotinylated secondary antisera (Vector Laboratories) in TBS with 2% NGS and 0.3% Triton X-100. Sections were then rinsed again in TBS (3X5min), after which they were incubated for 60 min in avidin-biotin complex (ABC Elite Kit, Vector Laboratories). Diaminobenzidine tetrahydrochloride (10mg tablets; Sigma-Aldrich, St. Louis, MO) was dissolved in TBS and 0.012% hydrogen peroxide to visualize brown, Fos-immunoreactive (Fos-ir) nuclei. Sections were mounted onto slides, dehydrated using a graded

alcohol series, cleared in xylene, and coverslipped. Due to poor tissue quality after immunohistochemical processing, one BER from the BER w/PF group and one BER from the No PF group were excluded from the Fos expression analysis. This resulted in a final sample size of 8 total BEP (n=5 in BEP w/PF and n=3 in the No PF group) and 9 total BER rats (n=6 in BER w/PF and n=3 in the No PF group) for the Fos analysis.

Quantification of Fos-ir in the Mesocorticolimbic Circuit

The total number of Fos-ir cells in each region of interest was estimated using unbiased stereological methods. The optical fractionator method in Stereoinvestigator (Microbrightfield Biosciences, Willingston, VT) was used to estimate Fos-ir cells in each region of interest within the NA and mPFC, and all tracings and cell counts were performed on an Olympus BX51 microscope and Q-Imaging Color 12 bit camera. An experimenter blind to the behavioral phenotype and exposure status of each animal performed cell counts in each region of interest. Analyzed sections in the medial prefrontal cortex (mPFC) corresponded to plates 9-12 (+3.72mm to +2.76mm from Bregma) of the Paxinos and Watson rat brain atlas (**Figure 1.2**) [145]. The prelimbic cortex (PrL), infralimbic cortex (IL), and cingulate cortex (Cg1) were all traced relative to the forceps minor (fmi) and in accordance with contour tracing of the mPFC used by Chisholm and Juraska, 2012 [146]. Tracings of the mPFC were performed under a 4X (NA 0.13) air objective, and counts were performed with a 40X (NA 0.85) air objective. For stereological estimates of the total number of Fos-ir cells in the mPFC, the counting frame was set to $125\mu\text{m}^2$ within a grid size of $400\mu\text{m}^2$, and the optical dissector height was set to $6\mu\text{m}$ with top and bottom guard zones of $2\mu\text{m}$. Analyzed sections in the nucleus accumbens (NA) corresponded to plates 16-23 (+2.04 mm to +1.2mm from Bregma) of the Paxinos and Watson (2005) rat brain atlas (**Figure 1.2**). The NA core (NAC) and NA shell (NAS) were traced using

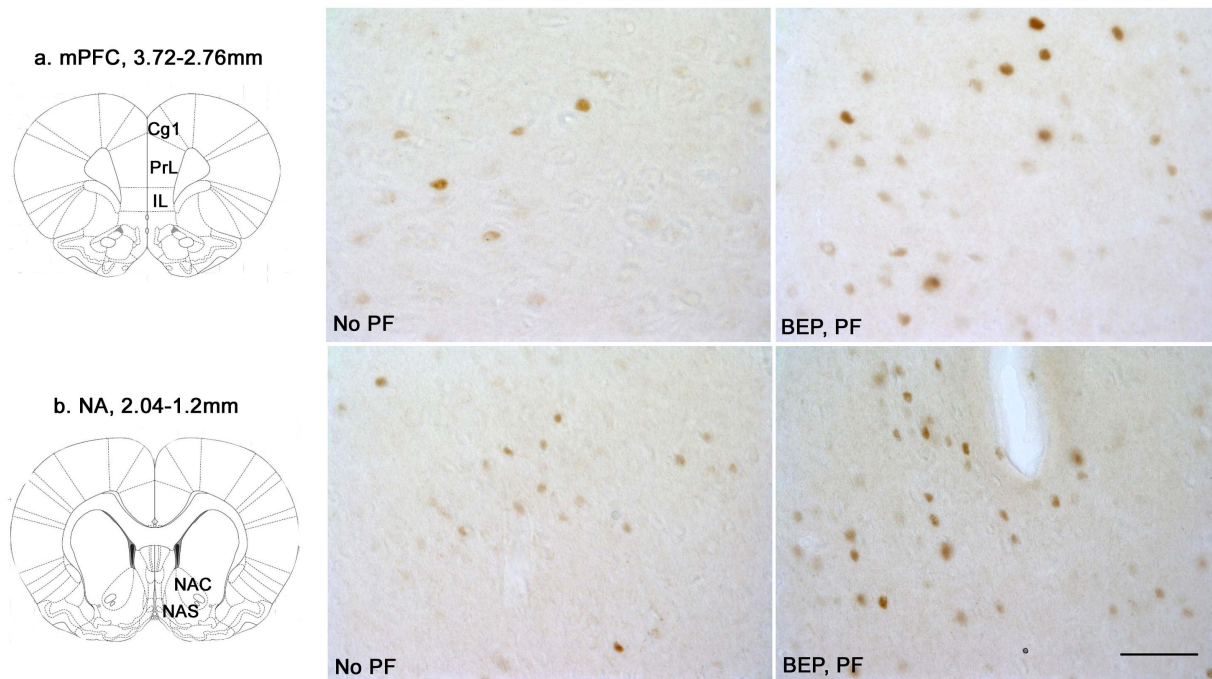


Figure 1.2) Regions of interest and representative Fos images from the mPFC and NA,
CH 1

Atlas images (Paxinos and Watson Rat Brain Atlas, 2005) depicting contours used for tracing the mPFC (a) and the NA (b). Adjacent images show representative images of Fos-ir cells in the mPFC or NA of a “No PF” rat and a BEP rat exposed to PF prior to sacrifice. Scale bar represents 50 μ m.

a 4X (NA 0.13) air objective, and cell counts within each contour were conducted using a 40X (NA 0.85) air objective. For stereological estimates of the number of Fos-ir cells in the NA, the counting frame was set to $125\mu\text{m}^2$ within a grid size of $350\mu\text{m}^2$, and the optical dissector height was set to $6\mu\text{m}$ with top and bottom guard zones of $2\mu\text{m}$.

Statistical Analyses

Preliminary Analyses of Feeding Test Data

Mixed design ANOVA models were used to examine mean differences in 4hr PF consumption, 4hr chow consumption, 24hr chow consumption, and body weights (measured at 24hrs only) between BEP and BER groups across the three-week feeding test period. The within-group variables were 4hr PF consumption, 4hr chow consumption, 24hr chow consumption, or body weights, while the between subjects factor was BEP/BER phenotype. Given prior research (e.g., [16, 131, 133-135]), these analyses were necessary to confirm that BEP rats consumed significantly more PF than BER rats and to verify that BEP and BER rats did not differ in average body weights across the study.

Fos-ir in the NA and mPFC

Although individual ANOVAs with *post-hoc* t-tests could have been used to test all pairwise group comparisons on mean Fos-ir cells in the NA and mPFC, we had *a priori* hypotheses that focused on two specific planned comparisons. Specifically, *a priori* hypotheses predicted that the BEP w/PF group would show the highest number of Fos-ir cells in each brain region of the NA and mPFC as compared to the other two experimental groups (No PF and BER w/PF rats). We therefore focused our analyses on specific planned comparisons only. Our

examination of only two comparisons is also consistent with recommendations for planned contrasts (i.e., conducting one less contrast than the number of groups: $k - 1$).

First, we conducted t-tests comparing mean Fos-ir cell number in each brain region between BEP w/PF and No PF rats. Higher mean Fos-ir cells in the BEP w/PF group, relative to the No PF group, would provide support for the hypothesis that BEP rats experience heightened neural responsiveness in the NA and mPFC following PF exposure as compared to no PF exposure. Second, we compared mean Fos-ir cells in each brain region between the BEP w/PF and the BER w/PF groups using individual ANCOVAs; ANCOVAs were used here to control for the total amount of PF consumed during the 1hr, pre-sacrifice exposure period. Statistically controlling for between-rat variation in total 1-hour PF intake (via ANCOVA models) was an important consideration since the BEP w/PF group consumed more PF than the BER w/PF group during the pre-sacrifice testing period (PF in grams: BEP M (SD) = 8.46 (1.47), BER M (SD) = 6.60 (1.78), Hedges' g = 1.02; PF in grams standardized by body weight: BEP M (SD) = 0.24 (0.04); BER M (SD) = 0.19 (0.05), Hedges' g = 0.98). ANCOVA models therefore ensured that higher total Fos-ir cells in the BEP w/PF group, relative to the BER w/PF group, could not be accounted for merely by between-rat variation in the absolute amount of 1-hour PF intake prior to sacrifice; instead, between-group differences would be indicative of differences in the neural responsiveness to PF.

All planned comparisons used one-tailed p -values given our unidirectional *a priori* hypothesis that the BEP w/PF group would show more Fos-ir cells than each of the other two experimental groups. Given the smaller sample sizes in this study, Hedges' g effect sizes, which is a variation of Cohen's d that corrects for biases when data consist of small sample sizes [147],

were also computed to provide a standardized measure of the magnitude of mean differences between groups (small, $g = .20$; medium, $g = .50$; large, $g = .80$).

Results

Preliminary Analyses of Feeding Test Data

Results from the mixed design ANOVAs for PF and chow consumption during the eight feeding tests are shown in Table 1 and Figure 2. BEP rats ate significantly more PF than BER rats throughout the entire testing period, yet BEP rats ate significantly less chow than BER rats on both feeding test days and non-feeding test days (**Table 1.3 & Figure 1.3**). BEP rats also ate less chow than BER rats during the 4hr period on feeding test days, though this difference did not reach statistical significance. BEP and BER rats showed non-significant, but medium effect size, differences in body weight (**Table 1.3 & Figure 1.3**). However, consistent with prior research [135], mean body weights for both the BEP and BER groups were within the normal weight range for age (see Growth Curve data for Sprague Dawley rats: www.Harlan.com; Harlan Laboratories, Inc.), indicating the BEP rats did not gain excessive weight during the feeding test paradigm.

Fos Expression in the NA and mPFC

Fos-ir cell count comparisons between BEP w/PF and No PF rats largely supported hypotheses. The BEP w/PF group had significantly higher Fos expression in the NAC and PrL and a statistical trend towards higher Fos expression in the NAS and IL, as compared to No PF rats (**Table 1.4 and Figure 1.4**), with effect sizes being large in magnitude (NAC: Hedge's $g = 1.25$; NAS: Hedge's $g = 0.89$; PrL: Hedges' $g = 1.15$; IL: Hedges' $g = .97$). In the Cg1 region,

Table 1.3) Differences in PF intake, chow intake, and body weights between BEPs and BERs, CH 1

Mean Comparisons between BEP and BER Rats on PF, Chow, and Body Weight from the Eight Feeding Tests.

Mean (S.E.)	<u>BEP vs. BER Mean Comparisons</u>				
	<i>Statistics</i>		<i>Effect Size</i>		
	<i>F</i> (1,17)	<i>p</i>	Hedges <i>g</i>		
<u>Body Weight (g)</u>					
BEP	212.72 (3.47)		1.24	.28	0.48
BER	207.63 (2.96)				
<u>Feeding Test Days</u>					
<u>Palatable Food (4hr, g)</u>					
BEP	0.39 (0.009)		128.42	<.001	4.63
BER	0.26 (0.008)				
<u>Palatable Food (4hr, kcal)</u>					
BEP	63.72 (1.57)		114.13	< .001	4.74
BER	41.63 (1.34)				
<u>Chow (4hr, g)</u>					
BEP	0.03 (0.007)		3.78	.07	1.02
BER	0.05 (0.006)				
<u>Chow (24hr, g)</u>					
BEP	0.04 (0.01)		57.65	<.001	3.79
BER	0.16 (0.01)				
<u>Non-Feeding Test Days</u>					
<u>Chow (24hr, g)</u>					
BEP	0.35 (0.005)		49.09	<.001	2.75
BER	0.39 (0.004)				

Note: Mean values (in grams only) for palatable food and chow are standardized scores, adjusted for body weight (i.e., intake (g)/body weight (g)^{2/3}). Values for 4hr PF intake in kcal were calculated using the 4.73 kcal/gm value reported for the high fat pellets used here. Sample sizes: BEP, n = 8 and BER, n = 11. Estimates were calculated across 8 feeding tests, from P67 to P85. Two-tailed *p*-values are presented. Hedges' *g* values reflect effect sizes, and thus, provide a standardized measure of the magnitude of mean differences between groups (effect size interpretation: small, *g* = .20; medium, *g* = .50; large, *g* = .80).

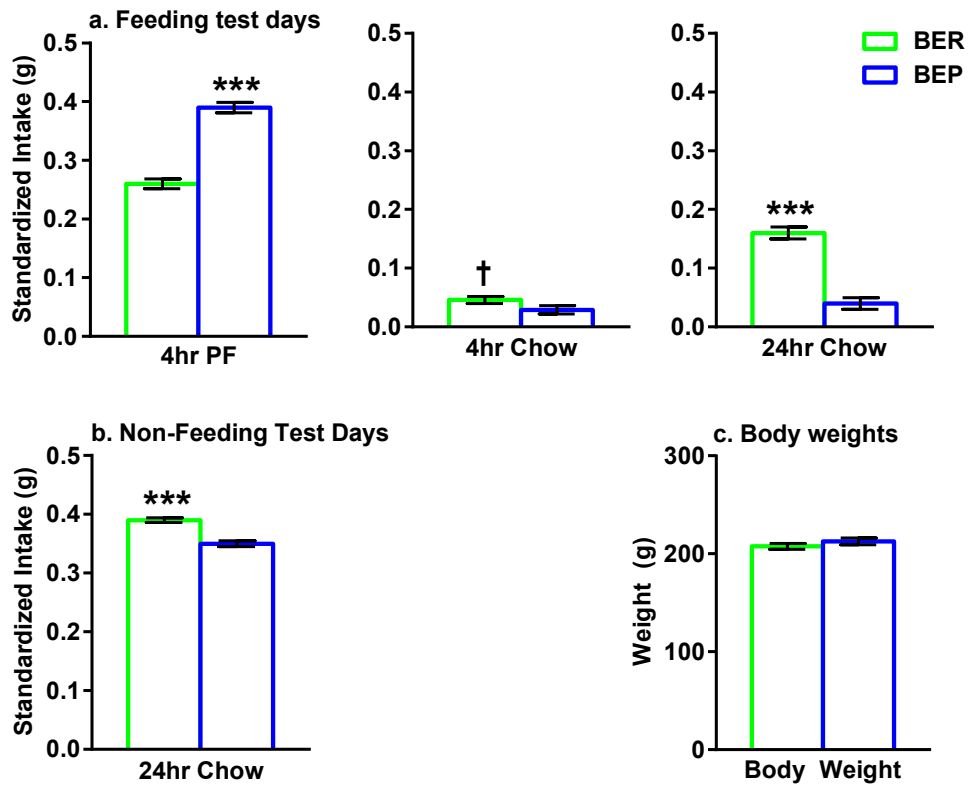


Figure 1.3) PF intake, chow intake, and body weights across the feeding test paradigm in BEPs and BERs, CH 1

BEP/BER differences in (a) PF and chow intake on feeding test days, (b) chow intake on non-feeding test days, and (c) body weights. Values represent average measurements across the three week testing period. Standardized intake: intake (g)/BW(g)^{2/3}; Error bars represent one S.E.M.

*** $p < 0.001$; † $p < 0.10$.

we found medium-to-large effect sizes for higher mean Fos-ir cell counts in BEP w/PF than No PF rats (Hedges' $g = .62$), even though the statistical test failed to reach significance (**Table 1.4**).²

Consistent with hypotheses, Fos-ir cell counts were significantly higher in BEP w/PF rats versus BER w/PF rats in the PrL, IL, and Cg1, and approached statistical significance in the NAC and NAS, after adjusting for total PF consumption prior to sacrifice (**Table 1.5 and Figure 1.4**). Effect sizes were large in magnitude for all neural regions (**see Table 1.5**): NAC (Hedge's $g = 1.02$), NAS (Hedge's $g = 0.82$), PrL (Hedges' $g = 2.59$), IL (Hedges' $g = 1.55$), and Cg1 (Hedges' $g = 1.64$).³ Thus, our findings suggest that differences in Fos expression between the BEP w/PF and BER w/PF groups cannot be accounted for by greater PF intake in BEP rats, as we statistically controlled for differences in pre-sacrifice PF intake, and instead reflect enhanced neural responsiveness to PF in BEP rats.

Discussion

Our study is the first to provide preliminary evidence that enhanced mesocorticolimbic responsiveness to PF is associated with a greater propensity to binge eat. First, we demonstrated that PF activates the NA core and shell and the PrL and IL cortices of the mPFC in BEP rats: BEP rats exposed to PF demonstrated greater Fos expression in these select brain regions as compared to rats not exposed to PF. The large effect sizes for all of these comparisons indicate

²As previously noted, BEP and BER rats in the No PF group did not significantly differ on the number of Fos-ir cells within any of the analyzed brain regions, and thus, were combined into one group for analyses. It is unlikely that our results were unduly affected by this decision; in general, BEP w/PF showed substantially higher mean Fos-ir cells as compared to the BEP rats in the No PF group (all neural regions: Hedges' $g = .83$ - 1.29 , mean $g = 1.03$) and the BER rats in the No PF group (with exception of Cg1, all other neural regions: Hedges' $g = .72$ - $.98$, mean $g = .85$).

³ANCOVA models controlled for between-rat differences in 'absolute levels (in grams)' of 1-hour PF consumption prior to sacrifice, but notably, similar results were obtained when 'body-weight adjusted' 1-hour PF consumption values were used as the covariate (i.e., large effect sizes in all neural regions; data available upon request).

biological significance. The NA shell is home to a hedonic hot spot for PF reward, regulating the affective response to PF [101, 148], whereas the NA core is necessary for instrumental learning associated with food reward [149] and the execution of motor behaviors to obtain food reward [150]. Moreover, the PL and IL cortices, respectively, project to the NA core and shell [151], encode the palatability of food rewards [103], and are activated in response to PF (e.g., high fat or chocolate pellets) and chow intake [56, 78, 144]. Thus, compared to chow alone (i.e., No PF group), PF consumption in BEPs more strongly activates brain regions involved in 1) the perception of the hedonic properties of PF, and 2) the motivation to attain and consume PF. Second, we found greater PF-induced neural activation of the NA core and shell and of all regions of the mPFC in BEP rats as compared to BER rats, even after statistically controlling for the total amount of PF consumed prior to sacrifice. Effect sizes for all comparisons were large in magnitude, but in mPFC, the group means were statistically significant and effect sizes were ~1.5-2 times greater than those in the NA, indicating that differences in neural activation between BEP and BER rats are more robust in the mPFC than in the NA. Thus, while binge eating proneness is associated with enhanced activity in both cortical and subcortical reward-related brain regions during PF exposure, our results suggest that binge eating proneness may be more strongly linked to dysregulated executive control of PF consumption than to heightened responsiveness to food reward within limbic circuitry.

Table 1.4) Fos expression in the mPFC and NA of BEP rats exposed to PF and No PF control rats, CH 1

Mean Comparisons on Fos Expression between BEP w/PF and No PF Groups				
Experimental Group	Mean (S.E.)	<i>Planned Pairwise Comparisons:</i> BEP w/PF > No PF		
		<i>Statistics</i>		<i>Effect Size</i>
		<i>t</i> (1, 9)	<i>p</i>	Hedge's <i>g</i>
<i><u>Nucleus Accumbens</u></i>				
<i><u>NA Core (NAC)</u></i>				
No PF	5791.42 (951.87)	-2.14	.04	1.25
BEP w/PF	11424.82 (2460.34)			
<i><u>NA Shell (NAS)</u></i>				
No PF	6925.79 (1186.59)	-1.62	.07	0.89
BEP w/PF	10428.15 (1896.81)			
<i><u>Prefrontal Cortex</u></i>				
<i><u>Prelimbic (PrL)</u></i>				
No PF	22611.74 (2204.77)	-1.99	<.05	1.15
BEP w/PF	32368.52 (4380.44)			
<i><u>Infralimbic (IL)</u></i>				
No PF	11573.19 (1523.60)	-1.78	.05	0.97
BEP w/PF	15737.90 (1803.93)			
<i><u>Cingulate (Cg1)</u></i>				
No PF	16711.54 (2507.99)	-1.13	.14	0.62
BEP w/PF	21018.31 (2888.68)			

Note: BEP w/PF=binge eating prone rats exposed to PF; BER w/PF=binge eating resistant rats exposed to palatable food; No PF = binge eating prone and binge eating resistant rats that were in the control condition, i.e., no exposure to PF. Sample sizes: No PF, n=6, BEP w/PF, n=5, and BER w/PF, n=6. Since *a priori* hypotheses predicted unidirectional mean differences between groups (i.e., BEP w/PF > No PF), planned comparisons were performed using one-tailed *p*-values. Hedges' *g* values reflect effect sizes, and thus, provide a standardized measure of the magnitude of mean differences between groups (effect size interpretation: small, *g* = .20; medium, *g* = .50; large, *g* = .80).

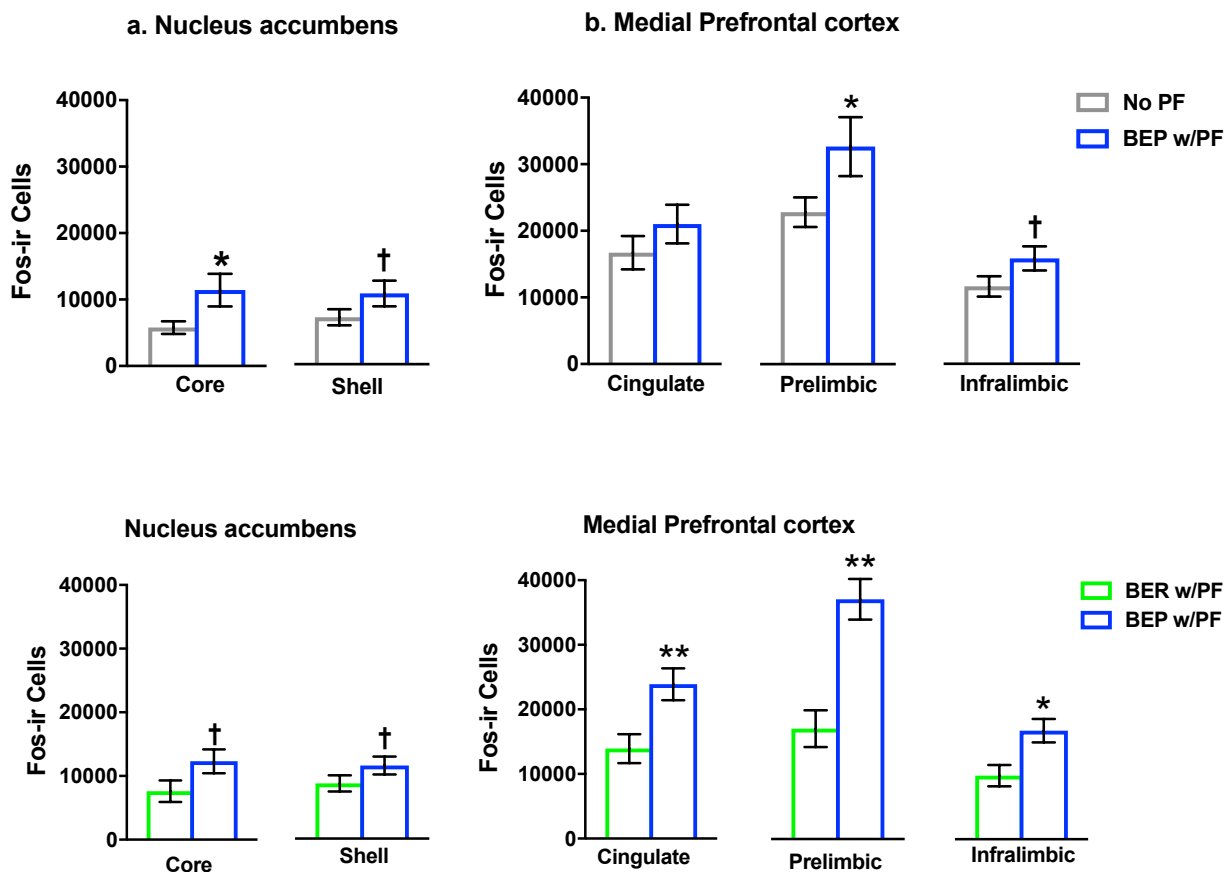


Figure 1.4) Fos expression within the mPFC and NA of No PF control rats, BEPs exposed to PF, and BERs exposed to PF, CH 1

Fos expression in the nucleus accumbens and medial prefrontal cortex. Top panel show mean comparisons of Fos expression in the nucleus accumbens (a) and medial prefrontal cortex (b) in BEP rats exposed to PF (BEP w/PF) versus No PF rats. Bottom panel represents mean comparisons of Fos expression in the nucleus accumbens (c) and medial prefrontal cortex (d) of BEP rats exposed to PF (BEP w/PF) versus BER rats exposed to PF (BER w/PF), controlling for total, 1hr PF consumption at sacrifice. Groups were compared using planned pairwise comparisons and one-tailed p values. Error bars represent one S.E.M.

**Table 1.5) Fos expression in the mPFC and NA of BEP and BER rats exposed to PF,
CH 1**

Mean Comparisons on Fos Expression between BEP with PF and BER with PF Groups,
Controlling for Palatable Food Consumption.

Experimental Group	Raw Descriptive Mean (S.D.)	ANCOVA Adjusted Mean (S.E.)	<i>Planned Pairwise Comparisons, controlling for PF Intake BEP w/PF > BER w/PF</i>		
			<i>Statistics</i>	<i>p</i>	<i>Effect Size</i>
			<i>F (1, 8)</i>		<i>Hedges' g</i>
<u>Nucleus</u>					
<u>Accumbens</u>					
<u>NA Core (NAC)</u>					
BER w/PF	8346.18 (1672.46)	7607.92 (1687.06)	3.00	.06	1.02
BEP w/PF	11424.82 (5501.49)	12310.73 (1875.35)			
<u>NA Shell (NAS)</u>					
BER w/PF	9414.59 (1722.21)	8605.65 (1254.28)	1.91	.10	0.82
BEP w/PF	10428.15 (4241.39)	11398.88 (1394.26)			
<u>Prefrontal Cortex</u>					
<u>Prelimbic (PrL)</u>					
BER w/PF	20425.51 (8668.29)	16853.90 (2802.38)	19.26	.001	2.59
BEP w/PF	32368.52 (9794.97)	36654.46 (3115.13)			
<u>Infralimbic (IL)</u>					
BER w/PF	10740.47 (3804.17)	9847.56 (1640.88)	6.94	<.02	1.55
BEP w/PF	15737.90 (4033.71)	16809.40 (1824.01)			
<u>Cingulate (Cg1)</u>					
BER w/PF	16314.52 (6811.50)	13922.14 (2223.90)	7.75	.01	1.64
BEP w/PF	21018.31 (6459.28)	23889.18 (2472.10)			

Note: ANCOVA models covaried 1-hour palatable food consumption at sacrifice. Raw Descriptive Mean = mean value for Fos expression that was not adjusted for palatable food consumption; ANCOVA Adjusted Mean = mean value of Fos expression that controls for 1-hour palatable food consumption. BEP w/PF=binge eating prone rats exposed to palatable food; BER w/PF=binge eating resistant rats exposed to palatable food. Sample sizes: BEP w/PF, n=5 and BER_PF, n=6. Since a priori hypotheses predicted unidirectional mean differences between the two groups (i.e., BEP w/PF > BER w/PF), one-tailed *p*-values are reported. Hedges' *g* values reflect effect sizes, and thus, provide a standardized measure of the magnitude of mean differences between groups (effect size interpretation: small, *g* = .20; medium, *g* = .50; large, *g* = .80).

Potential mechanisms explaining higher mesocorticolimbic responsiveness to PF in BEPs vs. BERs

The neurotransmitter systems in NA and mPFC that mediate the mesocorticolimbic responsiveness to PF remain to be identified. Two candidate neurotransmitters within NA are the dopamine and endogenous opiates (EOP) systems, which have both been linked to the coding of the hedonic properties and incentive salience of PF [101, 152]. Thus, the Fos response to PF in the NA may reflect either dopamine and/or EOP release and activation of their receptors on medium spiny neurons of the NAC and NAS. If so, then enhanced neurotransmission, either in the amount of neurotransmitter released or the magnitude of receptor signaling, could underlie the more extensive PF-induced activation of NA neurons in BEPs than in BERs. Within the mPFC, complex interactions between GABAergic, inhibitory interneurons and glutamatergic, excitatory projection neurons facilitate the executive control of goal-directed behaviors, including the amount and microstructure of chow and PF consumption [52, 78, 87, 110, 153, 154]. In mice, PF induces differential Fos expression in inhibitory and excitatory neurons of the mPFC; the vast majority of excitatory projection neurons are activated by PF, whereas only a small subset of inhibitory interneurons is activated by PF [78]. If PF also differentially activates excitatory and inhibitory neurons in the mPFC of rats, then *binge eating proneness may be related to differences in the particular pattern or proportions of excitatory and/or inhibitory neurons activated by PF in the mPFC of BEPs and BERs*. This possibility could be empirically probed by determining the phenotypes (i.e. excitatory vs. inhibitory) of the PF-activated mPFC neurons in BEPs and BERs.

Greater mesocorticolimbic responsiveness to food and food-related stimuli in human eating disorders

Of note, our results are consistent with recent human neuroimaging data that links aberrant activity mesocorticolimbic brain regions to binge eating and binge eating-related eating disorders. For example, mesocorticolimbic activity in response to high calorie liquid intake (e.g., Pepsi, chocolate milk, cream soda) increases linearly with self-reported scores of binge eating [28]. On the other hand, the responsiveness of select PFC sub-regions to images of high calorie foods (e.g., French fries, ice cream, cake, chips) is greater in women with bulimia, as compared to healthy controls [29], but is lower in response to ingestion of a palatable liquid as compared to healthy controls [155]. Ultimately, these variations in neuroimaging findings highlight the complexity of neural circuit dysfunction in eating disorders in the human condition, and point to the need for a combined effort employing both human and animal research to uncover the neurobiology underlying these conditions. Nonetheless, the overlap in findings between our animal data and several aspects of human neuroimaging data suggests that the BEP/BER model is a useful and appropriate model for future studies that aim to conduct translational research on the neurobiological mechanisms underlying binge eating.

Limitations to the current study

Despite the strengths of our current study, there are some important limitations that deserve comment. First, sample sizes in this study are small, due to 1) the number of BEP and BER rats that can be identified using BEP/BER criteria, and 2) the necessity to further separate BEP and BER groups into PF exposure and No PF control groups. However, in both sets of comparisons (BEP w/PF vs. No PF and BEP w/PF vs. BER w/PF), we found medium to large effect sizes for pairwise comparisons in all regions, even when they did not reach statistical

significance. Effect sizes indicated that group differences are substantial and biologically meaningful, yet future replications warrant the use of larger sample sizes. Second, although we statistically controlled for total PF intake by the use of ANCOVA models in this study, we cannot rule out the possibility that behaviors associated with higher PF intake (motor behaviors, licking behaviors) affected Fos expression. Future studies employing the Fos induction protocol used here could aim to equate the amount of PF available for BEP and BER rats to avoid this potential confound.

Third, in contrast to prior studies using the BEP/BER model in which chow consumption did not differ between the two phenotypes (e.g., [16, 131, 133, 135]), in the present study, BEP rats consumed *significantly less chow* than BER rats on both feeding test days and non-feeding test days. The phenotypic differences in chow consumption in the present study could be related to the type of PF used, which here had a higher fat content (45% kcal from fat, 35% kcal from carbohydrates) than the higher sugar content (15% kcal from fat, 69% kcal from carbohydrates) of the PF (vanilla frosting) that has been previously used in our lab. Because a high fat PF source is more energy dense than a PF source higher in sugar, it is possible that the larger reduction in chow consumption in BEP rats was a direct consequence of consuming more fat when PF was available. We also note that the proportions of BEP and BER rats found in this study are slightly less than what has been found previously in our lab using the BEP/BER protocol [16, 131, 133, 134]. Again, the higher fat content of the PF used in this study may have contributed to this outcome, as rats may be less likely to consistently consume high amounts of a PF source (i.e., be classified as BEP) that is higher in fat versus one that is higher in sugar. Future studies should, therefore, consider the possibility that different types of PFs could induce different levels of binge eating proneness in addition to qualitative (i.e., regional specificity) or

quantitative (i.e., magnitude of Fos expression) differences in neural activity in the mesocorticolimbic circuit.

Finally, we did not monitor estrous cycles in the present study, which could be an important factor driving PF consumption, given the significant contribution of estradiol and progesterone to food intake and energy homeostasis [156]. However, it is unlikely that estrous cycles, alone, contributed to the consistent behavioral differences between BEPs and BERs, since animals in both groups were likely in various stages of the estrous cycle across the course of the feeding test period. In the future, it may be beneficial to either monitor estrous cycles throughout the study or experimentally control ovarian hormone exposure, as doing so could ensure that circulating hormone concentrations are equal between all rats throughout the feeding test period and on the day of the Fos induction protocol. Moreover, future work could investigate the role of ovarian hormones in contributing to the BEP/BER differences in neural responsiveness to PF within the mesocorticolimbic circuit, in light of the fact that ovarian hormones exert significant control over mesocorticolimbic responsiveness to other “synthetic” rewards, such as drugs of abuse and alcohol [157-159]. Future studies would also benefit from similar analyses of neural correlates for binge eating proneness using male rats to investigate whether there exist sex-specific and/or hormone-dependent mechanisms underlying binge eating risk.

Conclusions

In conclusion, results from this study largely support our initial hypothesis that binge eating proneness is associated with greater mesocorticolimbic responsiveness to PF. Greater activation of NAC and NAS in BEP vs. BER rats suggests that binge eating prone and binge eating resistant phenotypes differ in their perception of food reward and/or the motivation to

consume PF. However, differences between BEP and BER rats in the magnitude of PF-induced neural activity in the mPFC were more robust than in the NAC and NAS, suggesting that variations in executive control of PF consumption may be more strongly associated with binge eating risk. Overall, our findings prompt additional investigation of the relative contributions of reward-related mechanisms and executive functions to PF consumption in binge eating prone individuals.

Chapter 2

Activation of excitatory and inhibitory neurons in the mPFC following palatable food exposure in binge eating prone and binge eating resistant female rats

Introduction

Binge eating, defined as the consumption of a large amount of food (typically palatable food, PF), in a short period of time, is a core, maladaptive eating behavior that cuts across all major sub-types of eating disorders (EDs) that predominantly affect women, including anorexia, bulimia, binge eating disorder and other non-specified, sub-threshold EDs [124, 160]. Binge eating is associated with a loss of control over food intake [124], and women with EDs, and who binge-eat, possess trait characteristics that suggest abnormal behavioral regulation, such as high impulsivity, behavioral rigidity, and co-morbid substance abuse and dependence [33, 34, 161]. Because the prefrontal cortex (PFC) subserves the core executive functions that are disrupted in women with EDs, dysfunctional, PFC-mediated behavioral regulation may be an etiologic factor in the development of pathological eating behaviors that are inherent to EDs.

The rodent medial PFC (mPFC) is of particular relevance to the study of neural mechanisms underlying eating pathology, as the rodent mPFC also subserves the executive functions (i.e., behavioral inhibition, impulse control, action selection [82, 83, 153]) that appear to be disrupted in women with EDs. To date, however, few studies have directly assessed the role of the rodent mPFC to food intake, or the significance of mPFC neural activity to binge eating. Our lab recently sought to address this gap by characterizing patterns of neural activation (i.e., expression of the neural activation marker Fos) within the mPFC in response to a PF stimulus in a well-validated model of binge eating, which identifies binge eating prone (BEP)

and binge eating resistant (BER) rats based on consistently high or low intake of intermittently-presented PF [16, 131, 133-135]. Specifically, we found greater responsiveness of the cingulate (CG), prelimbic (PL), and infralimbic (IL) sub-regions of the mPFC in BEP rats as compared to BER rats, suggesting that differential engagement of the mPFC in response to a PF stimulus correlates with binge eating proneness [132]. One question that remains, however, is whether the PF-activated neurons in the mPFC of BEPs and BERs are primarily excitatory, glutamatergic projection neurons or inhibitory, GABAergic interneurons, and whether the proportions of PF-activated excitatory vs. inhibitory neurons differ between BEPs and BERs. This is of particular relevance to the mPFC as both excitatory and inhibitory neurons contribute to the executive functions subserved by the mPFC [61, 66, 69], and both excitatory and inhibitory neurons of the mPFC are activated (i.e., express Fos) in male rats during PF exposure and consumption [78].

Excitatory neurons of the mPFC comprise up to 80-90% of the total neuronal pool and project to several downstream targets (i.e., the nucleus accumbens, lateral hypothalamus, basolateral amygdala) that are implicated in food intake and motivated behaviors [44, 48]. In addition, parvalbumin (PV), somatostatin (SOM), and vasoactive intestinal peptide (VIP) neurons, which comprise 90% of the total inhibitory neuron pool [70], serve to regulate intrinsic excitability within the mPFC and fine-tune cortical circuitry during complex behavioral tasks [61, 154]. Though no studies, to date, have specifically investigated the contribution of excitatory vs. inhibitory neurons to food intake, *per se*, pharmacological inactivation of the mPFC leads to an increase in highly palatable food intake in male rodents, suggesting that the mPFC serves as a behavioral “brake” or limit over excessive PF intake [110, 111]. Since, pharmacological inactivation techniques primarily “turn off” *excitatory neuron activity*, such

studies indirectly suggest that, at baseline, the excitatory neurons of the mPFC facilitate the mPFC-mediated behavioral brake over PF intake.

Here, we sought to expand upon our initial finding of differential engagement of the mPFC by PF in BEP and BER female rats by identifying the magnitude of excitatory and inhibitory neuron responsiveness to PF in the two phenotypes. Specifically, since BEP rats consistently consume more PF than BER rats, we hypothesized that the mPFC-mediated, behavioral brake over PF intake is weaker in BEP rats as compared to BER rats. Since the mPFC-mediated limit on PF intake appears to be subserved by excitatory neurons of the mPFC, we specifically hypothesized that weaker control over PF intake in BEPs occurs as a consequence of ***lower excitatory*** neuron responsiveness to PF in BEPs relative to BERs. As an alternative, we also hypothesized that the mPFC-mediated brake over PF intake could be weaker in BEPs as compared to BERs because of ***greater inhibitory*** neuron responsiveness to PF in BEPs as compared to BERs. Greater inhibitory tone onto excitatory neurons of the mPFC during PF exposure could effectively dampen the strength of the excitatory neuron limit over PF intake in BEPs. To test these hypotheses, we induced Fos expression in the mPFC of BEP and BER female rats using an acute exposure to PF, and then employed double-label immunohistochemistry, using the excitatory neuron marker special AT-rich sequence-binding protein 2 (Satb2, [162]) and three, non-overlapping inhibitory neuron markers PV, SOM, and VIP, to identify the neuronal phenotypes of Fos-expressing neurons of BEPs and BERs. Specifically, we predicted that either 1) fewer excitatory neurons would be responsive to PF, or 2) more inhibitory neurons would be responsive to PF in BEPs than in BERs; the proportion of Fos-expressing excitatory neurons would be lower, while the proportion of Fos-expressing inhibitory neurons would be higher in BEPs as compared to BERs. Either outcome would

suggest that weaker, mPFC-mediated behavioral control over PF intake, due to either lower excitatory tone or greater inhibitory tone during PF exposure, contributes to binge eating proneness in female rats.

Methods

Animals and Housing

A total of 100 young adult (post natal day 60) female, Sprague-Dawley rats were obtained from Harlan Laboratories (Madison, Wisconsin) and were run in two separate cohorts of N=70 rats (cohort 1) and N=30 rats (cohort 2), due to spatial constraints within animal housing facilities. Upon arrival, rats were individually housed in clear Plexiglass cages (45 x 23 x 21 cm³) with enrichment and *ad libitum* access to chow (Harlan Teklad Global Diets: 8640, Madison, Wisconsin) and water. Rats were maintained on a 12:12 reverse light-dark cycle with lights out at 10:00AM, and were treated in accordance with the NIH Guide for the Care and Use of Laboratory Animals. All animal procedures were approved by the Michigan State University Institutional Animal Care and Use Committee.

Feeding Test Paradigm

Rats were allowed one week of acclimation to housing conditions and experimenter handling prior to the start of the feeding test period. Thereafter, all animals underwent two weeks of feeding tests, which included 6 total feeding test days. Feeding test days occurred on MWF and consisted of 4hrs of access to PF (~25g Betty Crocker® creamy vanilla frosting, 15% kcal from fat, 70% kcal from carbohydrate, 0% kcal from protein). PF was provided ~10 min prior to lights out via hanging food dishes in the home cages; standard rat chow (50-70g on cage tops) remained freely available during the PF exposure period. PF and chow were weighed at

the beginning of the feeding test and at the end of the 4hr exposure period using a standard electronic balance, and values were rounded to the nearest tenth of a gram. Any remaining PF at the end of 4hrs was removed from home cages, while chow remained freely available. On both feeding test days and non-feeding test days (i.e., days when PF was not provided) body weights and 24hr chow consumption were measured and recorded just before lights out.

Identifying BEP and BER Female Rats

Identification of BEP and BER rats followed the protocol previously published by Boggiano et al., 2007 [135], and used a tertile approach based on the 4hr PF intake values from each of the 6 feeding test days. The 4hr intake values were used for identification of BEP and BER phenotypes here, given that binge eating can be readily observed in animals within this discrete window of PF exposure [16, 131, 134, 135]. Four hour PF intake values from each feeding test day were divided into top, middle, and bottom tertiles; each rat scored within one of the three tertiles on each feeding test day. Rats were classified as BEP if they scored within the

Table 2.1) Proportions of BEP and BER rats identified in cohorts 1 and 2, CH 2

Sample sizes and proportions of BEP and BER rats from cohorts 1 and 2		
Phenotype	Cohort 1 (N = 70)	Cohort 2 (N = 30)
BER	14/70 (20%)	8/30 (27%)
BEP	21/70 (30%)	8/30 (27%)

highest tertile on at least 3 of the 6 (i.e., at least 50%) feeding test days and never in the lowest tertile; rats were classified as BER if they scored within the lowest tertile on at least 3 of the 6 feeding test days and never in the highest tertile. This method for identifying BEP or BER rats based on the consistency and frequency of high or low intake of intermittently-presented PF,

respectively, is similar to methods used in the human population for classifying binge eating status and identifying binge eaters and non-binge eaters [124, 131]. **Table 2.1** outlines the sample sizes and the proportions of BEPs and BERs that were identified using this method in each cohort.

Induction of Fos expression by PF exposure

One to three days following the final feeding test, all BEPs and BERs from cohorts 1 and 2 were given an additional 1hr of access to PF (~25g vanilla frosting) in their home cages in order to induce the expression of the neural activation marker Fos. The Fos induction paradigm began at lights out, in order to emulate feeding test conditions (i.e., exposure to PF at the onset of the dark cycle) as closely as possible. Chow and water remained in each rat's cage for the duration of the 1hr period of access to PF. At the end of 1hr, remaining PF was removed from each rat's cage, and 30 min later, rats were given a lethal dose of sodium pentobarbital (Fatal Plus®, 150mg/kg i.p.). A randomly selected group of 10 binge eating neutral rats (i.e., non-BEP/non-BER) served as no-PF controls, and were removed from their home cages 30-40 min after lights out and given a lethal dose of sodium pentobarbital (150mg/kg). Thereafter, all rats were intracardially-perfused with a buffered saline rinse for 15 min followed by 4% paraformaldehyde for 20 min. Following perfusions, brains were harvested, post-fixed overnight in 4% paraformaldehyde, and stored in 20% sucrose until sectioning. Brains were then cryostat-sectioned at 40µm into 4 series and tissue sections were stored at -20°C until further processing for single and double label Fos immunohistochemistry.

Single and Double Label Fos Immunohistochemistry (IHC)

Single label Fos IHC

One series of tissue sections through the mPFC of all BEPs and BERs from cohorts 1 and 2 and all no-PF control rats was processed for single label Fos immunohistochemistry. For immunohistochemical detection of Fos, all rinses were performed using Tris-Buffered Saline (TBS) and all antibody solutions were made in TBS containing 0.3% Triton X-100 and 2% normal goat serum. Tissue sections from the mPFC were rinsed three times and then incubated in a 1% hydrogen peroxide solution to quench endogenous peroxidase activity. Following three rinses, sections were incubated for 30 min in blocking solution containing 20% normal goat serum in TBS with 0.3% Triton X-100. Thereafter, sections were incubated in rabbit polyclonal anti-c-Fos (EMD Millipore, ABE457, 1:10,000) for 48hr at 4°C. Following three rinses, sections were incubated for 1hr in biotinylated goat anti-rabbit IgG (Vector Labs, 1:500), then rinsed three times before a 1hr incubation in avidin-biotin-peroxide complex diluted in TBS (ABC Elite kit, Vector Labs). Following three rinses, staining was completed using 3,3'-diaminobenzidine (DAB, 0.025% with 0.012% H₂O₂) in TBS to yield a brown nuclear reaction product. Fos-stained sections were mounted onto glass slides, air-dried, dehydrated using a series of ethanols, and coverslipped. Control tissue, which excluded primary and secondary antibodies, was run using mPFC tissue from binge eating neutral rats that were exposed to PF prior to sacrifice. Control tissue yielded no Fos staining and little to no non-specific background staining. Of note, this same control tissue was used in all four of the double label experiments listed below, and in each run, little to no non-specific background staining was visualized.

Double Label Fos-Satb2 Immunofluorescence

An additional series of tissue sections from all BEPs (N=21) and BERs (N=14) from cohort 1 were processed for Fos-Satb2 immunofluorescence following a sequential double-labeling protocol. Specifically, two anatomically matched tissue sections from the caudal half of the mPFC from each BEP and BER were processed for Fos-Satb2 immunofluorescence. Fluorescent probes were used for the detection of Fos-Satb2 labeling as both Fos and Satb2 are nuclear markers [162]. All rinses were performed using Tris-Buffered Saline (TBS) and all antibody solutions were made in TBS containing 0.3% Triton X-100 with 2% normal goat serum and 5% bovine serum albumin. Tissue sections were first rinsed three times and then incubated in a 0.1% sodium borohydride solution to quench endogenous aldehyde activity and reduce auto-fluorescence. Following three rinses, sections were incubated for 30 min in blocking solution containing 20% normal goat serum and 10% bovine serum albumin in TBS with 0.3% Triton X-100. Thereafter, sections were incubated in rabbit polyclonal anti-c-Fos (Santa-Cruz, #sc-52, 1:10,000) for 48hr at 4°C. Following three rinses, sections were incubated overnight at 4°C in biotinylated goat anti-rabbit IgG (Vector Labs, 1:500), then rinsed six times before incubating for 2hr in Cy3-conjugated streptavidin (Jackson labs, 1:1000) in order to amplify the Fos signal. Following another six rinses, sections were incubated in mouse monoclonal anti-Satb2 (Abcam, SATBA4B10, 1:200) for 48hr at 4°C. Thereafter, sections were rinsed three times and incubated overnight at 4°C in Cy2-conjugated goat anti-mouse IgG (Jackson labs, 1:500). After six rinses, stained sections were mounted onto glass slides, air-dried, and coverslipped with *SlowFade*® Gold Antifade Mountant (ThermoFisher Scientific). Slides were sealed and kept at -20°C until microscopic analyses were performed.

Double Label Fos-PV, Fos-SOM, Fos-VIP IHC

An additional series of tissue sections through the mPFC from one half of BEPs and one half of BERs from cohort 1 was processed for either Fos-PV or Fos-SOM immunohistochemistry using a sequential, double-labeling protocol. For Fos-PV, sample sizes were N=11 BEP and N=7 BER; for Fos-SOM sample sizes were N=10 BEP and N=7 BER. In addition, all BEPs (N=8) and BERs (N=7) from cohort 2 were processed for Fos-VIP, also using a sequential double-labeling protocol. Tissue sections through the mPFC were first processed for Fos immunohistochemistry following the protocol outlined above (see **Single Label Fos IHC**), except Fos staining was completed using Nickel-DAB (Nickel Sulphate 2.5%; DAB, 0.02% with 0.003% H₂O₂) in sodium acetate buffer, yielding a black nuclear reaction product. For Fos-PV or Fos-VIP, tissue sections were then incubated for an additional 48hr at 4°C in mouse monoclonal anti-PV (Sigma-Aldrich, PARV-19, 1:100,000) or rabbit polyclonal anti-VIP (Immunostar, #20077, 1:4,000). Following three rinses, sections were incubated for 1hr in either biotinylated goat anti-mouse IgG, for Fos-PV, or biotinylated goat anti-rabbit IgG for Fos-VIP (Vector Labs, 1:500 for both PV and VIP). Sections were then rinsed three times before incubating for 1hr in ABC diluted in TBS. Following three rinses, staining was completed using DAB (0.025% with 0.012% H₂O₂) in TBS to yield brown cytoplasmic reaction products. For Fos-SOM, following single Fos staining with Nickel-DAB, tissue sections were incubated for an additional 1hr in blocking solution (20% normal goat serum with 20 µg/mL goat anti-rat Fab fragment in TBS with 0.3% Triton X-100). Thereafter, sections were incubated for 72hr at 4°C in rat monoclonal anti-SOM (Millipore, MAB354, 1:100), and following three rinses, sections were incubated for 1hr in biotinylated goat anti-rat IgG (Vector Labs, 1:500). Sections were rinsed three times before incubating for 1hr in ABC diluted in TBS. Following three rinses,

staining was completed using DAB in TBS to yield a brown cytoplasmic reaction product. All Fos-PV, Fos-VIP, and Fos-SOM labeled sections were mounted onto glass slides, air-dried, dehydrated using a series of ethanols, and coverslipped.

Quantification of Fos-expressing excitatory and inhibitory neurons in the mPFC

Stereological estimates of single label Fos-immunoreactive (Fos-ir) Cell Number

The total number of Fos-ir cells in the cingulate (CG), prelimbic (PL), and infralimbic (IL) sub-regions of the mPFC was estimated using unbiased stereological methods with the optical fractionator method in StereoInvestigator (MicroBrightfield Biosciences, Willingston, VT). Tracings of each sub-region and all cell counts were performed using an Olympus BX51 microscope and Q-Imaging Color 12 bit camera by an experimenter blind to the experimental group (i.e., No PF control, BER, or BEP) of each animal. Four sections through the rostro-caudal extent of the mPFC were counted for each animal, with sections corresponding to plates 9–12 (+3.72mm to +2.76mm from Bregma) of the Paxinos and Watson rat brain atlas [145]. The CG, PL and IL sub-regions were all traced relative to the forceps minor (fmi). Tracings of the mPFC were performed under a 4X (NA 0.13) air objective, and counts were performed with a 40X (NA 0.85) air objective. Within the optical fractionator probe, the counting frame was set to $100\ \mu\text{m}^2$ within a grid size of $250\ \mu\text{m}^2$, and the optical dissector height was set to $6\ \mu\text{m}$ with top and bottom guard zones of $2\ \mu\text{m}$.

Quantification of Fos-Satb2 Immunofluorescence

Quantification of Fos-Satb2 immunofluorescence was performed by an experimenter blind to the experimental group of the animal under epi-illumination using an Olympus BX51 microscope equipped with a mercury arc lamp and both FITC and TRITC filters. Two sections through the caudal half of the mPFC were analyzed for each animal, with sections corresponding

to plates 11 and 12 (+3.00mm to +2.76mm from bregma) of the rat brain atlas. CG, PL and IL sub-regions were traced relative to the fmi under a 4X (NA 0.13, UPlanFl) air objective, and counts were performed with a 40X (NA 0.85, UPlanApo) air objective using the meander scan function in Neurolucida (Version 7, Microbrightfield, Willingston, VT). Single label Fos and double label Fos-Satb2 were counted in each mPFC sub-region, in order to identify 1) the proportion of all Fos-ir neurons that co-localized with Satb2, and 2) the total number of Satb2⁺ neurons that expressed Fos. For proportional analyses in each mPFC sub-region, the total number of double-labeled cells was first calculated by summing across each tissue section and across both hemispheres. The total number of double-labeled Fos⁺/Satb2⁺ neurons was then divided by the total number of Fos-ir neurons across each tissue section and across both hemispheres: (#Fos-Satb2⁺ neurons) / (#Fos-Satb2⁺ neurons + #Fos⁺ neurons).

Quantification of Double-Label Fos-PV, Fos-SOM, Fos-VIP IHC

Quantification of Fos-PV, Fos-VIP, and Fos-SOM was performed by an experimenter blind to the experimental group of each animal under brightfield microscopy using an Olympus BX51 microscope. Four sections through the rostro-caudal extent of the mPFC were analyzed for each animal, with sections corresponding to plates 9–12 (+3.72mm to +2.76mm from Bregma) of the rat brain atlas. CG, PL and IL sub-regions were traced relative to the fmi under a 4X (NA 0.13) air objective, and counts were performed with a 40X (NA 0.85) air objective using the meander scan function in Neurolucida (Version 7, Microbrightfield). Single label Fos, double label Fos-PV, Fos-VIP, or Fos-SOM, and single label PV, VIP, or SOM were counted in each mPFC sub-region, in order to identify 1) the proportions of all Fos-ir neurons that co-localized with each inhibitory neuron marker, 2) the total numbers of inhibitory neurons that were activated by PF, and 3) the proportions of all PV-ir, SOM-ir, or VIP-ir neurons that co-

localized with Fos. The proportions of all Fos-ir neurons that co-localized with PV, SOM, or VIP were calculated as outlined above for *Satb2*. The proportions of all PV-ir, SOM-ir, or VIP-ir neurons that expressed Fos were calculated in a similar fashion: (#double-labeled GABA neurons) / (#double-labeled neurons + #PV⁺, SOM⁺, or VIP⁺).

Statistical Analyses

All statistical analyses were conducted using the Statistical Package for the Social Sciences (SPSS), version 22.0, with the alpha level set to $p < 0.05$ for all analyses

Behavioral differences between BEPs and BERs

PF and chow consumption and body weights were compared between BEPs and BERs using individual mixed design ANOVAs; the within-subjects factor was test day while the between subjects factor was binge phenotype. Cohort was included as a covariate in the model. Cohen's d effect sizes were calculated for each dependent variable, to determine the magnitude of the mean differences between the two phenotypes (small: $d = 0.20$; medium: $d = 0.50$; large: $d = 0.80$).

Single label Fos IHC

Total Fos-ir cell number was analyzed between the three experimental groups in each brain region using individual one-way ANOVAs with two planned contrasts when the overall ANOVA was significant: 1) BEP+BER vs. Control (i.e., PF vs. No PF), and 2) BEP vs. BER. Planned contrasts allowed for a direct analysis of the effect of PF, alone, on the magnitude of neural activation in the mPFC, as well as a specific analysis of phenotypic differences in neural responsiveness to PF in the mPFC. As a follow up analysis, ANCOVAs, using total PF consumed at sacrifice as the covariate, were calculated for the BEP vs. BER comparison in each

brain region, to ensure that BEP vs. BER differences in Fos expression were not simply driven by between-phenotype differences in the absolute amount of PF consumed prior to sacrifice. This was an important consideration, here, as PF intake during the 1hr access period on the Fos induction day was significantly higher in BEPs than in BERs {M (*S.E.*), **BEP**: 5.33 (0.27); M (*S.E.*), **BER**: 3.93 (0.22); $t(50) = -3.90, p < 0.01$ }. Cohen's *d* effect sizes were also calculated for the BEP vs. BER comparisons, using ANCOVA-adjusted means, in each brain region.

Double label Fos IHC

The proportions of total Fos-ir cells expressing Satb2, PV, SOM, and VIP were compared between BEPs and BERs using independent samples t-tests in each brain region. The total number of double-labeled cells, for each neuronal marker, was compared between BEPs and BERs using individual ANCOVAs in each brain region, with the amount of PF consumed at sacrifice included as a covariate. Similarly, for each inhibitory neuron marker, the proportions of all PV, VIP, or SOM-ir neurons that expressed Fos were also compared between BEPs and BERs using individual ANCOVA analyses within each brain region, also using PF consumed at sacrifice as the covariate. Cohen's *d* effect sizes were calculated for each comparison listed above (i.e., for both proportional comparisons and for the comparisons of total, double-labeled number) within each brain region.

Results

Behavioral differences between BEPs and BERs across the feeding test period

Results from the mixed design ANOVAs for PF, chow, and body weights from the feeding test period are displayed in **Table 2.2**. As expected, on feeding test days, BEPs

Table 2.2) PF and chow intake and body weights in BEPs and BERs, CH 2

Mean comparisons between BEP and BER rats on PF, chow, and body weights across the feeding test period

Variable	Mean (S.E.)	BEP vs. BER Mean Comparisons	
		Statistics	Effect Size
		<i>F</i> (1,49)	Cohen's <i>d</i>
Body weights (g)			
BER	196.03 (1.61)	0.47	0.19
BEP	197.52 (1.43)		
<i>Feeding test days</i>			
PF intake (4h, g)			
BER	5.97 (0.14)	289.45***	4.77
BEP	9.16 (0.12)		
PF intake (4h, kcal)			
BER	25.26 (0.61)	276.03***	4.63
BEP	38.89 (0.55)		
Chow intake (4h, g)			
BER	2.46 (0.15)	0.35	0.16
BEP	2.58 (0.13)		
Chow intake (24h, g)			
BER	9.82 (0.25)	24.85***	1.39
BEP	8.17 (0.22)		
<i>Non-feeding test days</i>			
Chow intake (24h, g)			
BER	13.67 (0.21)	3.52†	0.53
BEP	13.14 (0.19)		

Note: PF intake in kcal calculated based on the value of 4.24 kcal/gm for the vanilla frosting. Cohen's *d* interpretation: small, *d* = 0.20; medium, *d* = 0.50; large, *d* = 0.80.

****p* < 0.001; †*p* < 0.10.

consumed significantly more PF in 4hr as compared to BERs, with no differences in 4hr chow consumption. BERs consumed more chow in 24hr on feeding test days as compared to BEPs; this outcome is expected given the high consumption of PF by BEPs on feeding test days. Chow consumed in 24hr on non-feeding test days did not differ between the two phenotypes nor did body weights across the testing period.

Neural Responsiveness to PF in the mPFC

Owing to poor tissue quality following perfusions or poor staining quality following Fos immunohistochemistry, tissue sections from 7 BEPs and 6 BERs were omitted from the single label Fos analysis, leaving a final sample size of N=10 no-PF controls, N=16 BERs, and N=22 BEPs. ANOVAs revealed significant main effects of experimental group in the CG $\{F(2, 45) = 3.85, p = 0.029\}$, the PL $\{F(2, 46) = 6.37, p = 0.004\}$, and the IL $\{F(2, 46) = 5.26, p = 0.009\}$ (**Figure 2.1 and Table 2.3**). Significant main effects in each brain region were solely driven by the comparison of PF exposure (i.e., BEP + BER) to no PF exposure (i.e., Controls). Specifically, planned contrasts revealed significant differences between the combined group of BEPs + BERs vs. the no PF controls in each brain region (CG: $p = 0.01$; PL: $p = 0.001$; IL: $p =$ revealed only small effects for the BEP vs. BER comparisons in each brain region (**Table 2.3**).

Excitatory neuron responsiveness to PF in the mPFC of BEPs and BERs

Tissue sections from 1 BER and 2 BEPs were omitted from the Fos-Satb2 analysis because of poor staining quality, yielding a final sample size of N=13 BERs and N=19 BEPs. BEPs and BERs did not differ in the proportion of Fos⁺ neurons co-localized with Satb2 in any brain region (**Figure 2.2 and Table 2.4**). In both BEPs and BERs, approximately 85% of all Fos⁺ neurons were co-localized with Satb2 (**Figure 2.2 and Table 2.4**).

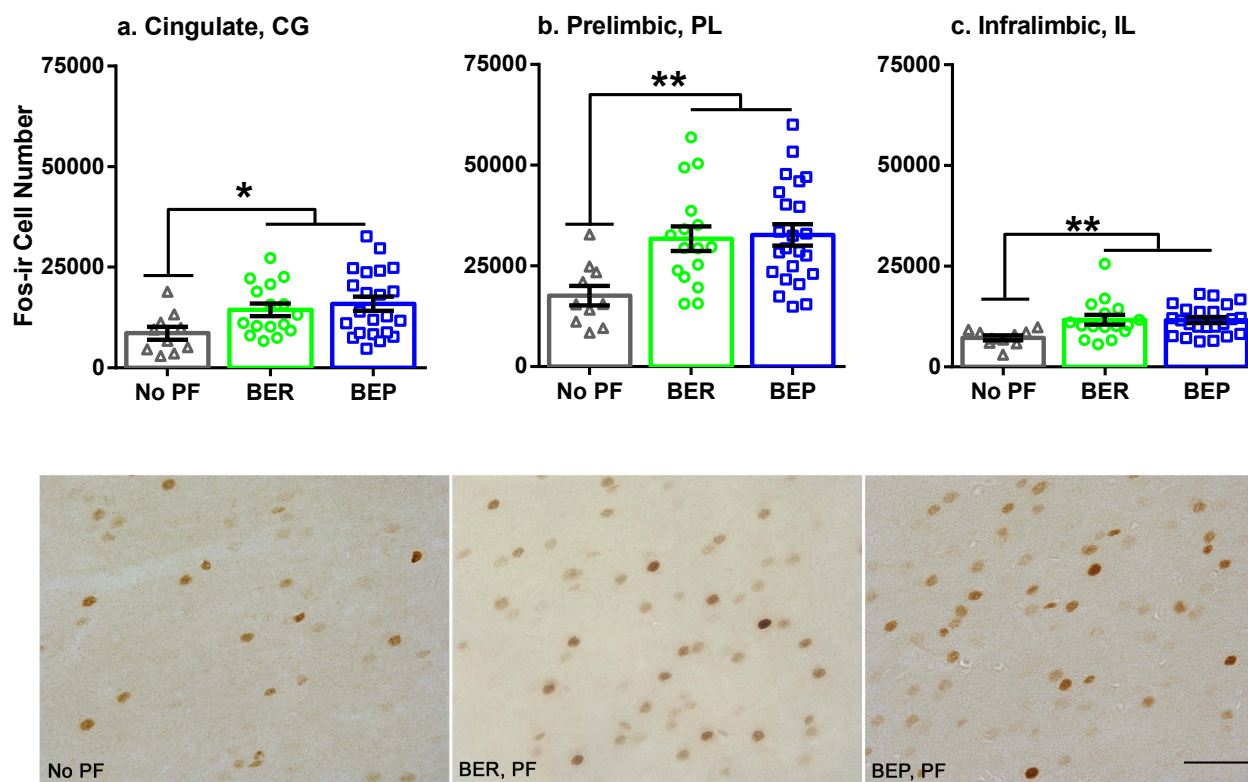


Figure 2.1) Single Fos expression in the CG, PL, and IL cortex of No PF control rats, BEPs and BERs, CH 2

Total number of Fos-ir cells in the CG (a), PL (b), and IL (c) of No PF control rats and BEP and BER rats exposed to PF just prior to sacrifice. Error bars represent one S.E.M. Bottom panel shows representative Fos-ir cells in the PL of a No PF control (left), a BER exposed to PF (center), and a BEP exposed to PF (right). Scale bar represents 50 μ m.

* $p < 0.05$, ** $p < 0.01$ based on planned contrast comparing BEP+BER rats (PF) to controls (no PF).

Table 2.3) Single Fos expression in No PF control rats and BEP and BER rats exposed to PF

Mean comparisons of Fos expression in the mPFC between No PF control rats and BEPs and BERs exposed to PF

Brain Region					<i>Pairwise Comparisons</i>		
	Mean (S.E.)		Group Main Effect		Planned contrast		Effect size ²
	No PF ¹	BER	BEP	<i>F</i> (df)	<i>t</i> -value		Cohen's <i>d</i>
					PF vs. No PF	BEP vs. BER	BEP vs. BER
Cingulate	8576.1 (1587.57)	14403.2 (1570.20)	15909.9 (1729.76)	3.85* (2, 45)	-2.64**	-0.66	0.18
Prelimbic	17603.38 (2448.49)	31730.66 (3053.49)	32646.03 (2606.90)	6.37** (2, 46)	-3.53**	-0.24	0.07
Infralimbic	7237.37 (628.05)	11666.72 (1215.53)	11618.17 (748.61)	5.26** (2, 46)	-3.24**	-0.04	0.01

Note: ¹No PF group included non-BEP/non-BER that served as home-cage controls.

²Cohen's *d* values for BEP v. BER comparisons were calculated using ANCOVA-adjusted means, with the total amount of PF consumed at sacrifice as the covariate; ** $p \leq 0.01$; * $p < 0.05$.

Though the proportions of Fos-ir neurons that were of the excitatory neuron phenotype did not differ between BEPs or BERs in any brain region, ANCOVA analyses of the total number of Fos⁺/Satb2⁺ neurons within the mPFC (co-varied by PF intake) revealed that total Fos⁺/Satb2⁺ neuron number *was lower* in the PL and IL of BEPs relative to BERs (**Figure 2.3 and Table 2.5**). Specifically, the BEP vs. BER comparison of total Fos⁺/Satb2⁺ neuron number reached trend level significance in the PL $\{F(1, 29) = 3.10, p = 0.08\}$ and was significantly lower in BEPs than in BERs in the IL $\{F(1, 26) = 5.61, p = 0.02\}$. These data suggest that while the absolute number of mPFC neurons that are activated by PF is similar in BEPs and BERs (i.e., assessed by the stereological analysis of Fos-ir cell number), the magnitude of ventral mPFC excitatory neurons that are activated by PF is lower in BEPs as compared to BERs.

Inhibitory neuron responsiveness to PF in the mPFC of BEPs and BERs

Inhibitory neurons in the mPFC of BEPs and BERs were responsive to PF, but they comprised only a small proportion, between 5-20%, of the total population of Fos⁺ neurons in BEPs and BERs (**Figure 2.2 and Table 2.4**). Moreover, BEPs and BERs did not differ in the proportions of Fos⁺ neurons that co-localized with each inhibitory neuron marker. In BERs, an average of 2.1% of Fos⁺ neurons co-localized with PV, 14.1% with SOM, and 1.5% of Fos⁺ with VIP. Similarly, in BEPs, an average of 2.4% of Fos⁺ neurons co-localized with PV, 15.1% with SOM, and 1.6% with VIP.

The total numbers of Fos⁺/PV⁺, Fos⁺/SOM⁺, and Fos⁺/VIP⁺ neurons (co-varied by PF intake) did not differ, statistically, between BEPs and BERs in any brain region, but effect size estimates revealed medium-to-large effects for the Fos⁺/PV⁺ and Fos⁺/SOM⁺ comparisons, in select brain regions, between the two phenotypes (**Figure 2.4 and Table 2.6**). The total number of Fos⁺/PV⁺ neurons was consistently higher in *BERs vs. BEPs*, with a small effect size in the IL,

($d = 0.28$), but large effect sizes in the CG ($d = 0.75$) and the PL ($d = 0.87$). On the other hand, the total number of Fos⁺/SOM⁺ neurons was consistently higher in *BEPs* vs. *BERs*, with a small effect size in the PL ($d = 0.37$), but medium-to large effects in the CG ($d = 0.79$) and the IL ($d = 0.80$). The number of Fos⁺/VIP⁺ neurons did not differ between BEPs and BERs in any brain region, and effect size estimates were only small-to-medium in magnitude (CG: $d = 0.04$; PL: $d = 0.47$; IL $d = 0.03$).

The magnitude of PV, SOM, and VIP neuron responsiveness to PF (co-varied by PF intake) also did not differ between BEPs and BERs in any brain region, though there were marked differences in the degree of neuronal activation (i.e., upon visual inspection) when comparing across each sub-type of inhibitory neuron (**Figure 2.4 and Table 2.7**). In BERs, an average of 32.9% of all SOM neurons and an average of 16.7% of all VIP neurons were Fos⁺, while only 1.7% of all PV neurons expressed Fos following PF exposure. Similarly, in BEPs, average proportions were 32.6% for all SOM neurons, 17.3% for all VIP neurons, but only 1.7% for all PV neurons.

Discussion

Our study is the first to identify that both excitatory and inhibitory neurons of the mPFC are responsive to PF in female rats and in a model of binge eating proneness. First, we demonstrate that although PF, alone, induces significant neural activation in the mPFC, BEPs and BERs do not appear to differ in their overall, global responsiveness to PF within the mPFC. We also demonstrate that a vast majority of PF-activated neurons within the mPFC are excitatory projection neurons, regardless of binge phenotype, suggesting that the excitatory neuron population facilitates the mPFC-mediated “brake” on PF intake in both BEPs and in BERs. In

Table 2.4) Proportions of Fos⁺ neurons co-localized with excitatory and inhibitory markers in the mPFC of BEP and BER rats

Mean comparisons between BEP and BER rats in proportions of all Fos⁺ neurons co-localized with excitatory marker Satb2 and inhibitory markers PV, SOM, and VIP

Neuronal Marker	Mean % (S.E.) ¹	<i>Mean Comparisons</i>	
		BEP vs. BER	
		Statistics	Effect Size
		<i>t</i> (df)	<i>Cohen's d</i>
<i>Proportion Fos⁺ with Satb2</i>			
Cingulate			
BER	89.8 (0.02)	-0.83 (31)	0.33
BEP	91.5 (0.01)		
Prelimbic			
BER	85.8 (0.01)	-0.43 (31)	0.14
BEP	86.3 (0.01)		
Infralimbic			
BER	78.8 (0.02)	-0.13 (31)	0.05
BEP	79.2 (0.02)		
<i>Proportion Fos⁺ with PV</i>			
Cingulate		<i>t</i> (df)	<i>Cohen's d</i>
BER	1.01 (0.41)	0.28 (16)	0.14
BEP	0.86 (0.33)		
Prelimbic			
BER	2.58 (0.29)	-0.66 (16)	0.25
BEP	3.07 (0.55)		
Infralimbic			
BER	2.66 (0.60)	-1.06 (16)	0.53
BEP	3.43 (0.45)		
<i>Proportion Fos⁺ with SOM</i>			
Cingulate		<i>t</i> (df)	<i>Cohen's d</i>
BER	13.91 (2.65)	-0.45 (15)	0.23
BEP	15.56 (2.42)		
Prelimbic			
BER	13.56 (2.15)	0.36 (15)	0.18
BEP	12.69 (1.38)		
Infralimbic			
BER	14.73 (2.48)	-0.87 (15)	0.43
BEP	17.09 (1.50)		
<i>Proportion Fos⁺ with VIP</i>			
Cingulate		<i>t</i> (df)	<i>Cohen's d</i>
BER	1.54 (0.20)	-0.31 (11)	0.18
BEP	1.66 (0.34)		
Prelimbic			

Table 2.4 (cont'd)			
BER	1.44 (0.13)	0.30 (12)	0.16
BEP	1.38 (0.16)		
Infralimbic			
BER	1.66 (0.22)	0.13 (12)	0.07
BEP	1.59 (0.46)		

[†] Percentages represent all Fos⁺ neurons co-localized with Satb2, PV, SOM, or VIP

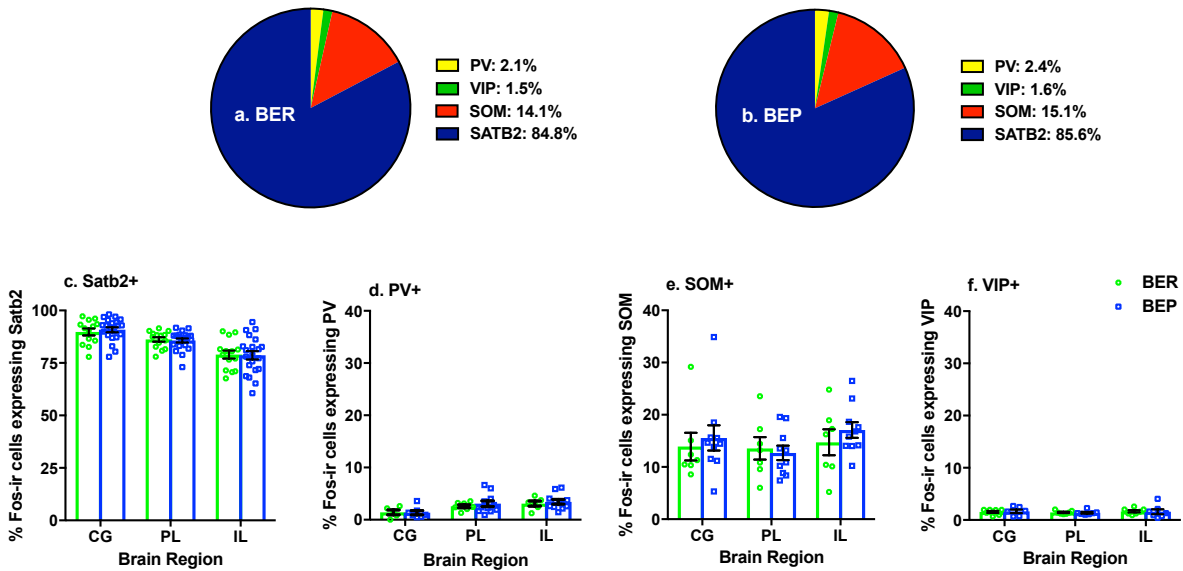


Figure 2.2) Proportions of Fos-expressing excitatory and inhibitory neurons within the mPFC of BEP and BER rats

Pie charts represent mean proportions (averaged across brain region) of all Fos⁺ neurons co-localized with excitatory and inhibitory neuron markers in BERs (a) and BEPs (b). Bottom panel shows proportions of Fos⁺ neurons, separated by brain region, co-localized with excitatory neuron marker Satb2 (c) or inhibitory neuron markers PV (d), SOM (e), and VIP (f). Error bars represent one S.E.M.

Table 2.5) Total number of Fos⁺ neurons co-localized with excitatory neuron marker Satb2 in the mPFC of BEP and BER rats

Mean comparisons between BEPs and BERs on the total number of Fos⁺ neurons expressing Satb2 in the mPFC

Brain Region	Mean (S.E.) ¹	<u><i>Mean Comparisons</i></u> BEP vs. BER	
		Statistics	Effect Size ²
		<i>F</i> (df)	Cohen's <i>d</i>
Cingulate			
BER	218.9 (37.93)	1.38 (1, 29)	0.44
BEP	158.9 (30.82)		
Prelimbic			
BER	449.5 (55.47)	3.10† (1, 29)	0.66
BEP	318.1 (45.07)		
Infralimbic			
BER	170.8 (17.35)	5.61* (1, 26)	0.92
BEP	117.1 (13.32)		

Note: ¹Means represent ANCOVA adjusted means using PF consumed prior to sacrifice as the covariate; ²Effect sizes were calculated using ANCOVA-adjusted means; * $p < 0.05$; † $p < 0.09$.

addition, though BEPs and BERs did not differ in the *proportions* of PF-activated excitatory vs. inhibitory neurons within the mPFC, the *number* of PF-activated excitatory neurons was *lower* in BEPs as compared to BERs. Thus, our data support our initial hypothesis that weaker, mPFC-mediated control over PF intake, due to reduced activation of mPFC excitatory neurons during PF exposure, may be associated with binge eating proneness.

PF elicits neural activation in the mPFC, but overall mPFC responsiveness to PF does not differ between BEPs and BERs

BEPs and BERs exposed to PF, as a whole, displayed significantly higher neural activation in each sub-region of the mPFC as compared to rats without exposure to PF, which replicates past studies in our lab [132] and confirms that PF intake strongly engages neurons within the mPFC. Surprisingly, however, we found *no differences* in Fos expression between BEPs and BERs in any sub-region of the mPFC, despite the significant effects (BEP>BER, all sub-regions) in a previous study from our lab [132]. Notably, however, the types of PFs used for both the feeding test paradigm and the Fos induction protocol differed substantially between the two studies, and likely contributed to the discrepancy in outcomes. In our previous study we used high-fat pellets (45% kcal from fat, 35% kcal from carbohydrates), rather than the vanilla frosting used here (15% kcal from fat, 70% kcal from carbohydrates), for the feeding tests and for the Fos induction protocol. Though BEPs ate significantly more PF than BERs in both studies, the magnitude of the difference in PF intake between BEPs and BERs when using the high fat pellets was higher. Here, BEPs ate, on average, ~13 kcal more than BERs across the testing period, while in our past study using high-fat pellets, BEPs ate, on average, ~22 kcal

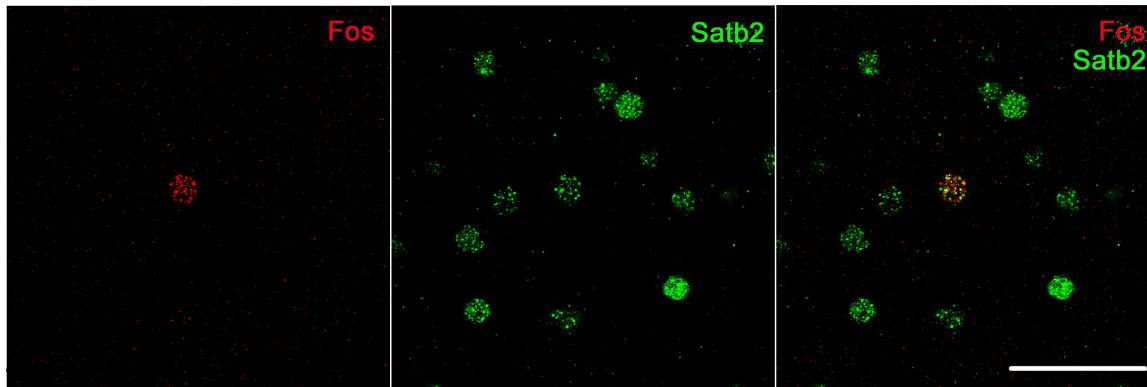
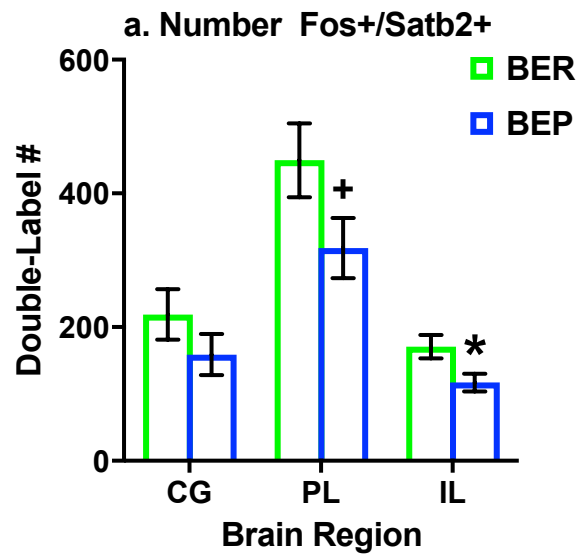


Figure 2.3) Number of activated excitatory neurons in the mPFC of BEP and BER rats

Total number of Fos⁺/Satb2⁺ neurons in the mPFC of BEP and BER rats (a). Values for double label # in BEPs and BERs represent ANCOVA-adjusted means, using PF consumed prior to sacrifice as the covariate. Error bars represent one S.E.M. Image panel depicts a Fos⁺ neuron co-localized with Satb2. Scale bar represents 50µm.

^{*} $p < 0.05$, ⁺ $p < 0.09$.

more than BERs across testing. In addition, both BERs and BEPs ate more of the high-fat PF, overall, than the vanilla frosting: on average BEPs ate 63.7 kcal of the high fat pellets, but only 38.9 kcal of the vanilla frosting, while BERs ate, on average, 41.6 kcal of the high fat pellets but only 25.3 kcal of the vanilla frosting [132]. Thus, the neural response of the mPFC to a high fat PF may also be inherently different, given the differences in total intake with the two types of PFs, than the response of the mPFC to the vanilla frosting, used here. That is, while the BEP vs. BER difference in PF intake was conserved across studies, regardless of the type of PF used, the magnitude of mPFC activation to PF, and consequently the degree of between-phenotype differences in mPFC responsiveness to PF, may vary depending on which PF source is used. In the future, it will be necessary to determine whether the macronutrient content of a particular PF source interacts with binge eating phenotype to affect the number of PF-activated neurons within the mPFC of female rats.

Reduced excitatory neuron responsiveness to PF may be associated with binge eating proneness

Our analysis of Fos expression in Satb2⁺ neurons, a marker for excitatory projection neurons of the mPFC [78, 162, 163], revealed that in both BEPs and BERs, most of the Fos⁺ neurons were co-localized with Satb2: an average of ~85% of all Fos⁺ neurons were Satb2⁺ in BERs and in BEPs. The high degree of Fos co-localization with Satb2⁺ was an expected finding given that up 80-90% of all neurons in the mPFC are excitatory neurons [44], and given that most of the mPFC neurons that are activated in response to high fat consumption in male mice are also primarily excitatory neurons [78]. Thus, our data extend results from other labs by demonstrating that most of the mPFC neurons that are activated by a high-fat/high-sugar PF source in female rats are of the excitatory phenotype. Moreover, our data confirm that the

functional relevance of the mPFC to PF consumption and to food reward in female rats appears to be primarily driven by excitatory neurons of the mPFC.

Despite a lack of BEP vs. BER differences in the proportions of Fos⁺ neurons co-localized with Satb2, our analysis of the total number of Fos⁺/Satb2⁺ neurons revealed that BEPs had a substantially lower number of Fos⁺/Satb2⁺ neurons in the PL cortex and a significantly lower number of Fos⁺/Satb2⁺ neurons in the IL cortex as compared to BERs. Thus, the magnitude of excitatory neuron responsiveness to PF was *lower* in BEPs relative to BERs, supporting our primary hypothesis that *reduced excitatory neuron responsiveness to PF is associated with binge eating proneness*. Reduced ventral mPFC (i.e., PL and IL) excitatory neuron responsiveness to PF in rats that are *prone* to binge eating is in line with the known function of the PL and IL in the context of basic behavioral regulation: the PL and IL facilitate behavioral inhibition and impulse control in rodents [82, 83, 87, 89]. Though this is typically demonstrated in cognitive behavioral tasks in rodents [80, 153], emerging evidence suggests that the ventral mPFC also exerts a behavioral control over food intake. Pharmacological inactivation of the ventral mPFC enhances the amount of time rats spend engaged in bouts of PF consumption [76, 110], and pharmacological inactivation of the PL significantly enhances intake of a high-fat diet [111]. Since we, here, identified that most of the PF-activated neurons of the mPFC are excitatory neurons, we can reasonably assume that the mPFC-mediated, behavioral “brake” over food intake is subserved by excitatory neurons of the mPFC. Thus, our data suggest that the strength of an mPFC-mediated “brake” over PF intake may be *weaker* in BEP rats due to reduced responsiveness of excitatory neurons in the presence of PF.

Future research with this model could confirm the downstream projection targets of the PF-activated excitatory neurons identified here, namely, that a large majority of PF-activated

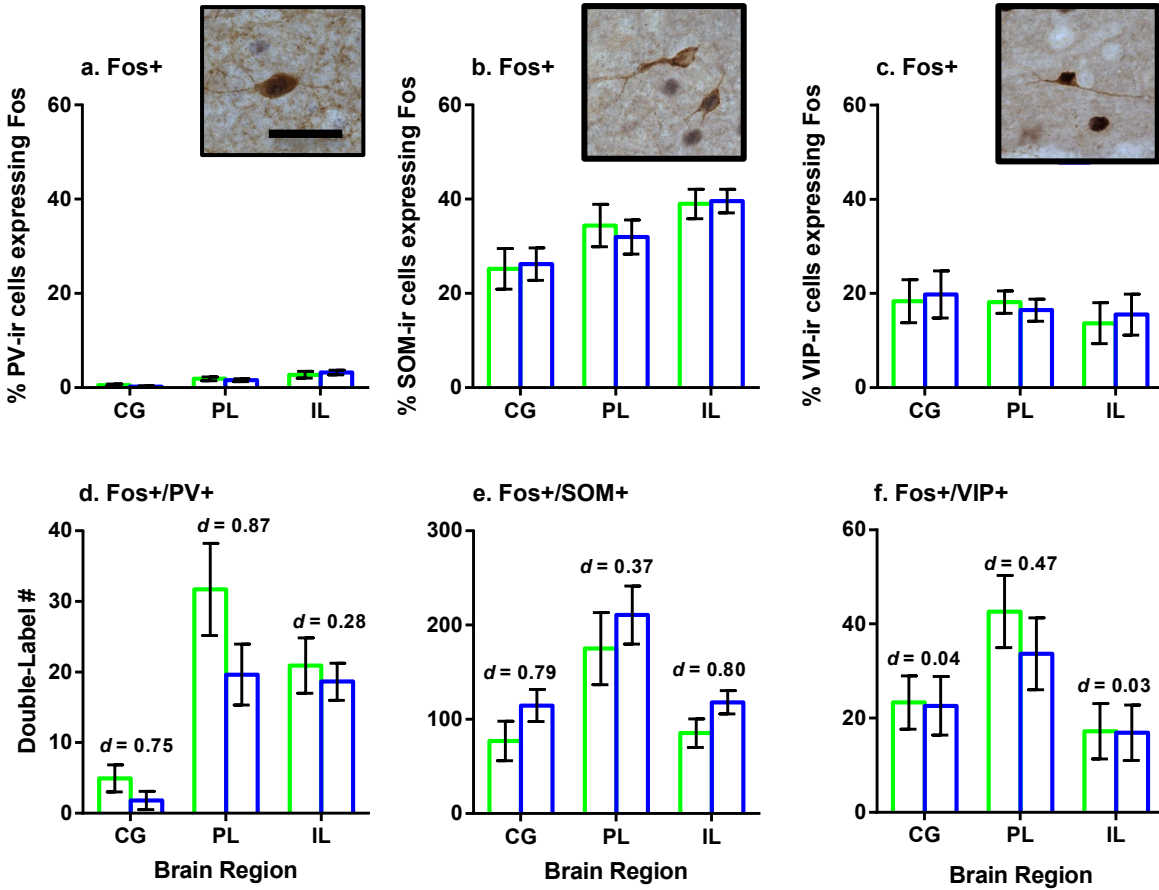


Figure 2.4) Proportions and total numbers of activated inhibitory neurons in the mPFC of BEP and BER rats

Top panel represents the proportions of all PV (a), SOM (b), or VIP⁺ (c) neurons expressing Fos in response to PF in the mPFC of BEPs and BERs, with representative images of Fos-PV, Fos-SOM, and Fos-VIP neurons. Scale bar represents 50 μ m. Middle panel represents total numbers of double-labeled PV (d), SOM (e), or VIP (f) neurons in the mPFC of BEP and BER rats. All values in a-f represent ANCOVA-adjusted means, using PF consumed prior to sacrifice as the covariate. Cohen's d effect sizes are presented for each BEP v. BER comparison in (d) – (f). Error bars represent one S.E.M.

excitatory neurons project to the nucleus accumbens. Confirming that a large majority of the PF-activated excitatory neurons project to the nucleus accumbens and that, perhaps, fewer accumbens-projecting mPFC neurons are activated by PF in BEPs vs. BERs would further suggest that the mPFC limits PF intake (to a lesser degree in rats prone to binge eating) through glutamatergic projections into accumbens circuitry. Specifically, we found a significant difference in the number of PF-activated excitatory neurons between BEPs and BERs in the IL cortex, and the IL cortex sends dense glutamatergic input to the accumbens shell. The nucleus accumbens shell houses a vast population of mu opioid receptors that not only enhance the hedonic, pleasurable response to food rewards, but that also increase the consumption of food rewards [101, 148, 152]. The increase in consumption that can be driven by the accumbens shell, however, is suppressed by activating glutamatergic signaling within the accumbens shell, much of which may originate from the IL cortex [112, 113, 115, 116]. Thus, future research could utilize combined retrograde labeling with Fos immunohistochemistry in the mPFC to identify the predominant downstream projection targets of the PF-activated excitatory neurons in the mPFC of BEPs and BERs.

Inhibitory neuron responsiveness to PF does not differ as a function of binge phenotype

As with the comparison of Fos-expressing neurons co-localized with *Satb2*, the proportions of Fos-expressing neurons that co-localized with each inhibitory neuron marker did not differ in any brain region between BEPs and BERs. In addition, only a small proportion of Fos-expressing neurons were of the inhibitory phenotype, suggesting that the contribution of GABAergic neurons to the regulation of PF intake is relatively minor as compared to the glutamatergic neuron population. Nonetheless, inhibitory neurons were indeed responsive to PF, suggesting that GABA-mediated regulation of glutamatergic neuron excitability within the

Table 2.6) Total number of Fos+ neurons co-localized with inhibitory neuron markers PV, SOM, or VIP in the mPFC of BEP and BER rats

Mean comparisons between BEP and BER rats on total numbers of Fos⁺ cells co-localized with GABAergic markers

BEP vs. BER	Mean # (S.E.) ¹	<i>Mean Comparisons</i>	
		Statistics	Effect Size
<i>Number Fos⁺/PV⁺</i>		<i>F</i> (df)	Cohen's <i>d</i>
Cingulate			
BER	4.96 (1.94)	1.56 (1, 12)	0.75
BEP	1.82 (1.29)		
Prelimbic			
BER	31.70 (6.51)	2.04 (1, 12)	0.87
BEP	19.65 (4.33)		
Infralimbic			
BER	20.93 (3.93)	0.20 (1, 12)	0.28
BEP	18.63 (2.61)		
<i>Number Fos⁺/SOM⁺</i>		<i>F</i> (df)	Cohen's <i>d</i>
Cingulate			
BER	76.99 (20.97)	1.62 (1, 14)	0.79
BEP	114.61 (16.90)		
Prelimbic			
BER	175.13 (38.36)	0.44 (1, 14)	0.37
BEP	210.81 (30.91)		
Infralimbic			
BER	85.39 (15.22)	2.31 (1, 14)	0.80
BEP	118.03 (12.27)		
<i>Number Fos⁺/VIP⁺</i>		<i>F</i> (df)	Cohen's <i>d</i>
Cingulate			
BER	23.21 (5.67)	0.00 (1, 10)	0.04
BEP	22.59 (6.23)		
Prelimbic			
BER	42.62 (7.65)	0.58 (1, 11)	0.47
BEP	33.67 (7.65)		
Infralimbic			
BER	17.24 (5.90)	0.00 (1, 11)	0.03
BEP	16.90 (5.90)		

¹ Mean values represent ANCOVA adjusted means, using total PF consumed prior to sacrifice as the covariate

Table 2.7) Proportions of PV, SOM, VIP+ neurons expressing Fos in response to PF intake in the mPFC of BEP and BER rats

Mean comparisons between BEP and BER rats on proportions of PV, SOM, or VIP⁺ neurons that express Fos

BEP vs. BER	Mean % (S.E.) ¹	<u>Mean Comparisons</u>	
		BEP vs. BER	
		Statistics	Effect Size
<i>Proportion PV⁺ with Fos</i>		<i>F (df)</i>	<i>Cohen's d</i>
Cingulate			
BER	0.54 (0.22)	1.29 (1, 15)	0.61
BEP	0.21 (0.17)		
Prelimbic			
BER	1.88 (0.39)	0.39 (1, 15)	0.34
BEP	1.56 (0.31)		
Infralimbic			
BER	2.73 (0.68)	0.27 (1, 15)	0.28
BEP	3.19 (0.54)		
<i>Proportion SOM⁺ with Fos</i>		<i>F (df)</i>	<i>Cohen's d</i>
Cingulate			
BER	25.23 (4.29)	0.03 (1, 14)	0.11
BEP	26.23 (3.46)		
Prelimbic			
BER	34.40 (4.54)	0.14 (1, 14)	0.26
BEP	31.98 (3.66)		
Infralimbic			
BER	39.01 (3.14)	0.02 (1, 14)	0.04
BEP	39.62 (2.53)		
<i>Proportion VIP⁺ with Fos</i>		<i>F (df)</i>	<i>Cohen's d</i>
Cingulate			
BER	18.35 (4.58)	0.04 (1, 10)	0.17
BEP	19.80 (5.03)		
Prelimbic			
BER	18.17 (2.38)	0.22 (1, 11)	0.31
BEP	16.45 (2.38)		
Infralimbic			
BER	13.68 (4.36)	0.08 (1, 11)	0.19
BEP	15.53 (4.36)		

¹Percentages represent all PV, SOM, or VIP+ GABAergic neurons co-localized with Fos, and values represent ANCOVA-adjusted means, using PF consumed prior to sacrifice as the covariate.

cortex, which is required for several mPFC-mediated executive functions [66, 71, 164], may extend to the regulation of PF intake as well.

When comparing the total numbers of Fos-expressing PV, SOM, and VIP neurons between BEPs and BERs, we found no significant differences between the two phenotypes in any brain region. Though we did find large effect sizes for select markers and in select brain regions, our data largely suggest that the magnitude of inhibitory neuron responsiveness to PF does not differ as a function of binge phenotype; greater inhibitory tone in the presence of PF *does not appear* to contribute to binge eating proneness. As such, the overall conclusion from our set of double labeling experiments, here, is that between-phenotype differences in the strength of an mPFC-mediated behavioral brake over PF intake is primarily driven by reduced excitatory neuron responsiveness to PF, with no effect of inhibitory neurons, in BEPs as compared to BERs.

Individual sub-types of inhibitory neurons differ in the magnitude of their responsiveness to PF

Examining the proportions of all PV, SOM, and VIP neurons that expressed Fos in response to PF revealed that, despite a lack of BEP vs. BER differences, SOM and VIP neurons were more strongly responsive to PF than were PV neurons. Approximately 30% of all SOM neurons and ~20% of all VIP neurons were activated in response to a PF stimulus, while only ~2% of all PV neurons were responsive to PF. Differential responsiveness of each sub-type of inhibitory neuron to PF has been previously demonstrated in the mPFC of male mice [78], suggesting that the unique cellular and functional properties of each type of inhibitory neuron may render them more or less likely to respond to food rewards.

PV neurons, for example, are primarily responsible for feed-forward and feed-back inhibition within the cortex [62], as well as the regulation of gamma oscillations within the cortex [165], for basic attentional processing. As such, a PF stimulus may not engage PV neurons beyond their baseline level of firing activity that is needed for basic cortical processing and attention. On the other hand, SOM neurons have a high degree of spontaneous firing activity [61], which likely explains the high magnitude of SOM neurons, in general, within this study. SOM neurons also synapse onto distal dendrites of pyramidal cells [61, 166], to regulate incoming excitation onto excitatory neuron dendrites, so the relatively high level of SOM neuron activation may also reflect greater input to the mPFC (i.e., via incoming glutamate, dopamine, serotonin) during PF exposure and consumption. Finally, VIP neurons subserve dis-inhibitory control within the cortex by inhibiting, primarily, SOM neuron activity [62, 74], so the relatively high level of VIP neuron activation may be secondary to the high level of SOM neuron activation (i.e., as a means for regulating SOM neuron activity). VIP neurons also contain mu opioid receptors [75], and since opioid transmission within the mPFC is implicated in food intake and food reward [76, 77], VIP neuron activation may also reflect signaling through mu opioid receptors. Notably, however, we did not assess the magnitude of PV, SOM, or VIP neuron responsiveness to a control stimulus (i.e., no PF), so we cannot definitively say that the magnitude of PV, SOM, or VIP neuron activation is specific for the PF stimulus, as opposed to other salient stimuli (i.e., chow intake, water intake) that typically occur at the onset of an animal's dark cycle.

Conclusion

In conclusion, our study demonstrates that both excitatory and inhibitory neurons of the mPFC are activated by PF in female rats, and that the vast majority of PF-activated neurons are

excitatory projection neurons, regardless of binge eating phenotype. Moreover, our data suggest that the degree to which excitatory neurons, but not inhibitory neurons, are activated by PF serves as a neural correlate for binge eating proneness: *reduced* activation of excitatory neurons within the mPFC appears to be associated with the binge eating prone, behavioral phenotype. Going forward, it will be necessary to identify the functional relevance of mPFC excitatory neurons to food reward and to binge eating in female rats within this model. Doing so will identify the critical mechanisms by which the mPFC regulates PF intake and binge eating proneness, and, by extension, how disturbances within PFC circuitry in women contributes to the risk for ED development.

Chapter 3

Enhanced palatable food consumption following GABA-mediated inhibition of the medial prefrontal cortex in binge eating prone and binge eating resistant female rats

Introduction

Disturbances in executive functions, including high impulsivity and compulsivity as well as behavioral rigidity, exist in women with eating disorders (EDs), including anorexia nervosa (AN), bulimia nervosa (BN), and binge eating disorder (BED) [11, 33-35]. EDs are also associated with several psychiatric co-morbidities and psychological disturbances that are related to dysfunctional inhibitory control, including substance abuse and dependence in BN [36, 161] and obsessive-compulsive personality traits in AN [11]. Executive functions are behavioral constructs typically sub-served by the prefrontal cortex (PFC), suggesting that impaired prefrontal cortical activity, specifically in the context of food consumption, may be an etiologic factor in the development of eating pathology in women with EDs.

Imaging studies in humans have largely corroborated the hypothesis that aberrant neural activity in the PFC may underlie ED psychopathology. In fact, the magnitude of neural activation within the PFC, specifically during tasks that engage behavioral control mechanisms, tends to correlate with the extremes of eating behaviors that distinguish each sub-type of ED [22]. Women with restricting-type AN have abnormally high neural activity in sub-regions of the PFC in response to hunger and during basic monetary reward tasks [24], while women with BN and BED display reduced activation of select sub-regions of the PFC during cognitive tasks (i.e., Simon Spatial Incompatibility task, Stroop task) that engage behavioral control mechanisms [40-42, 167, 168]. Thus, imaging studies in humans indeed suggest that the striking

abnormalities in eating behavior in EDs may arise as a consequence of aberrant neural activity within PFC circuitry. However, while imaging studies in humans suggest that neural activity within the PFC, in select behavioral contexts, correlates with symptoms of EDs, they do not necessarily explain how the observed abnormalities in PFC activity contribute to the expression of eating pathology in women with EDs. Animal models are, therefore, critical for developing causal inferences related to the mechanistic role for the PFC in regulating food intake, food reward, and disordered eating behaviors.

The rodent PFC, specifically the medial PFC (mPFC) has several core executive functions (i.e., impulse control [87], behavioral inhibition [83, 88], behavioral flexibility [82]) that appear to be disrupted in women with EDs. The executive functions of the rodent mPFC are typically examined using neurocognitive behavioral tasks in rodents (i.e., 5-choice test, set-shifting tasks), yet relatively few studies, to date, have directly investigated whether the PFC exerts a similar degree of “executive” control over food intake and food reward in rodents. In male rats, pharmacological inactivation of the ventral mPFC alters the microstructure of sucrose licking and highly palatable liquid intake [110, 169]. In addition, inactivation of the ventral mPFC leads to an increase, albeit non-significant, in palatable liquid intake [76, 110], while inactivation of the prelimbic cortex of the mPFC leads to a significant increase in high fat intake [111]. The latter two studies, in particular, suggest that the rodent mPFC functions as a behavioral “brake” or limit over excessive palatable food intake. However, to date, few studies have investigated the functional relevance of the mPFC to food intake and food reward in a clinically relevant animal model of disordered eating, and no studies have used female rats. In particular, the use of female rats to study the mechanisms by which normative eating behaviors

become maladaptive seems necessary, given that women are up to 10x as likely as men to have an ED [36, 134].

To study the neural mechanisms that contribute to eating pathology, our lab uses a well-validated rat model of binge eating, as binge eating is 1) a core, maladaptive symptom that cuts across all major types of EDs, and 2) a critical diagnostic feature of other non-specified feeding and eating disorders in women [124]. In the animal model of binge eating used here, binge eating prone (BEP) and binge eating resistant (BER) rats are identified based on consistently high or low intake of intermittently-presented PF, respectively, and the behavioral differences between BEP and BER rats mirror core differences between binge eaters and non-binge eaters in the human condition [135]. Specifically, BEPs consume significantly more PF than do BERs, but they do not consume more chow nor do they gain more weight than BERs over the course of the feeding test period [16, 131-134]. Additionally, BEPs endure increasing levels of foot shock stress to obtain PFs, while BERs do not, suggesting a greater “loss of control” in BEPs in the presence of PF [136]. In support of a general role for the mPFC in the BEP/BER model, our lab has also demonstrated that neural responsiveness to PF (i.e., expression of the neural activation marker Fos) is higher in the mPFC of BEP vs. BER female rats [132], suggesting that between-phenotype differences in neural output from the mPFC during PF exposure may contribute to the specific behavioral differences between BEPs and BERs.

The aim of the present study was to delineate the functional role of the mPFC to PF intake in female rats and in a clinically relevant animal model of binge eating. In light of the fact that the mPFC acts as a behavioral “brake” over PF intake, we hypothesized that the mPFC-mediated brake on PF intake is *weaker* in BEP rats relative to BER rats. To test this hypothesis, we quantified changes in PF intake and scores of feeding behavior in BEP and BER female rats

following GABA-mediated pharmacological inactivation of the mPFC. Specifically, we predicted that pharmacological inactivation of the mPFC would increase PF intake in both BEPs and BERs but that the increase in PF intake following mPFC inactivation would be *higher* in BEPs vs. BERs. Such results would provide preliminary evidence that binge eating proneness may be driven by weaker mPFC-mediated control over hedonic, reward-driven feeding mechanisms.

Methods

Animals and Housing

A total of 79 young adult (P60) female, Sprague-Dawley rats were obtained from Harlan Laboratories (Madison, Wisconsin) and were run in three separate cohorts. Upon arrival, rats were individually housed in clear Plexiglass cages (45 x 23 x 21 cm³) with enrichment and *ad libitum* access to chow (Harlan Teklad Global Diets: 8640, Madison, Wisconsin) and water. Rats were maintained on a 12:12 reverse light-dark cycle with lights out at 11:00AM, 12:00PM, or 2:00PM depending on the cohort, and were treated in accordance with the NIH Guide for the Care and Use of Laboratory Animals. All protocols were approved by the Michigan State University Institutional Animal Care and Use Committee.

Feeding Tests for Identifying BEP and BER Rats

Rats were allowed one week of acclimation to housing conditions and experimenter handling prior to the start of the feeding test period. Thereafter, feeding tests were conducted using a protocol adapted from one that has been previously used in our lab [16, 131, 133, 134]. Intermittent feeding tests were run over a period of two weeks and included 6 total feeding test days. Feeding test days occurred on MWF and consisted of 4hrs of access to PF (~25g of Betty

Crocker® creamy vanilla frosting, 15% kcal from fat, 70% kcal from carbohydrate, 0% kcal from protein). PF was provided ~10 min prior to lights out via hanging food dishes in the home cages; standard rat chow (~70g on cage tops) remained freely available during the PF exposure period. PF and chow were weighed at the beginning of the feeding test and again after 1 and 4 hrs of access using a standard electronic balance, and values were rounded to the nearest tenth of a gram. Any remaining PF at the end of 4hrs was removed from home cages until the next feeding test day, while chow remained freely available. On both feeding test days and non-feeding test days (i.e., days when PF was not provided) body weights and 24hr chow consumption were measured and recorded just before lights out.

Table 3.1) Proportions of BEPs and BERs in cohorts 1, 2, and 3, CH 3

Sample sizes and proportions of BEPs and BERs in each cohort			
Phenotype	Cohort 1 (N = 20)	Cohort 2 (N = 30)	Cohort 3 (N = 29)
BEP	3 (15%)	7 (23%)	6 (21%)
BER	3 (15%)	9 (30%)	6 (21%)

Classifying rats as BEP or BER

Identification of BEP and BER rats followed protocols previously published by our lab [16, 131-134] and used a tertile approach based on the 4hr PF intake values from each of the 6 feeding test days. The 4hr intake values were used for identification of binge eating phenotypes, here, given that binge eating can be readily observed in animals within this discrete window of PF exposure [131, 133-135]. Four hour PF intake values from each feeding test day were divided into top, middle, and bottom tertiles; each rat scored within one of the three tertiles on each feeding test day. Rats were classified as BEP if they scored within the highest tertile on at

least 3 of the 6 ($\geq 50\%$) of feeding test days and never in the lowest tertile; rats were classified as BER if they scored within the lowest tertile on at least 3 of the 6 feeding test days and never in the highest tertile. **Table 3.1** provides the sample sizes and the proportions of BEPs and BERs that were identified in each of the three cohorts. All binge eating neutral rats (i.e., non-BEP and non-BER) from each cohort were reserved for separate behavioral studies in our lab.

Stereotaxic Surgical Procedures

Bilateral guide cannulae were stereotaxically targeted to the ventral half of the mPFC in all BEPs (N=16) and BERs (N=18). Surgical procedures were completed one to two days following the final feeding test day. Rats were anesthetized via inhaled isoflurane and were secured in a Kopf stereotaxic frame; body temperatures were maintained via a warm heating pad for the duration of surgery. After exposing the skull using antiseptic techniques, bilateral stainless steel guide cannulas (2.5 mm long, 26 gauge, Plastics One, Roanoke, VA) were inserted at a 19° angle from vertical into the ventral mPFC (+2.6 mm anterior to bregma, ± 2.0 mm lateral to the midline, and -2.5 mm from the skull surface). Guide cannulas were lowered into the mPFC such that the top of the cannulas were flush with the skull and the cannula tip landed 2.5mm above the targeted infusion site of -5.0 mm from the skull surface. Guide cannulas were anchored to the skull using two surgical anchor screws and dental acrylic, and stainless steel dummy cannulas (2.5 mm long, Plastics One) were inserted into guide cannulas to prevent blockage. Rats were given 5mg/kg s.c. ketoprofen for pain management, 5mg/kg of s.c. enrofloxacin antibiotic, and 1mL of s.c. sterile saline at the time of surgery, and were returned to their home cages on a warm heating pad upon awakening. Thereafter, rats were allowed a minimum of 5 days of recovery before any additional testing, during which body weights were monitored and rats were handled daily.

Intra-mPFC Infusions of Muscimol

Muscimol was obtained from Sigma-Aldrich and was diluted with 0.9% sterile saline to make a 10mg/mL stock solution. The specific doses of muscimol used here were then prepared from the stock solution prior to infusions.

Infusions began ~60 min before lights out to ensure that all rats were infused in the light before PF was delivered. Two days prior to the first infusion of muscimol or saline vehicle, all rats were given one “sham” infusion to acclimate rats to the handling procedures associated with drug infusions. During the sham infusion, infusion cannulas (30 gauge, Plastics One, projecting 2.5 mm beyond the tip of guide cannulas) were lowered into guide cannulas with no drug delivery, and infusion cannulas remained in place for a total of 3 min in order to simulate the time that would be needed for drug infusions on testing days. Two days later, muscimol infusions began following a within-subjects design: each BEP and BER received all three doses of muscimol: 0 (sterile saline), 15, and 30ng. Drug doses were chosen based on previous studies that inactivated the mPFC prior to PF exposure [76, 110], and based on results from pilot studies in our lab. Specifically, given that pilot studies in our lab found that the largest increase in PF intake occurred following infusion of 30ng muscimol (See **Figure 3.1**), with no further increase in PF intake between 30ng and 75ng muscimol, the 30ng dose and a lower dose of 15ng were chosen for this experiment. Using a lower dose, here, would allow for a detection of between-phenotype differences in the sensitivity to mPFC inactivation. During each infusion, rats were gently held in the lap of the experimenter as inner infusions cannulas were lowered into guide cannulas, and 0.5µL of drug was delivered at a rate of 0.25µL/min using a 5µL Hamilton syringe connected on one end to infusion cannulas, via polyethylene (PE 20) tubing, and on the other to

an automated microsyringe pump. Cannulas were held in place for one additional minute to prevent backflow of drug, after which infusion cannulas were removed, dummy cannulas were replaced, and rats were returned to their home cage until the start of the feeding test. The order in which the drug was delivered was randomized across animal and across testing day, and experimenters were blind to the dose of the drug during all infusions. One drug-free interim day was scheduled between each infusion day. Finally, upon the completion of all infusions on each test day (i.e., ~10min before lights out), PF was placed into each rat's home cage and feeding tests were conducted following the protocol outlined previously for the initial feeding test paradigm.

Analysis of Feeding, Locomotor, and Grooming Behavior

A random sample of BEP (N = 14) and BER (N = 14) rats that underwent feeding tests followed by muscimol infusions, as described above, were recorded and later scored for feeding, locomotor, and grooming behavior. Only a select number of BEPs and BERs were recorded due to constraints associated with available equipment for recording. Rats were recorded for the first hour of PF exposure, and recordings were scored using an event recorder by an experimenter blind to both binge phenotype and drug dose. Feeding behavior was scored for the full duration of the 1hr test while locomotor and grooming behaviors were scored for only the first 30 min of the 1hr test. The following behaviors were quantified for each feeding test:

1) Feeding behavior: latency to begin consuming PF, number of episodes of PF consumption, mean duration of all episodes of PF consumption, and total time spent consuming PF (i.e., the sum of all feeding episodes across the hour)

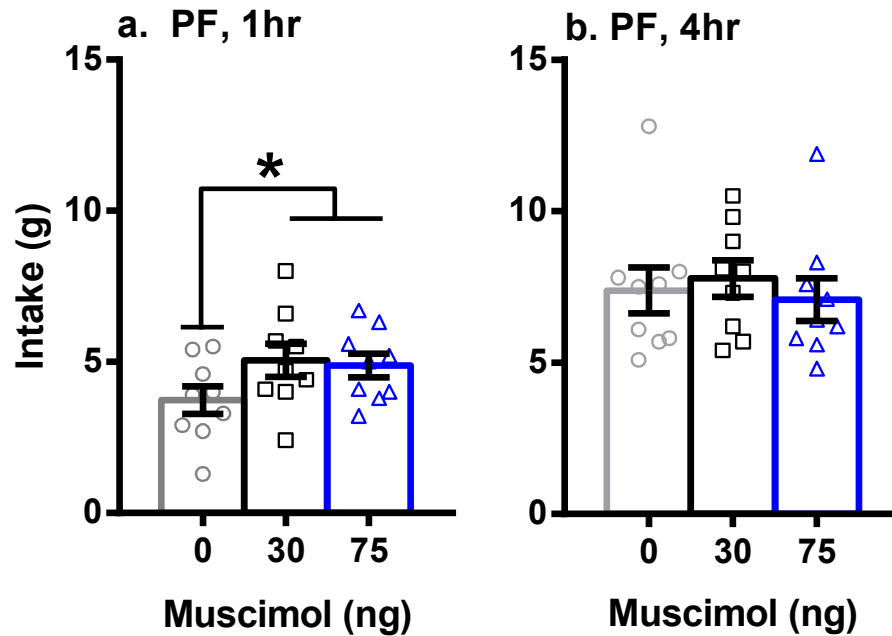


Figure 3.1) Initial pilot studies confirm that GABA-mediated inhibition of the mPFC leads to a significant increase in PF intake

Inactivation of the mPFC in female rats leads to a significant increase in 1hr (a) PF intake but not 4hr (b) PF intake. Doses of muscimol represent amount infused per hemisphere. Error bars represent one S.E.M. Total sample size, N = 9 female rats.

* $p < 0.05$, both doses as compared to saline.

2) Locomotor behavior: total number (counts) of cage crossings (i.e., moving past the midline of the cage in either direction) and total number (counts) of rears

3) Grooming behavior: total number of grooming maneuvers (counts), including bilateral head sweeps and full body sweeps

Verification of cannula placement and muscimol infusions within the mPFC

Two days after the final muscimol infusion and feeding test, all BEPs and BERs received an additional infusion of 30ng muscimol (bilateral, 0.5µl, 0.25µl/min) to induce Fos expression around the cannula tip in the mPFC. Fos expression in response to the muscimol infusion was used to estimate the spread of the drug and to provide evidence of neuronal survival and minimal glial scar around the cannula tip. One hour after muscimol infusions, rats received a lethal dose of sodium pentobarbital (Fatal Plus®, 150mg/kg i.p.) and rats were intracardially-perfused with a buffered saline rinse followed by 4% paraformaldehyde. Brains were harvested, post-fixed overnight in 4% paraformaldehyde and stored in a 20% sucrose solution until sectioning. Brains were then cryostat-sectioned at 40µm into 4 series and stored at -20°C in cryoprotectant until further processing. One series of tissue was mounted and stained with cresyl violet for verification of cannula placement and a second series of tissue was processed for Fos immunohistochemistry in the mPFC, following protocols previously published by our lab [170]. Briefly, sections were rinsed three times in tris buffered saline (TBS) before a 10 min incubation in 1% hydrogen peroxide. Following three rinses in TBS, sections were incubated for 30 min in 20% normal goat serum (NGS) in 0.1% Triton-X 100 in TBS. Sections were then incubated for 48hrs at 4°C in rabbit anti-c-fos primary antibody (sc-52, Santa Cruz, 1:10,000) diluted in 2% NGS. Thereafter, sections were rinsed three times in TBS before a 1hr incubation at room temperature in goat anti-rabbit secondary antibody (Vector Labs, 1:500) diluted in 2% NGS.

After three TBS rinses, sections were incubated for 1hr at room temperature in avidin-biotin-peroxidase complex (ABC Elite Kit, Vector labs), and following three final rinses in TBS, staining was completed using 3,3'-diaminobenzidine (DAB, 0.025% in TBS with 0.012% hydrogen peroxide) to yield a brown, nuclear reaction product. Sections were then mounted onto glass slides, air-dried, and dehydrated through a series of graded ethanol concentrations, and cover-slipped.

Statistical Analyses

SPSS Statistics software (version 24) was used for all statistical analyses, with the alpha level set to 0.05.

Behavioral differences between BEPs and BERs

During the initial feeding tests, individual mixed design ANOVAs were used to compare PF and chow consumption as well as body weights between BEPs and BERs, with the within-subjects factor being test day and the between-subjects factor being binge phenotype. Cohen's d effect sizes were calculated for each BEP vs. BER comparison in order to provide a standardized measure of the magnitude of the mean differences between the two phenotypes. Cohen's d effect sizes were interpreted as small ($d = 0.20$), medium ($d = 0.50$), or large ($d = 0.80$).

PF and chow intake following GABA-mediated inhibition of the mPFC

Data from two BER rats and one BEP rat were excluded from the analysis of PF and chow intake following inactivation of the mPFC due to either unilateral or bilateral occlusion of guide cannulae during the infusion protocol. This resulted in a final sample size of $N = 16$ BER and $N = 15$ BEP rats. For feeding tests following muscimol infusions, individual mixed design ANOVAs were used to analyze 1hr and 4hr PF consumption, 1hr and 4hr chow consumption,

and 24hr chow consumption (collected for cohorts 2 and 3 only), with drug dose as the within-subjects factor and binge phenotype as the between-subjects factor. Significant main effects of drug were followed up by pairwise comparisons using a Bonferroni correction and collapsed across phenotype if no drug*phenotype interaction was present. Cohen's *d* effect sizes were also calculated selectively for 1hr and 4hr PF intake within BEPs and BERs separately, in order to compare PF intake following infusion of saline to PF intake following infusion of 15ng or 30ng muscimol. For Cohen's *d* analyses, here, paired t-tests (i.e., intake at saline vs. intake at 15ng or 30ng) were first conducted for time point in each phenotype, individually, to determine the correlations between the means of PF intake. The correlations between the means were then included in the derivation of each effect size estimate, to correct for dependence among the means as a consequence of the within-subjects design [171]. In addition, the percent change in 1hr and 4hr PF intake, following infusion of 15ng and 30ng muscimol relative to saline, was also calculated for each phenotype separately. For each calculation, the individual group means of PF intake following infusion of saline were used (1hr: BER = 2.8g, BEP = 4.4g; 4hr: BER = 5.3g, BEP = 7.7g). The equation used for the calculation of the percent change in PF intake in each animal was (PF intake after 15 or 30ng muscimol – group mean of PF intake after 0ng) / (group mean of PF intake after 0ng). Thereafter, univariate ANOVAs were used to compare the percent change in PF intake between BEPs and BERs at each drug dose. Cohen's *d* effect sizes were also calculated for each BEP vs. BER comparison of percent change in PF intake.

Feeding, locomotor, and grooming behavior following GABA-mediated inhibition of the mPFC

Mixed design ANOVAs were used to analyze each score of feeding, locomotor, and grooming behavior, with drug dose as the within-subjects factor and binge phenotype as the between-subjects factor. Significant main effects of drug were followed up by pairwise

comparisons using a Bonferroni correction and collapsed across phenotype if no drug*phenotype interaction was present.

Results

BEPs consume significantly more PF than BERs during feeding tests

Results from the mixed design ANOVAs analyzing feeding test data are shown in **Table 3.2**. As expected, PF intake was significantly higher in BEP vs. BER rats at both the 1 and 4hr time points, with no differences between BEPs and BERs in chow intake [16, 131-134]. Though 24hr chow consumption on non-feeding test days did not differ between BEPs and BERs, 24hr chow consumption on feeding test days was significantly higher in BERs vs. BEPs, a finding consistent with previous work in our lab [132]. BEPs and BERs did not differ in body weights across the duration of the testing period.

GABA-mediated inhibition of the mPFC increases PF, but not chow, intake in BEP and BER rats

As expected, GABA-mediated inhibition of the mPFC induced a significant increase in PF intake at the 1hr time point in both BEPs and BERs ($F(2, 58) = 13.13, p < 0.001$, **Table 3.3a and Figure 3.2**), consistent with pilot studies from our lab (**Figure 3.1**). Follow up pairwise comparisons revealed that BEPs and BERs consumed significantly more PF in 1hr following infusion of 30ng muscimol as compared to both saline and 15ng. Specifically, 30ng muscimol yielded a 36.8% increase in 1hr PF intake in BERs and a 34.9% increase in 1hr PF intake in BEPs (**Table 3.3b**). In addition, there was a significant main effect of phenotype ($F(1, 29) = 23.03, p < 0.001$), with BEPs consuming more PF in 1hr than BERs at each drug dose.

Table 3.2) PF and chow intake and body weights in BEPs and BERs, CH 3

Mean comparisons between BEP and BER rats on PF, chow, and body weights across the feeding test period, prior to stereotaxic surgery

BEP vs. BER Group	Mean (S.E.)	BEP vs. BER Mean Comparisons	
		Statistics	Effect Size
		<i>F</i> (1,49)	Cohen's <i>d</i>
Body weights (g)			
BER	200.85 (2.20)	3.09†	0.64
BEP	206.39 (2.27)		
<i>Feeding test days</i>			
PF intake, 1h (g)			
BER	3.02 (0.22)	67.52***	2.96
BEP	5.61 (0.23)		
PF intake, 1h (kcal)			
BER	12.81 (0.93)	67.53***	2.94
BEP	23.77 (0.96)		
PF intake, 4h (g)			
BER	5.91 (0.26)	103.86***	3.66
BEP	9.76 (0.27)		
PF intake, 4h (kcal)			
BER	25.06 (1.12)	103.86***	3.67
BEP	41.39 (1.15)		
Chow intake, 1h (g)			
BER	1.17 (0.13)	0.00	0.01
BEP	1.17 (0.14)		
Chow intake, 4h (g)			
BER	2.37 (0.19)	1.08	0.37
BEP	2.09 (0.20)		
Chow intake, 24h (g)			
BER	9.73 (0.37)	9.25**	1.10
BEP	8.10 (0.38)		
<i>Non-feeding test days</i>			
Chow intake, 24h (g)			
BER	13.80 (0.38)	1.32	0.41
BEP	13.17 (0.39)		

Note: Values are based on data from only the BEPs (N=15) and BERs (N=16) that received muscimol infusions; effect size interpretation: small, $d = 0.20$; medium, $d = 0.50$; large, $d = 0.80$; *** $p < .001$; ** $p < .01$; † $p < .10$

The ANOVA revealed no drug*phenotype interaction for 1hr PF intake $\{F(2, 58) = 0.56, p = 0.57\}$, and supplementary Cohen's d effect size analyses, comparing PF intake following 0ng to PF intake following 30ng, revealed a medium-to-large effect size in BERs ($d = 0.64$) but a large effect in BEPs ($d = 1.18$, **Table 3.3a**). Notably, the effect size for this comparison in BEPs was almost double that of BERs, suggesting that although inactivation of the mPFC significantly enhanced 1hr PF intake in both phenotypes, the effect of mPFC inactivation on 1hr PF intake was stronger in BEPs than in BERs.

For 4hr PF intake, the ANOVA revealed only a statistical trend towards a main effect of drug $\{F(2, 58) = 2.68, p = 0.07$, **Table 3.3a and Figure 3.2**}, yet there remained a significant main effect of phenotype $\{F(1, 29) = 24.28, p < 0.001, \text{BEP} > \text{BER}\}$. Of note, there was also a statistical trend towards a drug*phenotype interaction $\{F(2, 58) = 2.37, p = 0.10\}$. BERs demonstrated virtually no change in 4hr intake (-0.57%) following infusion of the higher dose of muscimol, but 4hr PF intake increased by 10.26% in BEPs (**Table 3.3b**). In addition, the Cohen's d effect size for the comparison of percent change in 4hr PF intake between BEPs and BERs at the higher dose of muscimol was also medium in magnitude ($d = 0.44$). In addition, supplementary Cohen's d effect size analyses revealed that the comparison of 4hr PF intake following 0ng to 4hr PF intake following 30ng muscimol was negligible in BERs ($d = 0.02$), but was medium-to-large in BEPs ($d = 0.62$, **Table 3.3a**). Thus, the effect of pharmacological inactivation of the mPFC on increasing PF intake was sustained for the full duration of the 4hr exposure period in BEPs, but not in BERs.

Finally, chow consumption was unaffected by GABA-mediated inhibition of the mPFC, and did not differ between BEPs and BERs at any time point (**Table 3.3c and Figure 3.2**).

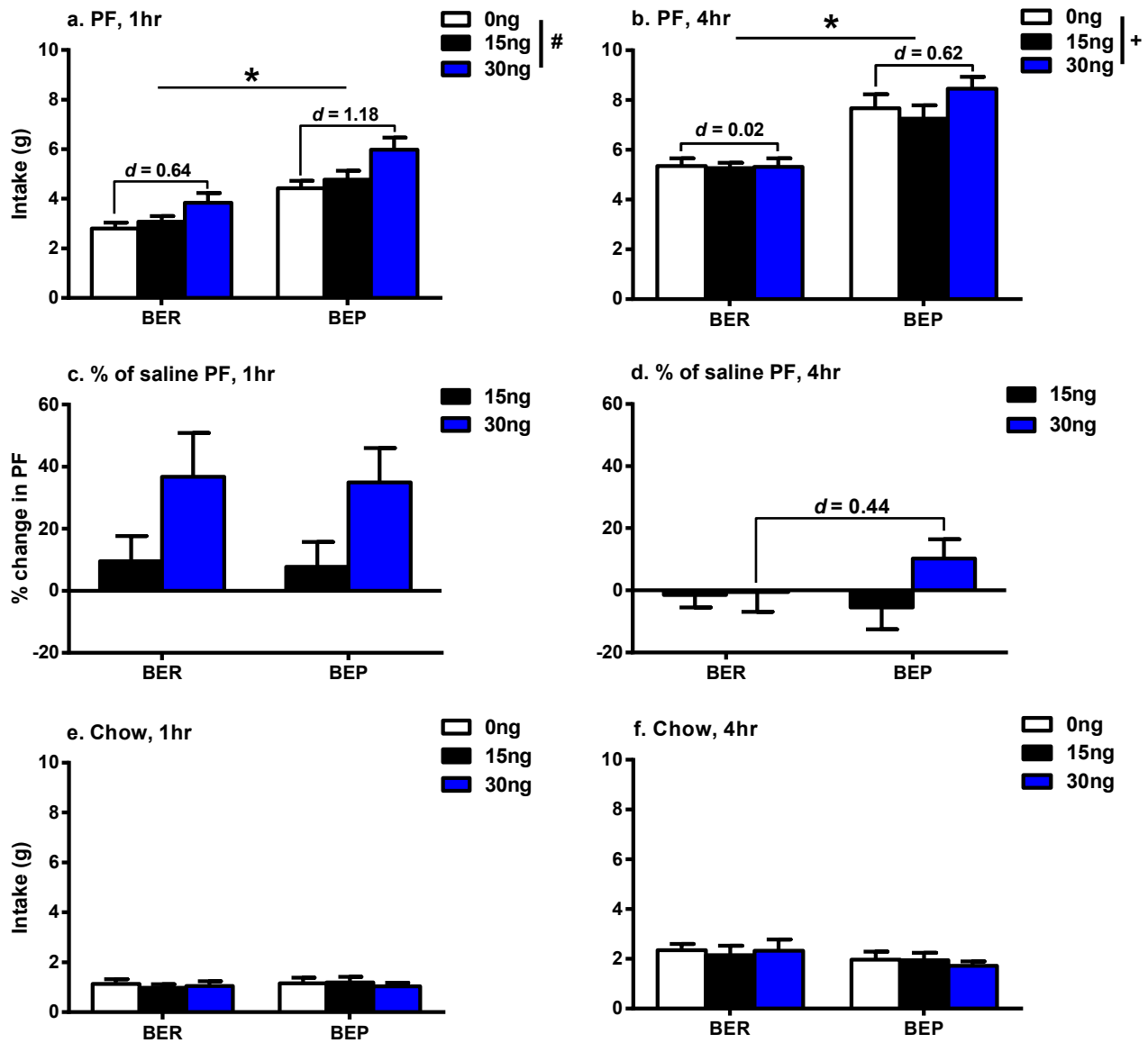


Figure 3.2) PF and chow intake in BEPs and BERs following GABA-mediated inhibition of the mPFC

Inactivation of the mPFC increased 1hr (a) and 4hr (b) PF consumption in BEPs and BERs. Cohen's d values in (a) and (b) represent the comparison of PF intake at 0ng to PF intake at 30ng muscimol, calculated within each phenotype individually. Middle panel displays the percent change in 1hr (c) or 4hr (d) PF intake, after the 15ng and 30ng infusions, relative to the individual group means of PF intake at the saline dose. Cohen's d value in (d) represents the mean comparison between BEPs and BERs, in percent change in PF intake, at the 30ng dose. One hour (e) and 4hr (f) chow intake were unaffected by inactivation of the mPFC. Doses of muscimol represent amount infused (in ng) into each hemisphere. Error bars represent one S.E.M.

* $p < 0.05$, M.E. of phenotype; # $p < 0.05$, + $p < 0.09$, M.E. of drug.

Table 3.3a) Increase in 1 and 4hr PF intake following GABA-mediated inhibition of the mPFC

Mean values for PF intake after 1 and 4hrs of exposure and following GABA-mediated inhibition of the mPFC in BEP and BER rats

Variable	Mean (S.E.)			<u>Cohen's <i>d</i> effect sizes</u>	
	Saline	15ng	30ng	<u>Saline vs.</u> 15ng	30ng
<i>PF intake,</i>					
<i>1hr (g)</i>					
BER	2.8 (0.24)	3.1 (0.23)	3.8 (0.40)	0.22	0.64
BEP	4.4 (0.29)	4.8 (0.36)	6.0 (0.49)	0.34	1.18
<i>PF intake,</i>					
<i>4hr (g)</i>					
BER	5.3 (0.32)	5.2 (0.21)	5.3 (0.34)	0.07	0.02
BEP	7.7 (0.56)	7.2 (0.54)	8.5 (0.48)	0.23	0.62

Note: Cohen's *d* effect size calculations were calculated for each drug dose comparison in each phenotype separately.

Table 3.3b) Percent change in 1 and 4hr PF intake following GABA-mediated inhibition of the mPFC

Percent change in 1hr and 4hr PF intake, relative to saline, following GABA-mediated inhibition of the mPFC in BEP and BER rats.

		<i>Mean Comparisons</i>	
Variable	Mean (S.E.)	BEP vs. BER	
		Statistics	Effect Size
		<i>F</i> (1, 29)	Cohen's <i>d</i>
<i>% change PF, 1hr¹</i>			
15ng muscimol			
BER	9.6% (7.9)	0.03	0.06
BEP	7.7% (8.2)		
30ng muscimol			
BER	36.8% (12.6)	0.01	0.05
BEP	34.9% (13.0)		
<i>% change PF, 4hr</i>			
15ng muscimol			
BER	-1.5% (5.6)	0.24	0.31
BEP	-5.5% (5.7)		
30ng muscimol			
BER	-0.6% (6.2)	1.49	0.44
BEP	10.3% (6.4)		

Note: ¹Percent change in PF intake calculated at each drug dose using group means of PF intake following saline infusion.

Table 3.3c) No change in 1, 4, or 24hr chow intake following GABA-mediated inhibition of the mPFC

Mean 1hr, 4hr, and 24hr chow consumption in BEPs and BERs following GABA-mediated inhibition of the mPFC

Variable	Mean (S.E.)			Drug Main Effect	Phenotype Main Effect
	Saline	15ng	30ng	<i>F</i> (df)	<i>F</i> (df)
<i>Chow intake, 1hr (g)</i>					
BER	1.13 (0.20)	0.98 (0.14)	1.04 (0.20)	0.04 (1, 28)	0.39 (2, 56)
BEP	1.15 (0.23)	1.19 (0.23)	1.04 (0.14)		
<i>Chow intake, 4hr (g)</i>					
BER	2.34 (0.25)	2.14 (0.38)	2.32 (0.46)	1.26 (1, 29)	0.27 (2, 58)
BEP	1.97 (0.31)	1.94 (0.31)	1.72 (0.18)		
<i>Chow intake, 24hr (g)</i>					
BER	9.99 (0.60)	9.49 (0.57)	9.83 (0.81)	0.05 (1, 23)	0.56 (2, 46)
BEP	10.03 (0.60)	9.76 (1.13)	8.93 (0.89)		

GABA-mediated inhibition of the mPFC alters the structure of feeding on PF in BEPs and BERs

There were no significant drug*phenotype interactions for any feeding behavior score, suggesting that the effect of GABA-mediated inhibition of the mPFC on feeding behavior was comparable between BEPs and BERs. First, mixed design ANOVAs revealed no main effect of drug on latency to begin consuming PF $\{F(2, 52) = 0.64, p = 0.53\}$, but a significant main effect of phenotype $\{F(1, 26) = 4.39, p = 0.04\}$; BEPs took significantly less time to start consuming PF than did BERs (**Figure 3.3**). On the other hand, inactivation of the mPFC led to a significant decrease in the number of episodes of PF consumption $\{F(2, 52) = 4.62, p = 0.01\}$, with significantly fewer episodes of PF consumption following infusion of 30ng muscimol as compared to saline ($p = 0.02$). Analysis of feeding episode number also revealed a significant main effect of phenotype $\{F(1, 26) = 8.12, p = 0.009\}$, with BEPs engaging in more episodes of PF consumption than BERs. Analysis of mean feeding episode duration revealed a significant main effect of drug $\{F(2, 52) = 9.38, p = 0.003\}$, with significantly longer episodes of PF consumption following infusion of 30ng muscimol as compared to both 0ng ($p = 0.01$) and 15ng muscimol ($p = 0.01$). Mean feeding episode duration did not, however, differ between BEPs and BERs $\{F(1, 26) = 0.20, p = 0.66\}$. Finally, the total amount of time spent consuming PF also increased as a function of drug dose $\{F(2, 52) = 5.72, p = 0.006\}$, with more time spent consuming PF following infusion of 30ng muscimol as compared to 0ng ($p = 0.01$). In addition, BEPs spent more time, overall, consuming PF than did BERs $\{F(1, 26) = 7.03, p = 0.01\}$.

GABA-mediated inhibition of the mPFC reduces locomotor and grooming behavior

There were no significant drug*phenotype interactions for any score of locomotor behavior or for the analysis of grooming counts. Mixed design ANOVAs revealed that the

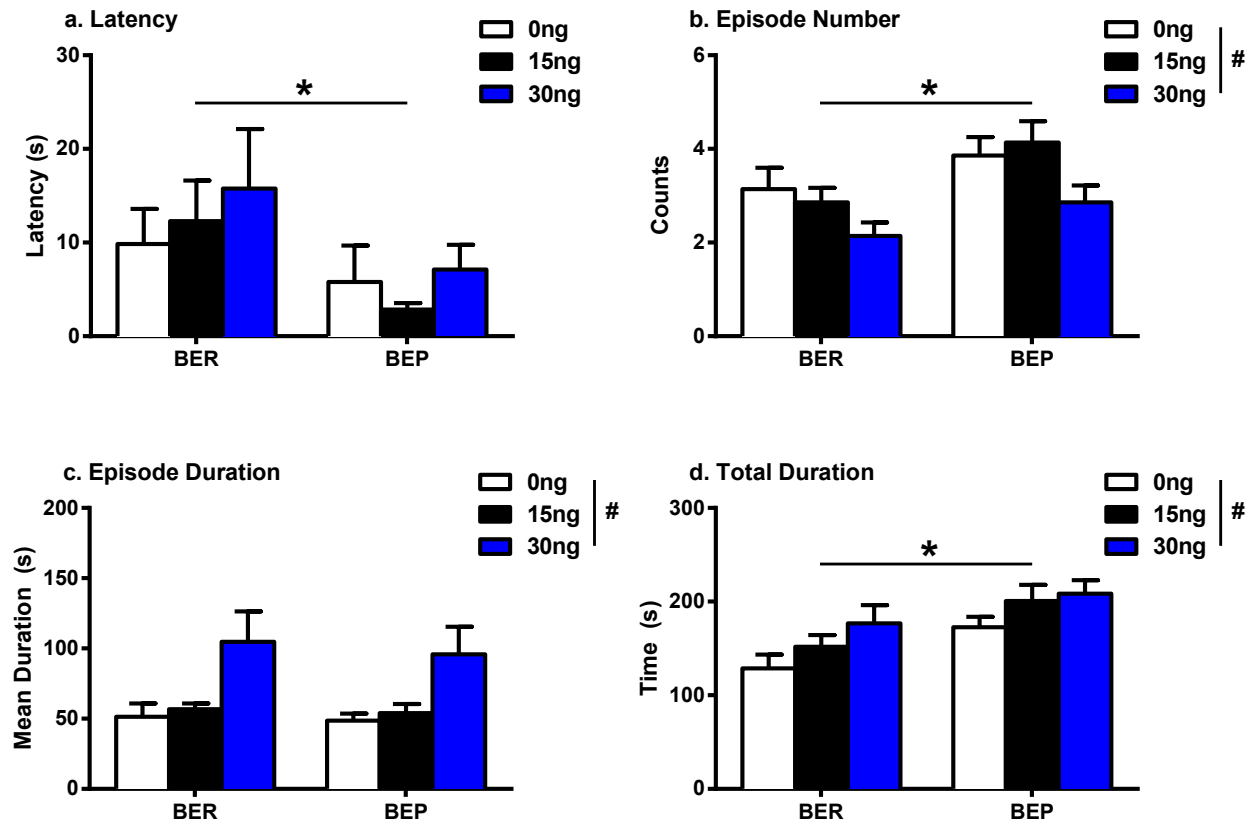


Figure 3.3) GABA-mediated inhibition of the mPFC alters the structure of PF consumption in BEP and BER rats

Changes in the structure of PF consumption in BEP and BER rats following inactivation of the mPFC. Error bars represent one S.E.M.

* $p < 0.05$, ME of phenotype; # $p < 0.05$, M.E. of drug.

number of cage crossings did not change as a function of drug dose $\{F(2, 52) = 1.56, p = 0.21\}$ and did not differ between BEPs and BERs $\{F(1, 26) = 0.06, p = 0.79, \textbf{Figure 3.4}\}$. Mixed design ANOVAs did reveal a statistical trend towards a decrease in the total number of rears as a function of drug dose $\{F(2, 52) = 2.98, p = 0.06\}$, but no differences between BEPs and BERs $\{F(1, 26) = 0.01, p = 0.93\}$. Furthermore, inactivation of the mPFC led to a significant decline in the total number of grooming counts $\{F(2, 50) = 15.66, p < 0.001\}$, with fewer total grooming counts following infusion of the higher dose of muscimol as compared to both saline ($p < 0.001$) and the lower dose of muscimol ($p = 0.007$), but grooming counts did not differ between BEPs and BERs $\{F(1, 25) = 0.05, p = 0.82\}$.

Cannula targets and muscimol-induced Fos expression in the mPFC

Cannula hit sites for BEPs and BERs are shown in **Figure 3.5**. All cannulas fell within the dorso-ventral and medial-lateral coordinates of the mPFC, yet there was a substantial rostro-caudal distribution. Nonetheless, in 80% (12/15) of BEPs and 81% (13/16) of BERs, right and left cannula targets were located within the same rostro-caudal distance from bregma, according to the Paxinos and Watson rat brain atlas [145]. On the other hand, right and left cannulas fell 96 μ m (i.e., 2 plates in the rat brain atlas) from each other in the rostro-caudal plane in 2 BEPs and 1 BER, while right and left cannulas fell 48 μ m (i.e., 1 plate) from each other in the rostro-caudal plane in 1 BEP and 2 BERs. In addition, visual inspection of Fos expression following infusion of 30ng muscimol revealed robust staining around the cannula tips and throughout the full medial-lateral and rostro-caudal extent of the ventral mPFC, indicating conserved neural activity and relatively minimal scar at the location of the infusions (**Figure 3.5**). Notably, Fos expression was not always restricted to a defined area around the cannula tips in BEPs and BERs, as Fos expression was also visualized in the dorsal half of the prelimbic cortex and in

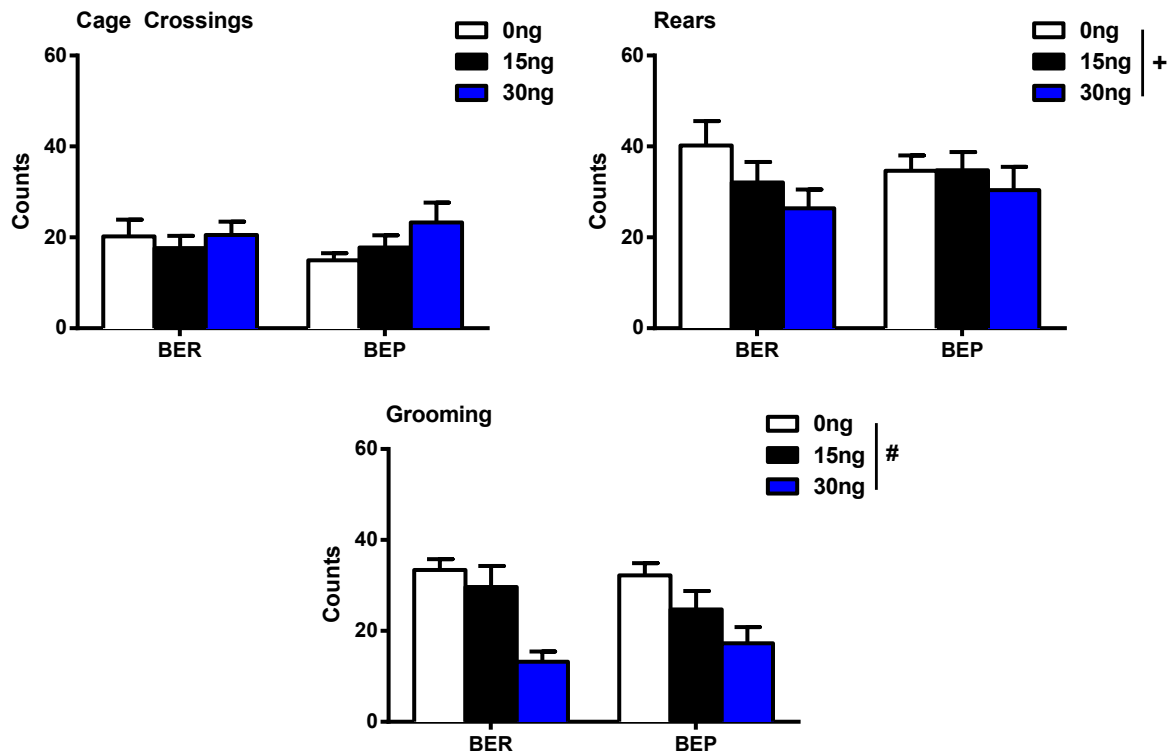


Figure 3.4) GABA-mediated inhibition of the mPFC alters rearing and grooming behavior in BEP and BER rats

Changes in locomotor and grooming behavior in BEP and BER rats following GABA-mediated inhibition of the mPFC. Error bars represent one S.E.

$p < 0.05$, + $p < 0.09$, M.E. of drug.

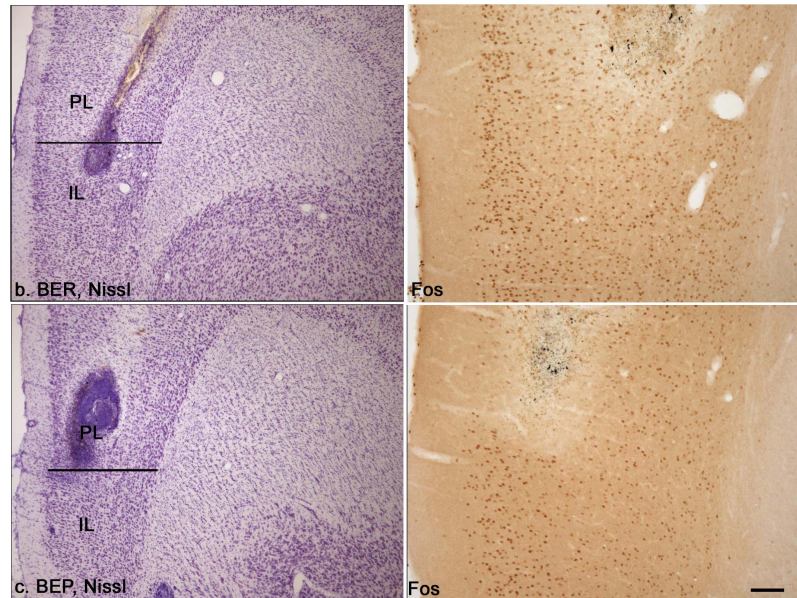
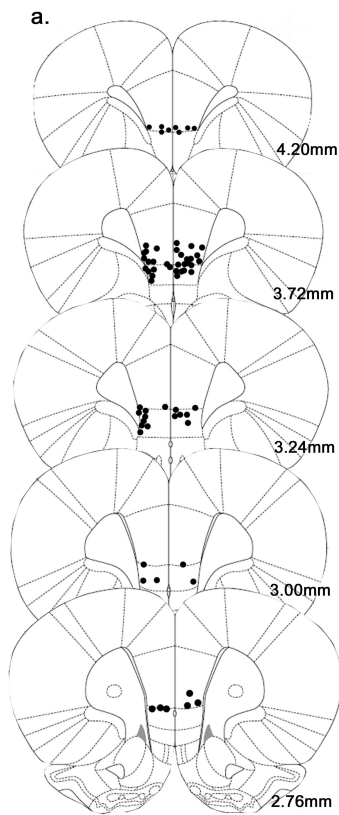


Figure 3.5) Cannula hit sites within the mPFC and Fos expression following pre-sacrifice infusion of muscimol within the mPFC of BEPs and BERs

Bilateral cannula placements within the mPFC (a). Representative Nissl stain, showing infusion cannula, and corresponding tissue section showing Fos expression following infusion of 30ng muscimol prior to sacrifice in a BER rat (b) and a BEP rat (c). Scale bar represents 100 μ m.

parts of the cingulate cortex. Thus we cannot rule out the possibility that muscimol spread to more dorsal areas of the mPFC over the course of infusions.

Discussion

Here we provide preliminary evidence that the ability for the mPFC to limit PF intake may be weaker in rats prone to binge eating. First, we show that the mPFC indeed serves as a behavioral “brake” on PF intake in female rats, as GABA-mediated inhibition of the mPFC led to a significant increase in PF intake, regardless of binge phenotype. In addition, BEPs displayed a stronger increase in PF intake (i.e., based on effect size analyses), after both 1 *and* 4hrs of exposure, than did BERs, suggesting that the brake over PF intake in BEP rats may be slightly weaker than in BER rats. Finally, our analysis of feeding behavior following inactivation of the mPFC identified two separate behavioral mechanisms for the increase in PF intake following inactivation of the mPFC and the differences in PF intake between BEPs and BERs. Thus, our data identify the functional significance of the mPFC not only to PF intake and the structure of PF consumption in female rats but also to binge eating proneness.

The mPFC serves as a behavioral limit over PF intake in female rats

In both BEP and BER rats, PF consumption increased significantly after GABA-mediated inhibition of the mPFC, suggesting that the function of the mPFC in the context of food reward is to restrict excessive consumption. The mPFC likely serves to limit PF intake by way of its dense glutamatergic projections into the nucleus accumbens [48], where dopaminergic and opioidergic signaling provide strong “go” signals in favor of PF consumption [101] Specifically, glutamatergic signaling within the accumbens, some of which may originate within the mPFC, regulates food intake: infusion of an AMPA receptor antagonist into the accumbens shell of male rats leads to a dramatic increase in chow intake while direct stimulation of AMPA receptors

within the accumbens shell reduces both chow and palatable liquid intake [112-114]. Thus, if PF intake is at least partially limited by the glutamatergic projections from the mPFC into the accumbens, then the rise in PF intake demonstrated here following inactivation of the mPFC might be a consequence of a more *dis-inhibited*, accumbens-mediated signal in favor of PF consumption. Here we induced global inactivation of the mPFC, but future work should aim to selectively and specifically target and manipulate mPFC-accumbens projections to more directly test this hypothesis.

In two previous studies using male rats, pharmacological inactivation of the mPFC had no significant effect on absolute consumption of a highly palatable liquid solution [76, 110]. Mena et al., 2011 and Baldo et. al., 2015 showed that inactivation of the mPFC indeed shifted the microstructure of feeding towards fewer and longer bouts of palatable liquid consumption, but without a resulting change in the global amount of palatable liquid consumed [76, 110]. The use of female rats, or even different types of PFs (i.e., solid PF vs. highly-palatable liquid) may have contributed to the fact that we, here, found a statistically significant increase in PF intake following mPFC inactivation, while other groups have not. In terms of a sex difference, neural responsiveness (i.e., Fos expression) to PF consumption, specifically to the type of PF used here, is stronger in the IL cortex of the mPFC as well as the nucleus accumbens core and shell of females as compared to males [170]. If PF consumption rises after inactivation of the mPFC because of a *release of inhibition* from the nucleus accumbens, then perhaps the resulting change in PF intake is greater in the female sex because of stronger, baseline accumbens responsiveness to PF in females as compared to males. In the future it will be necessary to determine if mPFC inactivation differentially affects PF intake in the female vs. the male sex, and if male BEPs and BERs also differ in the magnitude of the mPFC-mediated limit over PF intake.

The magnitude of mPFC-mediated control over PF intake is slightly weaker in BEPs vs. BERs

Inactivation of the mPFC led to an increase in PF intake in both BEPs and BERs, indicating that the mPFC limits PF intake regardless of binge phenotype, but the magnitude of the increase in PF intake was slightly higher in BEPs relative to BERs. This is most apparent in our data set through the effect size estimates for the comparison of 1hr PF intake following infusion of saline vs. 1hr PF intake following infusion of the higher dose of muscimol: the effect size for this comparison in BEPs ($d = 1.18$) was almost double that in BERs ($d = 0.64$), and at 4hrs the effect size was negligible for BERs ($d = 0.02$) but was medium-to-large in magnitude in BEPs ($d = 0.62$). In addition, BEPs showed a 10% increase in 4hr PF intake following infusion of the higher dose of muscimol, but 4hr PF intake in BERs after infusion of the higher dose of muscimol was virtually unchanged from saline. Thus, despite the non-significant drug*phenotype interactions for PF intake, our data at least partially suggest that inactivation of the mPFC yielded not only a higher, immediate increase in PF intake, but the effect of inactivation of the mPFC on PF intake was also sustained for a longer duration in BEPs as compared to BERs. In the future, it will be necessary to determine how PF intake changes following infusion of a higher dose of muscimol into the mPFC. Doses of up to 75ng have been used for the purpose of inactivating the mPFC prior to PF exposure [110]. Pilot studies in our lab using higher doses (i.e., 75ng, see **Figure 3.1**) revealed that the strongest increase in PF intake occurred following infusion of the 30ng dose that was used here, but our initial pilot studies utilized animals that had not been previously identified as being BEP or BER. Thus, future studies could utilize additional doses of musimol, specifically in BEPs and in BERs, to determine if stronger drug*phenotype interactions exist when higher doses of drug are used.

If we assume that the mPFC controls PF intake by at least partially limiting the drive for PF consumption coming from the nucleus accumbens, then between-phenotype differences in the strength of accumbens signals in favor of PF consumption could explain the larger increase in PF intake displayed by BEPs following inactivation of the mPFC. That is, the ability for the mPFC to control PF consumption in BEPs may *weaker* due to a *stronger* drive for PF intake coming from accumbens circuitry. In support of this hypothesis, previous work in our lab has also demonstrated greater PF-induced neural responsiveness (i.e., Fos expression) in the accumbens core and shell in BEPs as compared to BERs [132]. Thus, accumbens circuitry, at baseline, may exert a stronger “go” signal in favor of PF in BEPs, such that removing inhibition from the accumbens, by inactivating the mPFC as we have done here, results in a stronger increase in PF consumption in BEPs as compared to BERs.

Behavioral mechanisms underlying muscimol-induced increase in PF intake and differences in PF intake between BEPs and BERs

Inactivation of the mPFC induced a substantial shift in the basic structure of PF consumption in the first hour of PF exposure: BEPs and BERs engaged in fewer but longer episodes of PF intake following mPFC inhibition. This was mirrored by a decline in home-cage exploratory behavior (i.e., rears) and basic grooming behavior, suggesting that inactivating the mPFC shifted behavioral strategies towards PF consumption. Notably, previous work employing pharmacological inactivation of the mPFC in male rats demonstrated a virtually identical behavioral change in the context of PF intake, suggesting that, regardless of sex, inactivation of the mPFC increases the amount of time that animals spend engaged in consummatory behaviors [76, 110]. Baldo, B.A., et. al., 2015 noted that the lengthened bouts of PF consumption likely reflect a diminution in mPFC-mediated temporal control over PF consumption [110], given that

neuronal activity within mPFC regulates the onset and offset of basic consummatory behaviors [104]. As such, the mPFC likely controls PF intake by activating “on” and “off” signals for the initiation and cessation of bouts of PF intake. In this regard, neuronal output from mPFC appears to support decision-making and action selection (i.e., executive function [153]) in the specific context of food intake, in that it regulates how long an animal engages in feeding behavior instead of other, perhaps more advantageous, behaviors (i.e., exploring the environment, social interaction, mating) [110]. Because BEPs and BERs showed comparable changes, following inactivation of the mPFC, in the average duration of episodes of PF intake, the mPFC appears to function similarly in terms of the timing of episodes of PF intake in the two phenotypes. Thus, the heightened consumption of PF in BEPs is not necessarily due to a relative inability to terminate a bout of PF intake.

Rather, BEPs may be *more motivated* to consume PF than BERs, as they consistently approached the PF dish sooner and engaged in more frequent episodes of PF intake than did BERs. Data from studies of licking microstructure, using sucrose solutions, suggest that the number of sucrose licking bouts that are initiated reflects the motivational processes and post-ingestive negative feedback associated with consumption [172]. That is, the more motivated an animal is to start a new bout of sucrose licking, the better they are at suppressing inhibitory signals coming from the GI tract as it fills with substance [172]. Greater motivation for highly palatable liquids, based on licking microstructure data, has also been demonstrated in models of binge eating: rats who binge on a cream-oil sucrose solution initiate licking bouts of the cream-oil solution sooner and more often than rats in a non-binge group [173], and rats identified as being prone to sucrose bingeing (based on intake of a 20% sucrose solution) initiate sucrose licking bouts sooner and more often than rats identified as being resistant to sucrose bingeing

[174]. Certainly, we cannot make a direct comparison between the more precise measurements of licking microstructure obtained in [173] and [174] and the scores of feeding behavior used in the current study. However, if the neurobiological features of licking microstructure do extend to other forms feeding behaviors (i.e., ingestion of solid PFs), then our data may suggest that BEPs are more motivated to consume PF than BERs; they take significantly less time to start consuming PF and initiate more episodes of PF intake than do BERs. Notably, the enhanced motivation for PF in BEPs appears to be independent of the mPFC, given that BEPs had shorter latencies and more frequent episodes of PF intake than BERs even after inactivation of the mPFC. Thus, while the mPFC controls the distinct behavioral signature of PF intake in female rats, by regulating the timing of individual episodes of PF intake, the mPFC has little effect on the specific behavioral mechanisms, related to PF intake, that differentiate BEPs from BERs. In the future it will be necessary to assess whether the differences in feeding behavior observed here are also present when using a more precise study of licking microstructure, to confirm that differences in the motivational drive for PF underlie differences in intake between BEPs and BERs.

Conclusions

In summary, our data provide preliminary evidence that the mPFC of female rats serves as a behavioral “brake” on PF intake, as pharmacological inactivation of the mPFC led to a significant increase in PF intake and enhanced the amount of time rats spent engaged in episodes of PF intake. In addition, the rise in PF intake following inactivation of the mPFC was larger in BEPs vs. BERs, but since our data did not reach statistical significance, weaker mPFC-mediated behavioral control over PF intake only partially explains the observed differences in PF intake between BEPs and BERs in this model. In the future it will be necessary to identify other

potential neural and/or developmental mechanisms (i.e., enhanced reward circuit sensitivity to PF, altered CNS sensitivity to metabolic hormones, early life stress, sensitivity to gonadal hormones), that may interact with the mPFC-mediated brake over PF intake to drive binge eating proneness in female rats.

Conclusions

Historically, clinicians and scientists, alike, were under the assumption that EDs were primarily driven by psychosocial risk variables, such as personality traits, a history of dieting, and a drive for thinness. While personality and psychological trait characteristics certainly contribute to the development of EDs, the constant starvation and excessive exercise in AN and the dramatic ability to consume food (up to 4000 kcal at a time [123]) despite fullness in BN and BED also suggest underlying **biological** [175] abnormalities. So where, then, is the underlying abnormality? Thankfully, advances in human fMRI imaging have shed light on the neural circuits that appear to function sub-par in women with EDs. Human neuroimaging studies are probably the best tools that we currently have at our disposal for the purpose of identifying disturbances in neural function in individuals with EDs.

Several neuroimaging studies in women with EDs, to date, have identified altered patterns of neural activity within PFC circuitry, which begs the question of whether the typical function of the PFC in terms of behavioral regulation extends to the regulation of food intake as well. Studies in rodents suggest that, indeed, the mPFC serves as a behavioral limit on food intake, as inactivating neural activity in the mPFC leads to a rise in PF intake in rodents. Yet because almost all studies in rodents have been performed in male rats, and very few have used specific animal models of eating pathology, a direct application to EDs in the human condition is incomplete. As such, the experiments within this dissertation addressed this gap by identifying *the functional significance of the mPFC to eating pathology in female rats and in a model of binge eating proneness*.

First, we sought to determine whether the mPFC was at all relevant to PF consumption in female rodents and in our binge eating model. We found that, indeed, select sub-regions of the

mPFC were more strongly engaged by PF than a control, non-PF stimulus, and we found higher activation of each sub-region of the mPFC in BEP as compared to BER females. Hence, this initial study confirmed that the magnitude of activation within the mPFC in response to PF is associated with binge eating proneness.

To expand upon our initial finding, our second experiment sought to determine the neuronal phenotypes, that is, excitatory or inhibitory, of the PF-activated neurons within the mPFC of BEP and BER female rats. Studies in male rats that have used pharmacological inactivation of the mPFC suggest that the mPFC serves as a limit or behavioral “brake” over PF intake, so we hypothesized that the strength of this brake over PF intake is *weaker* in BEP rats as compared to BER rats. Since excitatory output from {excitatory neurons of} the mPFC facilitate this brake over PF intake, we predicted *reduced* activation of excitatory neurons following PF exposure would be present in the mPFC of BEP rats as compared to BER rats. We first assessed single-label Fos expression in the mPFC of BEP and BER rats, as in our first experiment, but found no differences in the magnitude of global activation of the mPFC in BEP rats as compared to BER rats. Though this particular outcome was different from our initial findings outlined above, the types of PF used in the two studies were quite different: one higher in fat (often used for diet-induced obesity) vs. one with a macronutrient content much more similar to that of foods typically consumed during a binge, particularly in women. We anticipate that the two different types of PF may induce inherently different patterns of neural activation, both qualitatively (in different brain regions) and quantitatively (the magnitude of activation), so it may be no surprise that the BEP vs. BER differences in the responsiveness of the mPFC to PF also varied across studies.

Nonetheless, the remaining double label immunohistochemical experiments within this second experiment revealed novel findings. First, the vast majority of neurons that expressed Fos in the mPFC were excitatory, projection neurons, regardless of binge phenotype, so BEPs and BERs do not differ in the *proportions* of Fos-ir neurons that co-localized with excitatory or inhibitory neuronal markers. On the other hand, the *absolute number* of PF-activated excitatory neurons, specifically within the ventral mPFC, was lower in BEPs than in BERs, supporting our hypothesis that predicted *reduced* excitatory neuron responsiveness to PF in rats prone to binge eating. Specifically, the fact that fewer excitatory neurons were activated by PF in BEPs as compared to BERs is in line with what we know about the role of the rodent mPFC in the context of food intake: excitatory neurons of the mPFC restrict PF intake. If less excitatory neurons are engaged by PF in BEPs than in BERs, perhaps this in part explains the observation that BEPs appear to be worse than BERs at controlling how much PF they consume, when given the opportunity.

Finally, our third experiment sought to identify the functional role of the mPFC to PF intake and to binge eating proneness. Since the mPFC appears to serve as a limit on PF intake, at least in male rodents, we predicted that pharmacological inactivation of the mPFC would lead to an increase in PF intake in both BEPs and in BERs. Yet, our over-arching hypothesis was that BEPs have weaker, mPFC-mediated control over PF intake, we predicted that the rise in PF intake following inactivation of the mPFC would be *larger in BEPs vs. BERs*. First, we demonstrated that inactivation of the mPFC led to a significant increase in PF intake, with no effect on the intake of chow, suggesting that the mPFC of female rats indeed serves as a behavioral limit over hedonic, reward-driven feeding. That is, the mPFC appears to tonically suppress reward-driven feeding when it is not, behaviorally, advantageous (i.e., when animals

are satiated). We did not find *statistically* significant differences between BEPs and BERs, in terms of the magnitude of the increase in PF intake following mPFC inactivation, but the rise in PF intake (both after 1 and 4hrs of exposure) was, nonetheless, *larger in BEPs than in BERs*. Thus, data from the final chapter of this dissertation supports our over-arching hypothesis that BEPs consistently consume more PF than BERs due to weaker, mPFC-mediated behavioral control over PF consumption. However, the lack of statistical significance found in this particular study also suggests that additional mechanisms, such as reward circuit responsiveness to PF or individual differences in sensitivity to gonadal or metabolic hormones, likely also contribute to the observed behavioral differences between BEPs and BERs. Such mechanisms could be empirically probed in future experiments with this model.

The mPFC in the context of sex differences in binge eating proneness and the onset of binge eating proneness during puberty

Here we show that female BEPs and BERs may differ in their ability to regulate how much PF is consumed. What might this mean for 1) the prominent sex difference (female > male) in binge eating proneness, and 2) the rise in binge eating proneness during adolescence? Our lab has demonstrated both phenomena using this model of binge eating. First, we have demonstrated a significant female bias in binge eating proneness, as female rats are significantly more likely to be identified as being BEP than are male rats [134]. We also have preliminary evidence that this sex difference in binge eating proneness may be due to enhanced behavioral and neural responsiveness to PF reward in females as compared to males. Specifically, females show a stronger CPP to PF than do males, and females display higher, PF-induced neural responsiveness in the IL cortex and accumbens core and shell than males [170]. So, we can say that sex differences in binge eating proneness may be due to sex differences in behavioral and

neural responsiveness to PF reward, but we cannot definitively say that the sex difference in binge eating proneness is also driven by high vs. low mPFC-mediated regulation of PF intake. One interesting finding from [170] however, was that our analysis of feeding behavior, which was similar to what was performed in the third chapter of this dissertation, revealed that females spent significantly more time, at each bout of PF intake, consuming PF than did males [170]. In the third chapter of this dissertation, we show that the mPFC appears to regulate this particular behavioral signature of PF intake, since “turning off” mPFC activity caused female rats to consume PF for much longer bouts of time. If, therefore, time spent consuming PF serves as a behavioral correlate for the magnitude of mPFC-derived regulation of PF intake, perhaps the finding that females spent more time consuming PF than did males does suggest that sex differences in binge eating proneness may be associated with between-sex differences in the mPFC-mediated control over PF intake. Future studies using male BEPs and BERs in the pharmacological inactivation studies used here could help answer this question. Moreover, such studies would help determine whether the neuro-behavioral differences between female BEPs and BERs also hold true for male BEPs and BERs as well.

In terms of the *adolescent* development of binge eating proneness [16], it is well documented that the mPFC undergoes extensive structural remodeling during adolescence, including cell death, cell birth, and synaptic pruning [176-178]. Recent work from the lab of Linda Wilbrecht has also shown that puberty is a critical time point for maturation of the excitatory vs. inhibitory balance within the mPFC, a process that is partially driven by organizational effects of ovarian hormones during puberty [179], and which is crucial for mPFC-driven behaviors like cognitive flexibility [179, 180]. In concert with mPFC remodeling, however, is active (and faster) maturation and growth of limbic, reward circuitry, adding to the

hypothesis that the “risky” behavior displayed by teens is a consequence of reward-driven behavior in the absence of mature executive functions within the mPFC [181, 182]. Thus far, we have evidence that binge eating proneness is partially driven by deficient mPFC-mediated regulation over PF intake, as demonstrated here, as well as higher responsiveness to food reward, which may be the case for sex differences in binge eating proneness; both neural constructs (i.e., reward and executive functions) essentially mature during puberty. Therefore, the adolescent development of binge eating proneness could be driven by 1) altered structural and functional development of the mPFC during puberty, namely, altered maturation of mPFC excitatory/inhibitory balance, or 2) an imbalance in the mPFC-mediated regulation over PF intake vs. the motivation for PF intake within limbic circuitry.

Implications for EDs in women

Here we identify the cellular players and functional relevance of the mPFC to PF intake and we identify a novel mechanism that may drive enhanced binge eating and ED risk in the female population. Thus, the data presented herein add to the growing body of literature that supports a role for the mPFC in having a direct, regulatory function in the context of food intake and eating pathology. In particular, we extend the theory that the mPFC serves as a behavioral limit over PF intake to *female rats* and to a *model of binge eating*. As such, the concept of deficits in mPFC-mediated behavioral regulation over PF intake, as a cause for ED psychopathology, is now even more relevant to the human condition where women are more often affected by EDs than are men. This critical step in determining how the mPFC functions in eating pathology in the female sex can now be expanded upon in the future, by identifying, for example, how ovarian hormones, during both adolescence and adulthood, might modify the strength of the mPFC-mediated brake over PF intake and eating pathology. For example, does

exposure to oral contraceptives during puberty alter the ability for the mPFC to control normative eating behavior? Are the fluctuations in the expression of eating pathology across the menstrual cycle in women associated with variations in how well the mPFC controls food intake [121]? The work within this dissertation provides the essential foundation upon which these questions can be probed in the future.

Finally, novel neuromodulatory treatment modalities for women with EDs that are currently under investigation *directly harness* neural activity within PFC circuitry. Specifically, repetitive transcranial magnetic stimulation (rTMS) and transcranial direct current stimulation (tDCS) are noninvasive methods for directly stimulating neuronal activity within sub-regions of the PFC that have shown promise for treating EDs in women [183]. For example, 20-30 sessions of rTMS of the dorsomedial PFC in women with binge-purge AN or BN reduced the frequency of both bingeing and purging by 80%, in those who responded to treatment [184], while 20 sessions of rTMS of the dorsolateral PFC in women with AN maintained BMI and improved symptoms of ED pathology in 3 of the 5 total participants [185]. Moreover, a single session of tDCS of the dorsolateral PFC reduced the urge to binge, improved self-regulatory control (i.e., using a monetary choice task), and improved bulimic behaviors for 24 hours post-stimulation in women with BN [186]. In men and women with BED, a single session of tDCS of the dorsolateral PFC decreased food cravings, total food intake, and the desire to binge-eat [187]. Several other trials, using rTMS or tDCS in women with AN, BN, and BED, are underway highlighting the potential that these techniques may have for the future of ED therapy [183]. However, the current state of neuromodulation is far from conclusive. To date, findings from neuromodulatory studies only provide good proof of concept that the approach is safe, tolerable, and somewhat effective for eating pathology [188]. The ability to specifically tailor

neuromodulatory techniques to each type of ED requires that we develop a more in-depth understanding of how cortical circuitry controls eating pathology. That is, identifying the neurotransmitter systems and the downstream projection targets by which the mPFC regulates food intake and eating pathology, especially in animal models, is crucial for determining how techniques like rTMS and tDCS can be made more effective in the long term. Data within this dissertation, therefore, provide a strong foundation upon which future research can more fully work towards this goal, in an attempt to identify novel age and sex-specific therapies for treating EDs in the human condition.

REFERENCES

REFERENCES

1. Wade, T.D., Keski-Rahkonen, A., and Hudson, J.I., *Epidemiology of eating disorders*, in *Textbook of Psychiatric Epidemiology*, M.T. Ming T. Tsuang, Peter B. Jones, Editor 2011, Wiley-Blackwell: Hoboken, New Jersey. p. 343-356.
2. Swanson, S.A., et al., *Prevalence and correlates of eating disorders in adolescents. Results from the national comorbidity survey replication adolescent supplement*. Arch Gen Psychiatry, 2011. **68**(7): p. 714-23.
3. Hoek, H.W. and D. van Hoeken, *Review of the prevalence and incidence of eating disorders*. Int J Eat Disord, 2003. **34**(4): p. 383-96.
4. Merikangas, K.R., et al., *Lifetime prevalence of mental disorders in U.S. adolescents: results from the National Comorbidity Survey Replication--Adolescent Supplement (NCS-A)*. J Am Acad Child Adolesc Psychiatry, 2010. **49**(10): p. 980-9.
5. Harris, E.C. and B. Barraclough, *Excess mortality of mental disorder*. Br J Psychiatry, 1998. **173**: p. 11-53.
6. Harris, E.C. and B. Barraclough, *Suicide as an outcome for mental disorders. A meta-analysis*. Br J Psychiatry, 1997. **170**: p. 205-28.
7. Herzog, D.B., et al., *Mortality in eating disorders: a descriptive study*. Int J Eat Disord, 2000. **28**(1): p. 20-6.
8. Arcelus, J., et al., *Mortality rates in patients with anorexia nervosa and other eating disorders. A meta-analysis of 36 studies*. Arch Gen Psychiatry, 2011. **68**(7): p. 724-31.
9. Becker, A.E., et al., *Eating disorders*. N Engl J Med, 1999. **340**(14): p. 1092-8.
10. Crow, S.J., et al., *Increased mortality in bulimia nervosa and other eating disorders*. Am J Psychiatry, 2009. **166**(12): p. 1342-6.
11. Walsh, B.T., *The enigmatic persistence of anorexia nervosa*. Am J Psychiatry, 2013. **170**(5): p. 477-84.
12. Papadopoulos, F.C., et al., *Excess mortality, causes of death and prognostic factors in anorexia nervosa*. Br J Psychiatry, 2009. **194**(1): p. 10-7.
13. Klump, K.L., *Puberty as a critical risk period for eating disorders: a review of human and animal studies*. Horm Behav, 2013. **64**(2): p. 399-410.
14. Bulik, C.M., *Eating disorders in adolescents and young adults*. Child Adolesc Psychiatr Clin N Am, 2002. **11**(2): p. 201-18.

15. Klump, K.L., K.M. Culbert, and C.L. Sisk, *Sex Differences in Binge Eating: Gonadal Hormone Effects Across Development*. Annu Rev Clin Psychol, 2017.
16. Klump, K.L., et al., *Binge eating proneness emerges during puberty in female rats: a longitudinal study*. J Abnorm Psychol, 2011. **120**(4): p. 948-55.
17. Klump, K.L., et al., *Changes in genetic and environmental influences on disordered eating across adolescence: a longitudinal twin study*. Arch Gen Psychiatry, 2007. **64**(12): p. 1409-15.
18. Kaye, W.H., J.L. Fudge, and M. Paulus, *New insights into symptoms and neurocircuit function of anorexia nervosa*. Nat Rev Neurosci, 2009. **10**(8): p. 573-84.
19. Kaye, W.H., et al., *Does a shared neurobiology for foods and drugs of abuse contribute to extremes of food ingestion in anorexia and bulimia nervosa?* Biol Psychiatry, 2013. **73**(9): p. 836-42.
20. Kaye, W., *Neurobiology of anorexia and bulimia nervosa*. Physiol Behav, 2008. **94**(1): p. 121-35.
21. Monteleone, P. and M. Maj, *Dysfunctions of leptin, ghrelin, BDNF and endocannabinoids in eating disorders: beyond the homeostatic control of food intake*. Psychoneuroendocrinology, 2013. **38**(3): p. 312-30.
22. Wierenga, C.E., et al., *Are Extremes of Consumption in Eating Disorders Related to an Altered Balance between Reward and Inhibition?* Front Behav Neurosci, 2014. **8**: p. 410.
23. Harrison, A., et al., *Sensitivity to reward and punishment in eating disorders*. Psychiatry Res, 2010. **177**(1-2): p. 1-11.
24. Wierenga, C.E., et al., *Hunger does not motivate reward in women remitted from anorexia nervosa*. Biol Psychiatry, 2015. **77**(7): p. 642-52.
25. Ely, A.V., et al., *Response in taste circuitry is not modulated by hunger and satiety in women remitted from bulimia nervosa*. J Abnorm Psychol, 2017. **126**(5): p. 519-530.
26. Radeloff, D., et al., *High-fat taste challenge reveals altered striatal response in women recovered from bulimia nervosa: A pilot study*. World J Biol Psychiatry, 2014. **15**(4): p. 307-16.
27. Oberndorfer, T.A., et al., *Altered insula response to sweet taste processing after recovery from anorexia and bulimia nervosa*. Am J Psychiatry, 2013. **170**(10): p. 1143-51.
28. Filbey, F.M., U.S. Myers, and S. Dewitt, *Reward circuit function in high BMI individuals with compulsive overeating: similarities with addiction*. Neuroimage, 2012. **63**(4): p. 1800-6.

29. Schienle, A., et al., *Binge-eating disorder: reward sensitivity and brain activation to images of food*. Biol Psychiatry, 2009. **65**(8): p. 654-61.
30. Uher, R., et al., *Medial prefrontal cortex activity associated with symptom provocation in eating disorders*. Am J Psychiatry, 2004. **161**(7): p. 1238-46.
31. Foerde, K., et al., *Neural mechanisms supporting maladaptive food choices in anorexia nervosa*. Nat Neurosci, 2015. **18**(11): p. 1571-3.
32. Gearhardt, A.N., M.A. White, and M.N. Potenza, *Binge eating disorder and food addiction*. Curr Drug Abuse Rev, 2011. **4**(3): p. 201-7.
33. Juarascio, A.S., et al., *Could training executive function improve treatment outcomes for eating disorders?* Appetite, 2015. **90**: p. 187-93.
34. Lee-Winn, A.E., et al., *Associations of Neuroticism and Impulsivity with Binge Eating in a Nationally Representative Sample of Adolescents in the United States*. Pers Individ Dif, 2016. **90**: p. 66-72.
35. Boeka, A.G. and K.L. Lokken, *Prefrontal systems involvement in binge eating*. Eat Weight Disord, 2011. **16**(2): p. e121-6.
36. Hudson, J.I., et al., *The prevalence and correlates of eating disorders in the National Comorbidity Survey Replication*. Biol Psychiatry, 2007. **61**(3): p. 348-58.
37. Gadalla, T. and N. Piran, *Co-occurrence of eating disorders and alcohol use disorders in women: a meta analysis*. Arch Womens Ment Health, 2007. **10**(4): p. 133-40.
38. Racine, S.E., et al., *Examining associations between negative urgency and key components of objective binge episodes*. Int J Eat Disord, 2015. **48**(5): p. 527-31.
39. Wu, M., et al., *Inhibitory control in bulimic-type eating disorders: a systematic review and meta-analysis*. PLoS One, 2013. **8**(12): p. e83412.
40. Marsh, R., et al., *An FMRI study of self-regulatory control and conflict resolution in adolescents with bulimia nervosa*. Am J Psychiatry, 2011. **168**(11): p. 1210-20.
41. Marsh, R., et al., *Deficient activity in the neural systems that mediate self-regulatory control in bulimia nervosa*. Arch Gen Psychiatry, 2009. **66**(1): p. 51-63.
42. Balodis, I.M., et al., *Divergent neural substrates of inhibitory control in binge eating disorder relative to other manifestations of obesity*. Obesity (Silver Spring), 2013. **21**(2): p. 367-77.

43. Reiter, A.M., et al., *Impaired Flexible Reward-Based Decision-Making in Binge Eating Disorder: Evidence from Computational Modeling and Functional Neuroimaging*. Neuropsychopharmacology, 2017. **42**(3): p. 628-637.
44. Giustino, T.F. and S. Maren, *The Role of the Medial Prefrontal Cortex in the Conditioning and Extinction of Fear*. Front Behav Neurosci, 2015. **9**: p. 298.
45. Linnman, C., et al., *Resting amygdala and medial prefrontal metabolism predicts functional activation of the fear extinction circuit*. Am J Psychiatry, 2012. **169**(4): p. 415-23.
46. Phelps, E.A., et al., *Extinction learning in humans: role of the amygdala and vmPFC*. Neuron, 2004. **43**(6): p. 897-905.
47. Motzkin, J.C., et al., *Ventromedial prefrontal cortex is critical for the regulation of amygdala activity in humans*. Biol Psychiatry, 2015. **77**(3): p. 276-284.
48. Hoover, W.B. and R.P. Vertes, *Anatomical analysis of afferent projections to the medial prefrontal cortex in the rat*. Brain Struct Funct, 2007. **212**(2): p. 149-79.
49. Vertes, R.P., *Differential projections of the infralimbic and prelimbic cortex in the rat*. Synapse, 2004. **51**(1): p. 32-58.
50. Gabbott, P.L., et al., *Prefrontal cortex in the rat: projections to subcortical autonomic, motor, and limbic centers*. J Comp Neurol, 2005. **492**(2): p. 145-77.
51. Floresco, S.B., et al., *Multiple dopamine receptor subtypes in the medial prefrontal cortex of the rat regulate set-shifting*. Neuropsychopharmacology, 2006. **31**(2): p. 297-309.
52. Kelley, A.E., *Ventral striatal control of appetitive motivation: role in ingestive behavior and reward-related learning*. Neurosci Biobehav Rev, 2004. **27**(8): p. 765-76.
53. Baldwin, A.E., K. Sadeghian, and A.E. Kelley, *Appetitive instrumental learning requires coincident activation of NMDA and dopamine D1 receptors within the medial prefrontal cortex*. J Neurosci, 2002. **22**(3): p. 1063-71.
54. Gourley, S.L. and J.R. Taylor, *Going and stopping: dichotomies in behavioral control by the prefrontal cortex*. Nat Neurosci, 2016. **19**(6): p. 656-64.
55. Wickens, J.R., et al., *Dopaminergic mechanisms in actions and habits*. J Neurosci, 2007. **27**(31): p. 8181-3.
56. Land, B.B., et al., *Medial prefrontal D1 dopamine neurons control food intake*. Nat Neurosci, 2014. **17**(2): p. 248-53.

57. Steketee, J.D., *Neurotransmitter systems of the medial prefrontal cortex: potential role in sensitization to psychostimulants*. Brain Res Brain Res Rev, 2003. **41**(2-3): p. 203-28.
58. Albert, P.R., F. Vahid-Ansari, and C. Luckhart, *Serotonin-prefrontal cortical circuitry in anxiety and depression phenotypes: pivotal role of pre- and post-synaptic 5-HT1A receptor expression*. Front Behav Neurosci, 2014. **8**: p. 199.
59. Bizot, J., et al., *Serotonin and tolerance to delay of reward in rats*. Psychopharmacology (Berl), 1999. **146**(4): p. 400-12.
60. Elston, G.N., *Cortex, cognition and the cell: new insights into the pyramidal neuron and prefrontal function*. Cereb Cortex, 2003. **13**(11): p. 1124-38.
61. Urban-Ciecko, J. and A.L. Barth, *Somatostatin-expressing neurons in cortical networks*. Nat Rev Neurosci, 2016. **17**(7): p. 401-9.
62. Tremblay, R., S. Lee, and B. Rudy, *GABAergic Interneurons in the Neocortex: From Cellular Properties to Circuits*. Neuron, 2016. **91**(2): p. 260-92.
63. Freund, T.F., *Interneuron Diversity series: Rhythm and mood in perisomatic inhibition*. Trends Neurosci, 2003. **26**(9): p. 489-95.
64. Pfeffer, C.K., et al., *Inhibition of inhibition in visual cortex: the logic of connections between molecularly distinct interneurons*. Nat Neurosci, 2013. **16**(8): p. 1068-76.
65. Kawaguchi, Y. and Y. Kubota, *GABAergic cell subtypes and their synaptic connections in rat frontal cortex*. Cereb Cortex, 1997. **7**(6): p. 476-86.
66. Lewis, D.A., et al., *Cortical parvalbumin interneurons and cognitive dysfunction in schizophrenia*. Trends Neurosci, 2012. **35**(1): p. 57-67.
67. Cardin, J.A., et al., *Driving fast-spiking cells induces gamma rhythm and controls sensory responses*. Nature, 2009. **459**(7247): p. 663-7.
68. Perova, Z., K. Delevich, and B. Li, *Depression of excitatory synapses onto parvalbumin interneurons in the medial prefrontal cortex in susceptibility to stress*. J Neurosci, 2015. **35**(7): p. 3201-6.
69. Murray, A.J., et al., *Parvalbumin-positive interneurons of the prefrontal cortex support working memory and cognitive flexibility*. Sci Rep, 2015. **5**: p. 16778.
70. Kawaguchi, Y. and S. Kondo, *Parvalbumin, somatostatin and cholecystokinin as chemical markers for specific GABAergic interneuron types in the rat frontal cortex*. J Neurocytol, 2002. **31**(3-5): p. 277-87.

71. Kvitsiani, D., et al., *Distinct behavioural and network correlates of two interneuron types in prefrontal cortex*. Nature, 2013. **498**(7454): p. 363-6.
72. Pinto, L. and Y. Dan, *Cell-Type-Specific Activity in Prefrontal Cortex during Goal-Directed Behavior*. Neuron, 2015. **87**(2): p. 437-50.
73. David, C., et al., *The innervation of parvalbumin-containing interneurons by VIP-immunopositive interneurons in the primary somatosensory cortex of the adult rat*. Eur J Neurosci, 2007. **25**(8): p. 2329-40.
74. Pi, H.J., et al., *Cortical interneurons that specialize in disinhibitory control*. Nature, 2013. **503**(7477): p. 521-4.
75. Ferezou, I., et al., *Extensive overlap of mu-opioid and nicotinic sensitivity in cortical interneurons*. Cereb Cortex, 2007. **17**(8): p. 1948-57.
76. Mena, J.D., K. Sadeghian, and B.A. Baldo, *Induction of hyperphagia and carbohydrate intake by mu-opioid receptor stimulation in circumscribed regions of frontal cortex*. J Neurosci, 2011. **31**(9): p. 3249-60.
77. Mena, J.D., R.A. Selleck, and B.A. Baldo, *Mu-opioid stimulation in rat prefrontal cortex engages hypothalamic orexin/hypocretin-containing neurons, and reveals dissociable roles of nucleus accumbens and hypothalamus in cortically driven feeding*. J Neurosci, 2013. **33**(47): p. 18540-52.
78. Gaykema, R.P., et al., *Characterization of excitatory and inhibitory neuron activation in the mouse medial prefrontal cortex following palatable food ingestion and food driven exploratory behavior*. Front Neuroanat, 2014. **8**: p. 60.
79. Chudasama, Y., *Animal models of prefrontal-executive function*. Behav Neurosci, 2011. **125**(3): p. 327-43.
80. Dalley, J.W., R.N. Cardinal, and T.W. Robbins, *Prefrontal executive and cognitive functions in rodents: neural and neurochemical substrates*. Neurosci Biobehav Rev, 2004. **28**(7): p. 771-84.
81. Walton, M.E., D.M. Bannerman, and M.F. Rushworth, *The role of rat medial frontal cortex in effort-based decision making*. J Neurosci, 2002. **22**(24): p. 10996-1003.
82. Chudasama, Y., et al., *Dissociable aspects of performance on the 5-choice serial reaction time task following lesions of the dorsal anterior cingulate, infralimbic and orbitofrontal cortex in the rat: differential effects on selectivity, impulsivity and compulsivity*. Behav Brain Res, 2003. **146**(1-2): p. 105-19.
83. Passetti, F., Y. Chudasama, and T.W. Robbins, *The frontal cortex of the rat and visual attentional performance: dissociable functions of distinct medial prefrontal subregions*. Cereb Cortex, 2002. **12**(12): p. 1254-68.

84. Bissonette, G.B., E.M. Powell, and M.R. Roesch, *Neural structures underlying set-shifting: roles of medial prefrontal cortex and anterior cingulate cortex*. Behav Brain Res, 2013. **250**: p. 91-101.
85. Ng, C.W., et al., *Double dissociation of attentional resources: prefrontal versus cingulate cortices*. J Neurosci, 2007. **27**(45): p. 12123-31.
86. Walton, M.E., et al., *Functional specialization within medial frontal cortex of the anterior cingulate for evaluating effort-related decisions*. J Neurosci, 2003. **23**(16): p. 6475-9.
87. Feja, M. and M. Koch, *Ventral medial prefrontal cortex inactivation impairs impulse control but does not affect delay-discounting in rats*. Behav Brain Res, 2014. **264**: p. 230-9.
88. Risterucci, C., et al., *Excitotoxic lesions of the prelimbic-infralimbic areas of the rodent prefrontal cortex disrupt motor preparatory processes*. Eur J Neurosci, 2003. **17**(7): p. 1498-508.
89. Murphy, E.R., et al., *Impulsive behaviour induced by both NMDA receptor antagonism and GABAA receptor activation in rat ventromedial prefrontal cortex*. Psychopharmacology (Berl), 2012. **219**(2): p. 401-10.
90. Tsutsui-Kimura, I., et al., *Neuronal codes for the inhibitory control of impulsive actions in the rat infralimbic cortex*. Behav Brain Res, 2016. **296**: p. 361-72.
91. Corbit, L.H. and B.W. Balleine, *The role of prelimbic cortex in instrumental conditioning*. Behav Brain Res, 2003. **146**(1-2): p. 145-57.
92. Killcross, S. and E. Coutureau, *Coordination of actions and habits in the medial prefrontal cortex of rats*. Cereb Cortex, 2003. **13**(4): p. 400-8.
93. Coutureau, E. and S. Killcross, *Inactivation of the infralimbic prefrontal cortex reinstates goal-directed responding in overtrained rats*. Behav Brain Res, 2003. **146**(1-2): p. 167-74.
94. Smith, K.S. and A.M. Graybiel, *A dual operator view of habitual behavior reflecting cortical and striatal dynamics*. Neuron, 2013. **79**(2): p. 361-74.
95. Wu, M., et al., *Set-shifting ability across the spectrum of eating disorders and in overweight and obesity: a systematic review and meta-analysis*. Psychol Med, 2014. **44**(16): p. 3365-85.
96. Fischer, S., G.T. Smith, and K.G. Anderson, *Clarifying the role of impulsivity in bulimia nervosa*. Int J Eat Disord, 2003. **33**(4): p. 406-11.

97. Waxman, S.E., *A systematic review of impulsivity in eating disorders*. Eur Eat Disord Rev, 2009. **17**(6): p. 408-25.
98. Kaye, W.H., et al., *Relationship of mood alterations to bingeing behaviour in bulimia*. Br J Psychiatry, 1986. **149**: p. 479-85.
99. Velazquez-Sanchez, C., et al., *High trait impulsivity predicts food addiction-like behavior in the rat*. Neuropsychopharmacology, 2014. **39**(10): p. 2463-72.
100. Moore, C.F., et al., *Neuroscience of Compulsive Eating Behavior*. Front Neurosci, 2017. **11**: p. 469.
101. Berridge, K.C., *'Liking' and 'wanting' food rewards: brain substrates and roles in eating disorders*. Physiol Behav, 2009. **97**(5): p. 537-50.
102. Stuber, G.D. and R.A. Wise, *Lateral hypothalamic circuits for feeding and reward*. Nat Neurosci, 2016. **19**(2): p. 198-205.
103. Jezzini, A., et al., *Processing of hedonic and chemosensory features of taste in medial prefrontal and insular networks*. J Neurosci, 2013. **33**(48): p. 18966-78.
104. Horst, N.K. and M. Laubach, *Reward-related activity in the medial prefrontal cortex is driven by consumption*. Front Neurosci, 2013. **7**: p. 56.
105. Ishikawa, A., et al., *Contributions of the amygdala and medial prefrontal cortex to incentive cue responding*. Neuroscience, 2008. **155**(3): p. 573-84.
106. Sangha, S., et al., *Alterations in reward, fear and safety cue discrimination after inactivation of the rat prelimbic and infralimbic cortices*. Neuropsychopharmacology, 2014. **39**(10): p. 2405-13.
107. Warren, B.L., et al., *Distinct Fos-Expressing Neuronal Ensembles in the Ventromedial Prefrontal Cortex Mediate Food Reward and Extinction Memories*. J Neurosci, 2016. **36**(25): p. 6691-703.
108. Warthen, D.M., et al., *Activation of Pyramidal Neurons in Mouse Medial Prefrontal Cortex Enhances Food-Seeking Behavior While Reducing Impulsivity in the Absence of an Effect on Food Intake*. Front Behav Neurosci, 2016. **10**: p. 63.
109. Parent, M.A., et al., *The medial prefrontal cortex is crucial for the maintenance of persistent licking and the expression of incentive contrast*. Front Integr Neurosci, 2015. **9**: p. 23.

110. Baldo, B.A., et al., *GABA-Mediated Inactivation of Medial Prefrontal and Agranular Insular Cortex in the Rat: Contrasting Effects on Hunger- and Palatability-Driven Feeding*. Neuropsychopharmacology, 2015.
111. Corwin, R.L., et al., *Binge-type eating disrupts dopaminergic and GABAergic signaling in the prefrontal cortex and ventral tegmental area*. Obesity (Silver Spring), 2016. **24**(10): p. 2118-25.
112. Kelley, A.E. and C.J. Swanson, *Feeding induced by blockade of AMPA and kainate receptors within the ventral striatum: a microinfusion mapping study*. Behav Brain Res, 1997. **89**(1-2): p. 107-13.
113. Maldonado-Irizarry, C.S., C.J. Swanson, and A.E. Kelley, *Glutamate receptors in the nucleus accumbens shell control feeding behavior via the lateral hypothalamus*. J Neurosci, 1995. **15**(10): p. 6779-88.
114. Stratford, T.R., C.J. Swanson, and A. Kelley, *Specific changes in food intake elicited by blockade or activation of glutamate receptors in the nucleus accumbens shell*. Behav Brain Res, 1998. **93**(1-2): p. 43-50.
115. Richard, J.M. and K.C. Berridge, *Prefrontal cortex modulates desire and dread generated by nucleus accumbens glutamate disruption*. Biol Psychiatry, 2013. **73**(4): p. 360-70.
116. Kelley, A.E., et al., *Corticostriatal-hypothalamic circuitry and food motivation: integration of energy, action and reward*. Physiol Behav, 2005. **86**(5): p. 773-95.
117. Hammerle, F., et al., *Thinking dimensional: prevalence of DSM-5 early adolescent full syndrome, partial and subthreshold eating disorders in a cross-sectional survey in German schools*. BMJ Open, 2016. **6**(5): p. e010843.
118. Sweeting, H., et al., *Prevalence of eating disorders in males: a review of rates reported in academic research and UK mass media*. Int J Mens Health, 2015. **14**(2).
119. Asarian, L. and N. Geary, *Sex differences in the physiology of eating*. Am J Physiol Regul Integr Comp Physiol, 2013. **305**(11): p. R1215-67.
120. Klump, K.L., et al., *Preliminary evidence that estradiol moderates genetic influences on disordered eating attitudes and behaviors during puberty*. Psychol Med, 2010. **40**(10): p. 1745-53.
121. Klump, K.L., et al., *The interactive effects of estrogen and progesterone on changes in emotional eating across the menstrual cycle*. J Abnorm Psychol, 2013. **122**(1): p. 131-7.

122. Avena, N.M. and M.E. Bocarsly, *Dysregulation of brain reward systems in eating disorders: neurochemical information from animal models of binge eating, bulimia nervosa, and anorexia nervosa*. Neuropharmacology, 2012. **63**(1): p. 87-96.
123. Walsh, B.T., *The importance of eating behavior in eating disorders*. Physiol Behav, 2011. **104**(4): p. 525-9.
124. American Psychiatric Association, *Diagnostic and Statistical manual of mental disorders*. 5th ed. 2013, Washington, DC.
125. Avena, N.M., P. Rada, and B.G. Hoebel, *Evidence for sugar addiction: behavioral and neurochemical effects of intermittent, excessive sugar intake*. Neurosci Biobehav Rev, 2008. **32**(1): p. 20-39.
126. Corwin, R.L., N.M. Avena, and M.M. Boggiano, *Feeding and reward: perspectives from three rat models of binge eating*. Physiol Behav, 2011. **104**(1): p. 87-97.
127. Hagan, M.M., et al., *A new animal model of binge eating: key synergistic role of past caloric restriction and stress*. Physiol Behav, 2002. **77**(1): p. 45-54.
128. Babbs, R.K., F.H. Wojnicki, and R.L. Corwin, *Effect of 2-hydroxyestradiol on binge intake in rats*. Physiol Behav, 2011. **103**(5): p. 508-12.
129. Colantuoni, C., et al., *Evidence that intermittent, excessive sugar intake causes endogenous opioid dependence*. Obes Res, 2002. **10**(6): p. 478-88.
130. Avena, N.M. and B.G. Hoebel, *A diet promoting sugar dependency causes behavioral cross-sensitization to a low dose of amphetamine*. Neuroscience, 2003. **122**(1): p. 17-20.
131. Klump, K.L., et al., *The effects of ovariectomy on binge eating proneness in adult female rats*. Horm Behav, 2011. **59**(4): p. 585-93.
132. Sinclair, E.B., et al., *Differential mesocorticolimbic responses to palatable food in binge eating prone and binge eating resistant female rats*. Physiol Behav, 2015. **152**(Pt A): p. 249-56.
133. Hildebrandt, B.A., et al., *Differential strain vulnerability to binge eating behaviors in rats*. Physiol Behav, 2014. **127**: p. 81-6.
134. Klump, K.L., et al., *Sex differences in binge eating patterns in male and female adult rats*. Int J Eat Disord, 2013. **46**(7): p. 729-36.
135. Boggiano, M.M., et al., *High intake of palatable food predicts binge-eating independent of susceptibility to obesity: an animal model of lean vs obese binge-eating and obesity with and without binge-eating*. Int J Obes (Lond), 2007. **31**(9): p. 1357-67.

136. Oswald, K.D., et al., *Motivation for palatable food despite consequences in an animal model of binge eating*. Int J Eat Disord, 2011. **44**(3): p. 203-11.
137. Culbert, K.M., et al., *Prenatal hormone exposure and risk for eating disorders: a comparison of opposite-sex and same-sex twins*. Arch Gen Psychiatry, 2008. **65**(3): p. 329-36.
138. Culbert, K.M., et al., *The emergence of sex differences in risk for disordered eating attitudes during puberty: a role for prenatal testosterone exposure*. J Abnorm Psychol, 2013. **122**(2): p. 420-32.
139. Telch, C.F. and W.S. Agras, *Obesity, binge eating and psychopathology: are they related?* Int J Eat Disord, 1994. **15**(1): p. 53-61.
140. Avena, N.M., et al., *Overlaps in the nosology of substance abuse and overeating: the translational implications of "food addiction"*. Curr Drug Abuse Rev, 2011. **4**(3): p. 133-9.
141. Herrera, D.G. and H.A. Robertson, *Activation of c-fos in the brain*. Prog Neurobiol, 1996. **50**(2-3): p. 83-107.
142. Valdivia, S., et al., *Acute high fat diet consumption activates the mesolimbic circuit and requires orexin signaling in a mouse model*. PLoS One, 2014. **9**(1): p. e87478.
143. Heusner, A.A., *Body size and energy metabolism*. Annu Rev Nutr, 1985. **5**: p. 267-93.
144. Blancas, A., et al., *Progressive anticipation in behavior and brain activation of rats exposed to scheduled daily palatable food*. Neuroscience, 2014. **281C**: p. 44-53.
145. Paxinos, G and C, Watson, *The Rat Brain in Stereotaxic Coordinates*. 5th ed., 2005, San Diego: Academic Press.
146. Chisholm, N.C. and J.M. Juraska, *Effects of long-term treatment with estrogen and medroxyprogesterone acetate on synapse number in the medial prefrontal cortex of aged female rats*. Menopause, 2012. **19**(7): p. 804-11.
147. Olkin, I and L.V. Hedges, *Statistical Methods for Meta-Analysis*, 1985, Orlando: Academic Press.
148. Pecina, S. and K.C. Berridge, *Hedonic hot spot in nucleus accumbens shell: where do mu-opioids cause increased hedonic impact of sweetness?* J Neurosci, 2005. **25**(50): p. 11777-86.
149. Smith-Roe, S.L. and A.E. Kelley, *Coincident activation of NMDA and dopamine D1 receptors within the nucleus accumbens core is required for appetitive instrumental learning*. J Neurosci, 2000. **20**(20): p. 7737-42.

150. Kelley, A.E., *Functional specificity of ventral striatal compartments in appetitive behaviors*. Ann N Y Acad Sci, 1999. **877**: p. 71-90.
151. Brog, J.S., et al., *The patterns of afferent innervation of the core and shell in the "accumbens" part of the rat ventral striatum: immunohistochemical detection of retrogradely transported fluoro-gold*. J Comp Neurol, 1993. **338**(2): p. 255-78.
152. Castro, D.C. and K.C. Berridge, *Opioid hedonic hotspot in nucleus accumbens shell: mu, delta, and kappa maps for enhancement of sweetness "liking" and "wanting"*. J Neurosci, 2014. **34**(12): p. 4239-50.
153. O'Doherty, J.P., *Contributions of the ventromedial prefrontal cortex to goal-directed action selection*. Ann N Y Acad Sci, 2011. **1239**: p. 118-29.
154. Constantinidis, C., G.V. Williams, and P.S. Goldman-Rakic, *A role for inhibition in shaping the temporal flow of information in prefrontal cortex*. Nat Neurosci, 2002. **5**(2): p. 175-80.
155. Bohon, C. and E. Stice, *Reward abnormalities among women with full and subthreshold bulimia nervosa: a functional magnetic resonance imaging study*. Int J Eat Disord, 2011. **44**(7): p. 585-95.
156. Yu, Z., N. Geary, and R.L. Corwin, *Individual effects of estradiol and progesterone on food intake and body weight in ovariectomized binge rats*. Physiol Behav, 2011. **104**(5): p. 687-93.
157. Becker, J.B. and M. Hu, *Sex differences in drug abuse*. Front Neuroendocrinol, 2008. **29**(1): p. 36-47.
158. Quinones-Jenab, V. and S. Jenab, *Progesterone attenuates cocaine-induced responses*. Horm Behav, 2010. **58**(1): p. 22-32.
159. Kuhn, C., et al., *The emergence of gonadal hormone influences on dopaminergic function during puberty*. Horm Behav, 2010. **58**(1): p. 122-37.
160. Hudson, J.I., et al., *Longitudinal study of the diagnosis of components of the metabolic syndrome in individuals with binge-eating disorder*. Am J Clin Nutr, 2010. **91**(6): p. 1568-73.
161. Calero-Elvira, A., et al., *Meta-analysis on drugs in people with eating disorders*. Eur Eat Disord Rev, 2009. **17**(4): p. 243-59.
162. Huang, Y., et al., *Expression of transcription factor Satb2 in adult mouse brain*. Anat Rec (Hoboken), 2013. **296**(3): p. 452-61.

163. Alcamo, E.A., et al., *Satb2 regulates callosal projection neuron identity in the developing cerebral cortex*. Neuron, 2008. **57**(3): p. 364-77.
164. Lovett-Barron, M., et al., *Dendritic inhibition in the hippocampus supports fear learning*. Science, 2014. **343**(6173): p. 857-63.
165. Freund, T.F. and I. Katona, *Perisomatic inhibition*. Neuron, 2007. **56**(1): p. 33-42.
166. Yavorska, I. and M. Wehr, *Somatostatin-Expressing Inhibitory Interneurons in Cortical Circuits*. Front Neural Circuits, 2016. **10**: p. 76.
167. Lock, J., et al., *Aberrant brain activation during a response inhibition task in adolescent eating disorder subtypes*. Am J Psychiatry, 2011. **168**(1): p. 55-64.
168. Balodis, I.M., et al., *Monetary reward processing in obese individuals with and without binge eating disorder*. Biol Psychiatry, 2013. **73**(9): p. 877-86.
169. Parent, M.A., et al., *Cholinergic and ghrelinergic receptors and KCNQ channels in the medial PFC regulate the expression of palatability*. Front Behav Neurosci, 2015. **9**: p. 284.
170. Sinclair, E.B., et al., *Preliminary evidence of sex differences in behavioral and neural responses to palatable food reward in rats*. Physiol Behav, 2017. **176**: p. 165-173.
171. Morris, S.B. and R.P. DeShon, *Combining effect size estimates in meta-analysis with repeated measures and independent-groups designs*. Psychol Methods, 2002. **7**(1): p. 105-25.
172. Johnson, A.W., *Characterizing ingestive behavior through licking microstructure: Underlying neurobiology and its use in the study of obesity in animal models*. Int J Dev Neurosci, 2017.
173. Lardeux, S., J.J. Kim, and S.M. Nicola, *Intermittent access to sweet high-fat liquid induces increased palatability and motivation to consume in a rat model of binge consumption*. Physiol Behav, 2013. **114-115**: p. 21-31.
174. Calvez, J. and E. Timofeeva, *Behavioral and hormonal responses to stress in binge-like eating prone female rats*. Physiol Behav, 2016. **157**: p. 28-38.
175. Klump, K.L., M. McGue, and W.G. Iacono, *Age differences in genetic and environmental influences on eating attitudes and behaviors in preadolescent and adolescent female twins*. J Abnorm Psychol, 2000. **109**(2): p. 239-51.
176. Koss, W.A., et al., *Dendritic remodeling in the adolescent medial prefrontal cortex and the basolateral amygdala of male and female rats*. Synapse, 2014. **68**(2): p. 61-72.

177. Markham, J.A., J.R. Morris, and J.M. Juraska, *Neuron number decreases in the rat ventral, but not dorsal, medial prefrontal cortex between adolescence and adulthood*. Neuroscience, 2007. **144**(3): p. 961-8.
178. Staffend, N.A., et al., *A decrease in the addition of new cells in the nucleus accumbens and prefrontal cortex between puberty and adulthood in male rats*. Dev Neurobiol, 2014. **74**(6): p. 633-42.
179. Piekarski, D.J., J.R. Boivin, and L. Wilbrecht, *Ovarian Hormones Organize the Maturation of Inhibitory Neurotransmission in the Frontal Cortex at Puberty Onset in Female Mice*. Curr Biol, 2017. **27**(12): p. 1735-1745 e3.
180. Piekarski, D.J., et al., *Does puberty mark a transition in sensitive periods for plasticity in the associative neocortex?* Brain Res, 2017. **1654**(Pt B): p. 123-144.
181. Giedd, J.N., et al., *Brain development during childhood and adolescence: a longitudinal MRI study*. Nat Neurosci, 1999. **2**(10): p. 861-3.
182. Op de Macks, Z.A., et al., *Risky decision-making in adolescent girls: The role of pubertal hormones and reward circuitry*. Psychoneuroendocrinology, 2016. **74**: p. 77-91.
183. Lutter, M., *Emerging Treatments in Eating Disorders*. Neurotherapeutics, 2017. **14**(3): p. 614-622.
184. Dunlop, K., et al., *Increases in frontostriatal connectivity are associated with response to dorsomedial repetitive transcranial magnetic stimulation in refractory binge/purge behaviors*. Neuroimage Clin, 2015. **8**: p. 611-8.
185. McClelland, J., et al., *Repetitive Transcranial Magnetic Stimulation (rTMS) Treatment in Enduring Anorexia Nervosa: A Case Series*. Eur Eat Disord Rev, 2016. **24**(2): p. 157-63.
186. Kekic, M., et al., *Single-Session Transcranial Direct Current Stimulation Temporarily Improves Symptoms, Mood, and Self-Regulatory Control in Bulimia Nervosa: A Randomised Controlled Trial*. PLoS One, 2017. **12**(1): p. e0167606.
187. Burgess, E.E., et al., *Effects of transcranial direct current stimulation (tDCS) on binge eating disorder*. Int J Eat Disord, 2016. **49**(10): p. 930-936.
188. Val-Laillet, D., et al., *Neuroimaging and neuromodulation approaches to study eating behavior and prevent and treat eating disorders and obesity*. Neuroimage Clin, 2015. **8**: p. 1-31.